GEOLOGICAL SURVEY OF DENMARK AND GREENLAND BULLETIN 10 • 2006

Review of Survey activities 2005

Edited by
Martin Sønderholm and A.K. Higgins

GEOLOGICAL SURVEY OF DENMARK AND GREENLAND
DANISH MINISTRY OF THE ENVIRONMENT

Geological Survey of Denmark and Greenland Bulletin 10

Keywords
Geological Survey of Denmark and Greenland, survey organisations, current research, Denmark, Greenland.

Cover photographs from left to right

1. The barrier reef complex fringing most of the Kenya coastline is also one of the most vulnerable environments to pollution. A new *Oil Spill Sensitivity Atlas* for Kenya helps to prioritise the emergency response on the most susceptible areas (see article, page 65). Photograph: John Tychsen, GEUS.
2. Vibro-seismic data were acquired on Stevns, Denmark to be able to correlate the Danian–Campanian cores drilled along the east coast of Stevns (see article, page 13). Photograph: Lars Stemmerik, GEUS.
3. Farming on the rooftops. Experiment carried out at GEUS to investigate concentrations of pathogens leached to drainage water as a result of different slurry manure application methods. Photograph: Peter K. Warna-Moors, GEUS.
4. Refuelling of helicopter on the Arctic Sea ice during seismic acquisition programme related to data collection for the *Continental Shelf Project* around Greenland. Photograph: Trine Dahl-Jensen, GEUS.

Frontispiece: facing page
Thrust sheet pair exposed in the Rubjerg Knude Glaciotectonic Complex, Vendsyssel, Denmark. Photograph: Stig A. Schack Pedersen, GEUS.

Chief editor of this series: Adam A. Garde
Scientific editors: Martin Sønderholm and A.K. Higgins
Editorial secretaries: Birgit Eriksen and Esben W. Glendal
External referees (numbers refer to first page of reviewed article): Lars Ole Boldreel (29), Michael Houmark-Nielsen (21, 61) and Kristine Thrane (25, 49, 53); Geological Institute, University of Copenhagen, Denmark. Asger Ken Pedersen (37, 41, 45); Geological Museum, Copenhagen, Denmark. Gregers Dam (9, 13, 33) and Michael Larsen (17); DONG Energy, Agern Alle 24–26, Hørsholm, Denmark
Illustrations: : Stefan Sølberg with contributions from Jette Halskov
Lay-out and graphic production: Annabeth Andersen, Carsten E. Thuesen
Printers: Schultz Grafisk, Albertslund, Denmark
Manuscripts submitted: 15 January – 27 February 2006
Final versions approved: 26 October 2006
Printed: 29 November 2006

ISSN 1603-9769, 1604-8156
ISBN-10: 87-7871-189-4
ISBN-13: 978-87-7871-189-2

Geological Survey of Denmark and Greenland Bulletin
The series *Geological Survey of Denmark and Greenland Bulletin* replaces *Geology of Denmark Survey Bulletin* and *Geology of Greenland Survey Bulletin*.

Citation of the name of this series
It is recommended that the name of this series is cited in full, viz. *Geological Survey of Denmark and Greenland Bulletin*.
If abbreviation of this volume is necessary, the following form is suggested: *Geol. Surv. Den. Green. Bull.* 10, 68 pp.

Available from
Geological Survey of Denmark and Greenland (GEUS) • Øster Voldgade 10 • DK-1350 Copenhagen K • Denmark
Phone: +45 38 14 20 00, fax: +45 38 14 20 50, e-mail: geus@geus.dk
or
Geografforlaget ApS • Rugårdsvej 55 • DK-5000 Odense C • Denmark
Phone: +45 63 44 16 83, fax: +45 63 44 16 97, e-mail: go@geografforlaget.dk

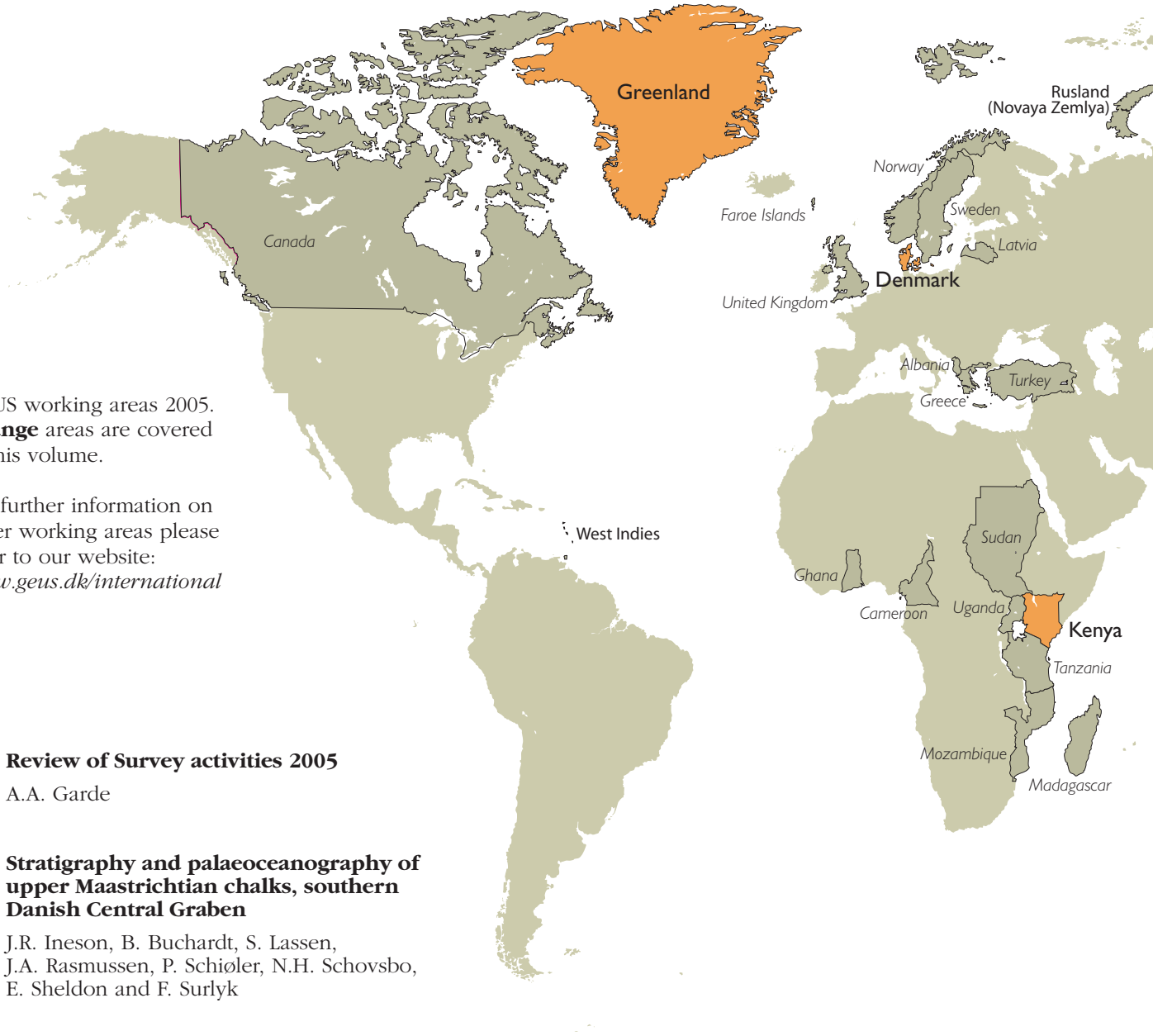

GEUS working areas 2005. **Orange** areas are covered in this volume.

For further information on other working areas please refer to our website: *www.geus.dk/international*

33. **Continental crust in the Davis Strait: new evidence from seabed sampling**

F. Dalhoff, L.M. Larsen, J.R. Ineson, S. Stouge, J.A. Bojesen-Koefoed, S. Lassen, A. Kuijpers, J.A. Rasmussen and H. Nøhr-Hansen

37. **An integrative and quantitative assessment of the gold potential of the Nuuk region, West Greenland**

B. Møller Stensgaard, T.M. Rasmussen and A. Steenfelt

41. **The Tikiusaaq carbonatite: a new Mesozoic intrusive complex in southern West Greenland**

A. Steenfelt, J.A. Hollis and K. Secher

45. **Archetypal kimberlite from the Maniitsoq region, southern West Greenland and analogy to South Africa**

T.F.D. Nielsen, M. Jebens, S.M. Jensen and K. Secher

49. **Using zircon geochronology to resolve the Archaean geology of southern West Greenland**

J.A. Hollis, D. Frei, J.A.M. van Gool, A.A. Garde and M. Persson

53. **Five slices through the Nuussuaq Basin, West Greenland**

A.K. Pedersen, L.M. Larsen, G. Krarup Pedersen and K.S. Dueholm

57. **Earthquake seismology in Greenland – improved data with multiple applications**

T.B. Larsen, T. Dahl-Jensen, P. Voss, T. Møller Jørgensen, S. Gregersen and H.P. Rasmussen

61. **Radical past climatic changes in the Arctic Ocean and a geophysical signature of the Lomonosov Ridge north of Greenland**

N. Mikkelsen, N. Nørgaard-Pedersen, Y. Kristoffersen, S. Juul Lassen and E. Sheldon

65. **KenSea – development of an environmental sensitivity atlas for coastal areas of Kenya**

J. Tychsen, O. Geertz-Hansen and J. Kofoed

Review of Survey activities 2005

Adam A. Garde
Chief editor

The present volume is the third issue of *Review of Survey activities* (RoSa). It contains 15 four-page contributions that cover a wide range of the current activities at the Geological Survey of Denmark and Greenland (GEUS). Thirteen of these are short scientific papers dealing with ongoing research by the Survey and its external partners. For the first time the research-based papers in the Review are now externally peer reviewed. A new standing panel of reviewers for RoSa has been established to ensure that the contributions are of general interest to a wide readership and that, within the limitations of space, they maintain the normal scientific standards of the Survey's publications. All articles are planned to be easily readable by non-specialists, and since this is a Review of Survey activities, it should be borne in mind that many papers are first accounts of ongoing research.

The fact that almost all contributions in the current volume are scientific in nature implies that while providing a timely panorama of current research at the Survey, they are far from embracing all projects undertaken by the Survey in Denmark, Greenland and other countries in 2005. A factual overview of the activities of GEUS as a whole can be obtained at GEUS' website.

In the present volume three papers deal with Cretaceous–Holocene onshore and offshore stratigraphy, sedimentology and palaeoceanography in Denmark, in part related to hydrocarbon exploration. A fourth paper from Denmark, that illustrates just one of the broad spectrum of the Survey's routine responsibilities undertaken on behalf of the state, addresses construction of 3D geological models to characterise the migration of point-source pollution in groundwater reservoirs.

Projects related to Greenland and the Arctic in general are represented in this volume by a group of nine papers. The first is a methodology paper describing advanced *in situ* geochronological and trace element microanalysis by laser ablation techniques, a now routine analytical tool at the Survey that has provided data for several of the subsequent articles, including a study of sediment provenance in the East Greenland – Faroe Islands – Shetland region, and an account of zircon geochronology applied to Archaean geological studies in southern West Greenland. Within the same region, a new method of integrative and quantitative assessment of the gold potential is presented, and two papers deal with newly discovered kimberlites and carbonatites and their potential economic significance. One paper describes five profiles through basalts and sedimentary rocks in the Nuussuaq Basin in West Greenland, constructed using geological photogrammetrical techniques along coastal cliffs and steep valley sides. Another paper presents new evidence for the presence of continental crust in the Davis Strait obtained from seabed sampling; this is an important new contribution to the long-standing debate of the nature of the crust under the Labrador Sea and Davis Strait and its stratigraphy. A report on ongoing studies of the deep crustal structure of Greenland using earthquake seismology is presented, and a last paper concerning the Arctic region describes radical former climatic changes in the Arctic Ocean and the geophysical signature of the Lomonosov Ridge north of Greenland, and discusses the sensitivity of the sea-ice cover to global warming.

The final paper in the present volume describes the development of an environmental sensitivity atlas for coastal areas of Kenya. This project is just one of several current GEUS projects where the Survey's broad technical and managing expertise is put to use in developing countries.

Stratigraphy and palaeoceanography of upper Maastrichtian chalks, southern Danish Central Graben

Jon R. Ineson, Bjørn Buchardt, Susanne Lassen, Jan A. Rasmussen, Poul Schiøler, Niels H. Schovsbo, Emma Sheldon and Finn Surlyk

Upper Maastrichtian chalks form important hydrocarbon reservoirs in the Danish sector of the North Sea and have been intensively studied, yet their lithological uniformity can frustrate attempts to develop a high-resolution stratigraphic subdivision and a genetic understanding of the factors controlling production and sedimentation of the pelagic carbonate ooze. Recent research into these topics, supported by the Danish Energy Authority, was carried out by the Geological Survey of Denmark and Greenland (GEUS) in collaboration with the Geological Institute, University of Copenhagen by means of a multidisciplinary study involving quantitative/semi-quantitative palynology, micropalaeontology (nannofossils, foraminifers) and isotope geochemistry, integrated with detailed sedimentology. Two key wells were selected, the M-10X well from the Dan Field and the E-5X well from the Tyra SE Field (Fig. 1), based on the extensive core coverage in these wells and on their position in the southern part of the Danish Central Graben where evidence of large-scale resedimentation (and consequent stratigraphic complexity) is uncommon within the Maastrichtian section.

In focusing on such a pelagic carbonate system, the ultimate aim is a holistic understanding of the marine system including temperature variation, nutrient supply and distribution, salinity, watermass layering, circulation and oxygen distribution. All these factors influence organic productivity and thus the accumulation of biogenic sediment. This study concentrated on a number of palaeoceanographic signals that can be derived from the sedimentary record, summarised in Fig. 2. Planktonic organisms, both phytoplankton (e.g. coccolithophores, some dinoflagellates) and zooplankton (e.g. foraminifers) provide a record of conditions in the upper watermasses, largely within the photic zone, while bottom conditions are indicated by epifaunal/infaunal organisms (e.g. benthic foraminifers) and bioturbation, and by the sedimentological evidence of depositional processes at the sea floor. On a larger scale, the input of terrestrial organic material relative to the marine component can provide an indirect measure of shoreline migration and thus relative sea-level change, a factor that is also reflected in the $\delta^{13}C$ isotopic composition of the seawater, as recorded by the biogenic carbonate ooze.

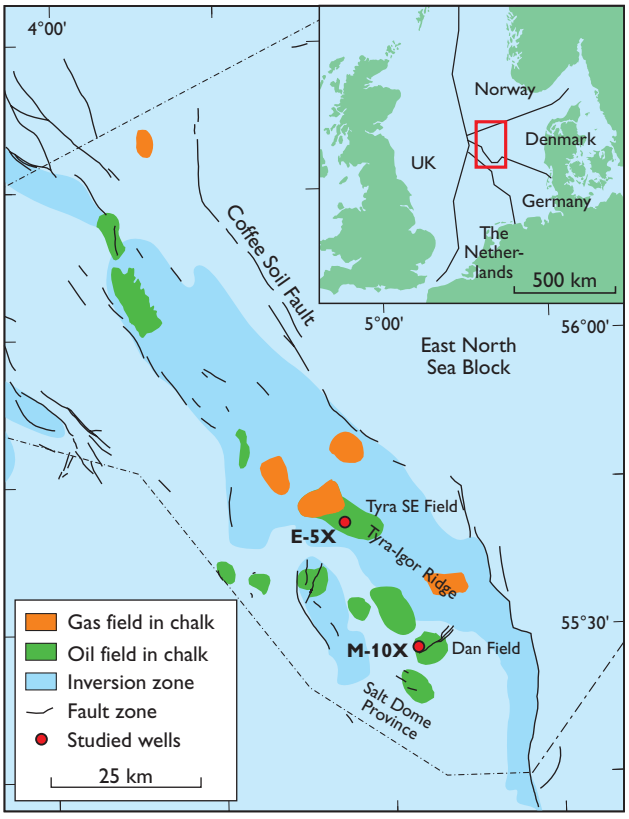

Fig. 1. Map showing the location of the two key wells, M-10X (Dan Field) and E-5X (Tyra SE Field), and the dominant Late Cretaceous structural elements in the Danish Central Graben.

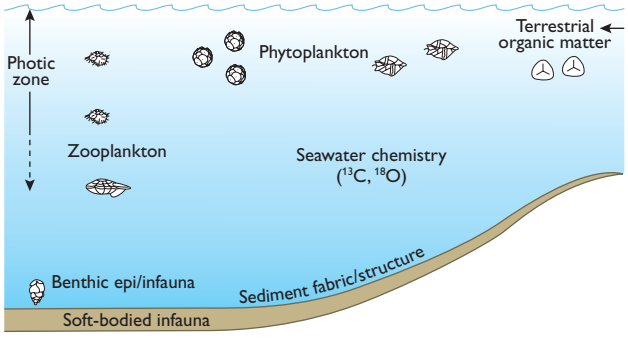

Fig. 2. Cartoon (scale arbitrary) showing the source of the palaeoceanographic signals utilised in the project; see text for explanation.

Stratigraphy

A prerequisite for this palaeoceanographic study was a well-constrained stratigraphic breakdown of the succession to permit confident intrabasinal correlation and comparison with regional/global events described in the literature. Although awaiting formal assignment, the upper Maastrichtian and Danian chalks of the Danish Central Graben are herein referred to the Tor and Ekofisk Formations, respectively, as defined from the Norwegian sector of the North Sea. Despite the numerous biostratigraphic studies undertaken on this stratigraphic interval in the Danish sector, much of the information is in the form of company reports, and published data are few. A high-resolution biostratigraphic study was thus undertaken to identify internationally recognised biozones related to the dinoflagellate cyst, nannofossil and microfossil floras and faunas. Detailed stable isotope investigations were incorporated to examine the potential role of chemostratigraphy. This resulted in a consistent framework for the uppermost Maastrichtian of the two key wells in the southern Danish Central Graben, exemplified by the subdivision of the M-10X cored section shown in Fig. 3. As a supplement to the zonal biostratigraphy, semi-quantitative data provide a second tier of stratigraphic constraints; these include dinoflagellate (*Palaeocystodinium denticulatum, Palynodinium grallator*), foraminifer (*Praebulimina laevis, Pseudotextularia elegans*) and nannofossil (*Watznaueria barnesiae*) acme events.

The Maastrichtian–Danian boundary in the M-10X and E-5X cored sections is marked by a distinctive hardground developed in the uppermost *c*. 1 m of the Tor Formation. The association of complex cross-cutting *Thalassinoides* networks, the cemented and bored upper layer and the irregular, pitted, glauconite-impregnated upper surface are indicative of a mature, evolved hardground surface, recording a protracted period of non-sedimentation at the sea floor. The occurrence of mixed late Maastrichtian and early Danian faunal and floral assemblages within the uppermost metre beneath the hardground surface suggests that the burrow systems remained open into Danian time, thus accumulating complex multi-generational fills. The lowermost Danian biozones are absent above the hardground indicating that this surface remained exposed at the sea floor for at least several hundred thousand years.

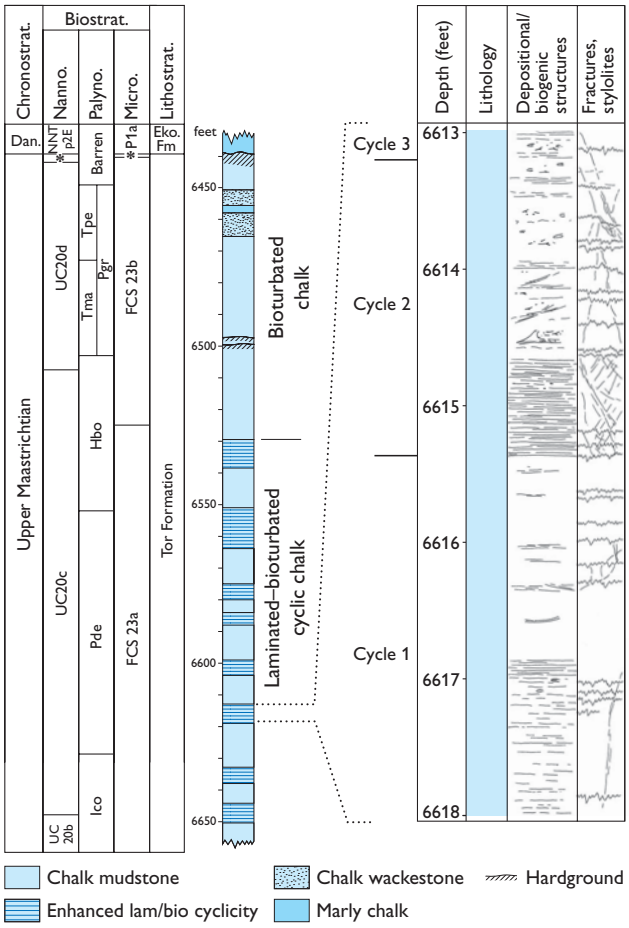

Fig. 3. Stratigraphic framework of the cored upper Maastrichtian section in the M-10X well showing the broad subdivision into lower cyclic and upper non-cyclic, bioturbated chalks; the expanded section shows two laminated–bioturbated cycles, characteristic of the lower cyclic chalks. **Dan.**, Danian; **Eko.**, Ekofisk. Palynological zones/subzones: **Ico**, *Isabelidinium cooksoniae*; **Pde**, *Palaeocystodinium denticulatum*; **Hbo**, *Hystrichostrogylon borisii*; **Pgr**, *Palynodinium grallator*; **Tma**, *Tanyosphaeridium magdalium*; **Tpe**, *Thalassiphora pelagica*. **Asterisk** indicates mixed floral and faunal assemblages of late Maastrichtian and Danian aspect associated with the top Tor Formation hardground.

Palaeoceanography

Analysis of palaeoceanographic trends and evolution in the late Maastrichtian in the study area has required integration of a wide range of detailed data, only a fraction of which can be reviewed in this summary. In the following, selected aspects of the full dataset (see Ineson *et al*. 2004a) are presented to provide the essential framework of the palaeoceanographic model.

Sedimentology

The upper Maastrichtian chalk succession in the southern Danish Central Graben is lithologically uniform, comprising pure coccolith-rich chalks with rare skeletal grains larger than silt grade, and a dominant 'lime mudstone' texture. In the Dan Field area, the cored upper Maastrichtian section is divisible into a lower cyclic succession, characterised by metre-scale laminated/bioturbated cycles, and an upper succession that is thoroughly bioturbated and overtly non-cyclic (Fig. 3). It has been proposed that the laminated facies in the

lower chalks represents an alternation of thin (millimetre-scale) chalk turbidites and hemipelagites; preservation of this primary sedimentary layering is thought to relate to low levels of oxygen on the sea floor (Damholt & Surlyk 2004). The alternation of laminated and bioturbated chalks thus records rhythmic shifts in bottom-water oxygenation; subtle shifts in the floral and faunal assemblages across these cycles suggest that such changes may have been controlled by variation in the degree of watermass stratification (Ineson *et al.* 2004b). In addition to the lack of overt cyclicity and the ubiquitous bioturbation, the upper chalks are also lithologically more variable, including rare incipient hardground surfaces, skeletal-rich chalks (wackestones) and an isolated marly chalk bed (Fig. 3). A subtle environmental change is thus indicated from a rhythmically stratified watermass to a more homogeneous watermass under which the sea floor was well ventilated and locally/periodically influenced by weak bottom currents.

Palynofacies and stable isotopes

A number of palynological parameters can be utilised to provide a sea-level record, such as the relative proportions of marine and non-marine palynomorphs and the relative abundance of the genus *Impagidinium* (an indicator of open ocean conditions) within the dinoflagellate assemblages. These parameters provide a consistent sea-level signal in the two Central Graben wells (Ineson *et al.* 2004a). The lower, cyclic chalks record an overall gradual sea-level fall culminating in a 'peak lowstand' near the base of the *P. grallator* dinoflagellate Zone (Fig. 4, *c.* 6500 ft) coinciding with the level of the incipient hardground surfaces. Palynofacies data from the succeeding bioturbated chalks record a subsequent sea-level rise and a variable signal up to the barren interval at the top of the Maastrichtian section.

It has been observed widely that the carbon isotope ($\delta^{13}C$) record broadly tracks the eustatic sea-level curve (e.g. Jarvis *et al.* 2002). The $\delta^{13}C$ values for the lower, cyclic chalks decrease gradually up-section, paralleling the palynofacies trend and adding support to the sea-level interpretation. In both wells, the lowest $\delta^{13}C$ values in the upper Maastrichtian section occur just beneath the base of the *P. grallator* Zone.

Nannoflora and foraminifers

The nannofloral assemblages are diverse (average species richness of 22) and show only minor compositional fluctuations with time, reflecting overall a stable, cool water (Boreal), oligotrophic (low nutrient) setting. Subtle shifts in the relative proportions of certain taxa, however, are thought to reflect changes in the nature of the upper watermasses, and although the precise control (i.e. temperature, nutrient level, salinity) can be difficult to isolate, interpretation can be facilitated by comparison with other datasets. Two examples are shown in Fig. 4. *Lucianorhabdus cayeuxii* has been demonstrated to occur preferentially in relatively inshore shelf sediments (Pospichal & Wise 1990); the general increase in the relative abundance of this species in the upper half of the studied sec-

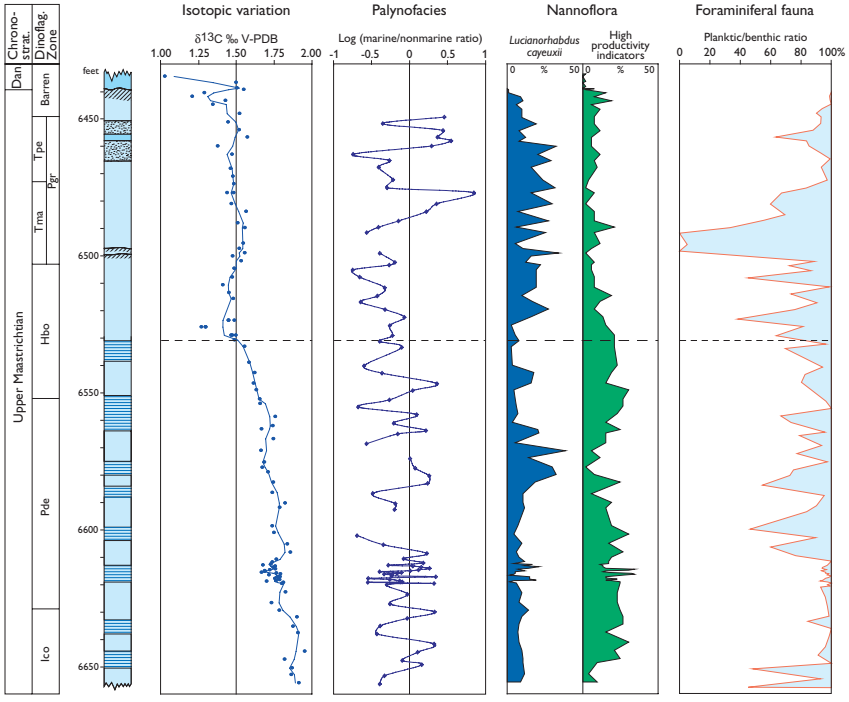

Fig. 4. Selected data from the M-10X well, illustrating the palaeoceanographic evolution in the late Maastrichtian, as discussed in the text. For stratigraphic terms and key, see Fig. 3; the horizontal **dashed line** indicates the boundary between the lower cyclic and upper non-cyclic chalks. The nannofossil genera grouped together to provide an indication of changing fertility levels are *Biscutum, Discorhabdus, Chiastozygus* and *Zeugrhabdotus*.

tion is thus compatible with the overall shallowing trend indicated by the sedimentological and palynological data. Certain nannofossil species are considered to be indicative of increased nutrient levels (e.g. Watkins 1989); the combined signal exhibited by these species clearly mirrors the subdivision of the succession into cyclic and non-cyclic chalks (Fig. 4), possibly reflecting a change in nutrient partitioning in the water column under different palaeoceanographic states.

The foraminifer assemblages are dominated by planktonic forms, particularly the ecologically tolerant *Heterohelix globulosa*, and plankton/benthos (P/B) ratios are typically over 70% (Fig. 4). The benthic fauna is of outer shelf aspect overall, with rare agglutinated forms. A feature of particular note in the M-10X foraminifer dataset is the anomalously low P/B values at 6490–6500 ft, associated with an increase in the relative abundance of a mid-shelf benthic foraminifer, *P. laevis*. This shallowing signal from the foraminifer data coincides with the sedimentological and palynofacies data indicating the 'peak lowstand' in the late Maastrichtian chalk sea.

Acme of the planktonic foraminifer *P. elegans* and the nannofossil *W. barnesiae* in the upper, non-cyclic chalks are indicative of warmer surface waters in the region at this time and are symptomatic of a global warming event in the latest Maastrichtian (Huber & Watkins 1992; Olsen *et al*. 2001).

Late Maastrichtian palaeoceanographic evolution

Palaeoecological data, from semi-quantitative analysis of foraminifer, coccolith and dinoflagellate faunas and floras, integrated with isotopic, palynofacies and sedimentological data has led to a model for the palaeoceanographic evolution of the Danish Central Graben in the late Maastrichtian involving two contrasting oceanographic systems. The lower half of the cored section records a cool-water, oligotrophic, deep shelf that was prone to stratification. Breakdown of this rhythmically stratified system accompanied a long-term gradual fall in sea level, perhaps reflecting a depth-related threshold beyond which stratification was no longer favoured. The upper half of the cored section records an increasingly dynamic and varied mid-shelf to deep shelf setting with a complex blend of environmental signals – sea-level change, watermass warming and evidence of low but variable productivity. Following turnover of the stratified system, the combined datasets record a progressive shallowing to a peak lowstand located just above the base of the *P. grallator* dinoflagellate Zone boundary; this sea-level event can be correlated with a key sequence boundary in the type Maastrichtian of the Netherlands (Schiøler *et al*. 1997).

Acknowledgement

The Danish Energy Authority (grant no.1313/01-0001) is thanked for financial support.

References

Damholt, T. & Surlyk, F. 2004: Laminated–bioturbated cycles in Maastrichtian chalk of the North Sea: oxygenation fluctuations within the Milankovitch frequency band. Sedimentology **51**, 1323–1342.

Huber, B.T. & Watkins, D.K. 1992: Biogeography of Campanian–Maastrichtian calcareous plankton in the region of the Southern Ocean: paleogeographic and paleoclimatic implications. In: Kennett, J.P. & Warnke, D.A. (eds): The Antarctic paleoenvironment: a perspective on global change. Antarctic Research Series **56**, 31–60.

Ineson, J.R., Buchardt, B., Lassen, S., Rasmussen, J.A., Schovsbo, N.H., Schiøler, P., Sheldon, E. & Surlyk, F. 2004a: Palaeontology, stable isotopes and sedimentology of the Upper Maastrichtian, Danish Central Graben: a record of palaeoclimatic and palaeoceanographic change. Danmarks og Grønlands Geologiske Undersøgelse Rapport **2004/81**, 20 pp.

Ineson, J.R., Buchardt, B., Lassen, S., Rasmussen, J.A., Schovsbo, N.H., Schiøler, P., Sheldon, E. & Surlyk, F. 2004b: On the origin of laminated–bioturbated chalk cycles in the Upper Maastrichtian, Danish Central Graben. Danmarks og Grønlands Geologiske Undersøgelse Rapport **2004/82**, 22 pp.

Jarvis, I., Mabrouk, A., Moody, R.T.J. & de Cabrera, S. 2002: Late Cretaceous (Campanian) carbon isotope events, sea-level change and correlation of the Tethyan and Boreal realms. Palaeogeography, Palaeoclimatology, Palaeoecology **2948**, 1–34.

Olsen, R.K., Wright, J.D. & Miller, K.G. 2001: Paleobiogeography of *Pseudotextularia elegans* during the latest Maastrichtian global warming event. Journal of Foraminiferal Research **31**, 275–282.

Pospichal, J.J. & Wise, S.W. 1990: Maastrichtian calcareous nannofossil biostratigraphy of Maud Rise ODP Leg 113 Sites 689 and 690, Weddell Sea. Proceedings of the Ocean Drilling Program, Scientific Results **113**, 465–487.

Schiøler, P., Brinkhuis, H., Roncaglia, L. & Wilson, G.J. 1997: Dinoflagellate biostratigraphy and sequence stratigraphy in the type Maastrichtian (Late Cretaceous), ENCI Quarry, The Netherlands. Marine Micropaleontology **31**, 65–95.

Watkins, D.K. 1989: Nannoplankton productivity fluctuations and rhythmically-bedded pelagic carbonates of the Greenhorn Limestone (Upper Cretaceous). Palaeogeography, Palaeoclimatology, Palaeoecology **74**, 75–86.

Authors' addresses

J.R.I., P.S., N.H.S. & E.S., *Geological Survey of Denmark and Greenland (GEUS), Øster Voldgade 10, DK-1350 Copenhagen K, Denmark.* E-mail: *ji@geus.dk*

B.B. & F.S., *Geological Institute, University of Copenhagen, Øster Voldgade 10, DK-1350 Copenhagen K, Denmark.*

S.L., *96 Settrington Road, London SW6 3BA, UK.*

J.A.R., *Geological Museum, University of Copenhagen, Øster Voldgade 5–7, DK-1350 Copenhagen K, Denmark.*

Shallow core drilling of the Upper Cretaceous Chalk at Stevns Klint, Denmark

Lars Stemmerik, Finn Surlyk, Kurt Klitten, Susanne L. Rasmussen & Niels Schovsbo

The Upper Cretaceous – Danian succession in Denmark and most of NW Europe is composed mainly of chalk and associated shallower water carbonates deposited in a wide epeiric sea during an overall global sea-level highstand (e.g. Surlyk 1997). The Maastrichtian–Danian chalk has been intensely studied over the last 20 years, since it forms the most important reservoir rock for hydrocarbons in the North Sea Central Graben (e.g. Surlyk *et al.* 2003; Klinkby *et al.* 2005). In Denmark, thousands of water wells have been drilled through the succession as about 35% of the water consumption is from Maastrichtian chalk and Danian bryozoan limestone.

During 2005 the new Cretaceous Research Centre (CRC) was established jointly at Geocenter Copenhagen by the Geological Institute, University of Copenhagen and the Geological Survey of Denmark and Greenland (GEUS) with financial support from the Danish Natural Science Research Council (FNU). CRC aims at studying the Earth System in a Greenhouse World, with special emphasis on the Upper Cretaceous – Danian chalk of NW Europe. The stable, long-lasting marine macro-environment represented by the chalk sea provides a unique opportunity to analyse and link the depositional, geochemical and biological responses to external forcing at time scales ranging from the sub-Milankovitch to the million year range. The studies will be based on a wide range of methods, including seismic stratigraphy, palaeoecology, sequence-, cyclo- and biostratigraphy, isotope geochemistry, sedimentology and time series analysis. This paper presents the first preliminary results of a CRC drilling cam-

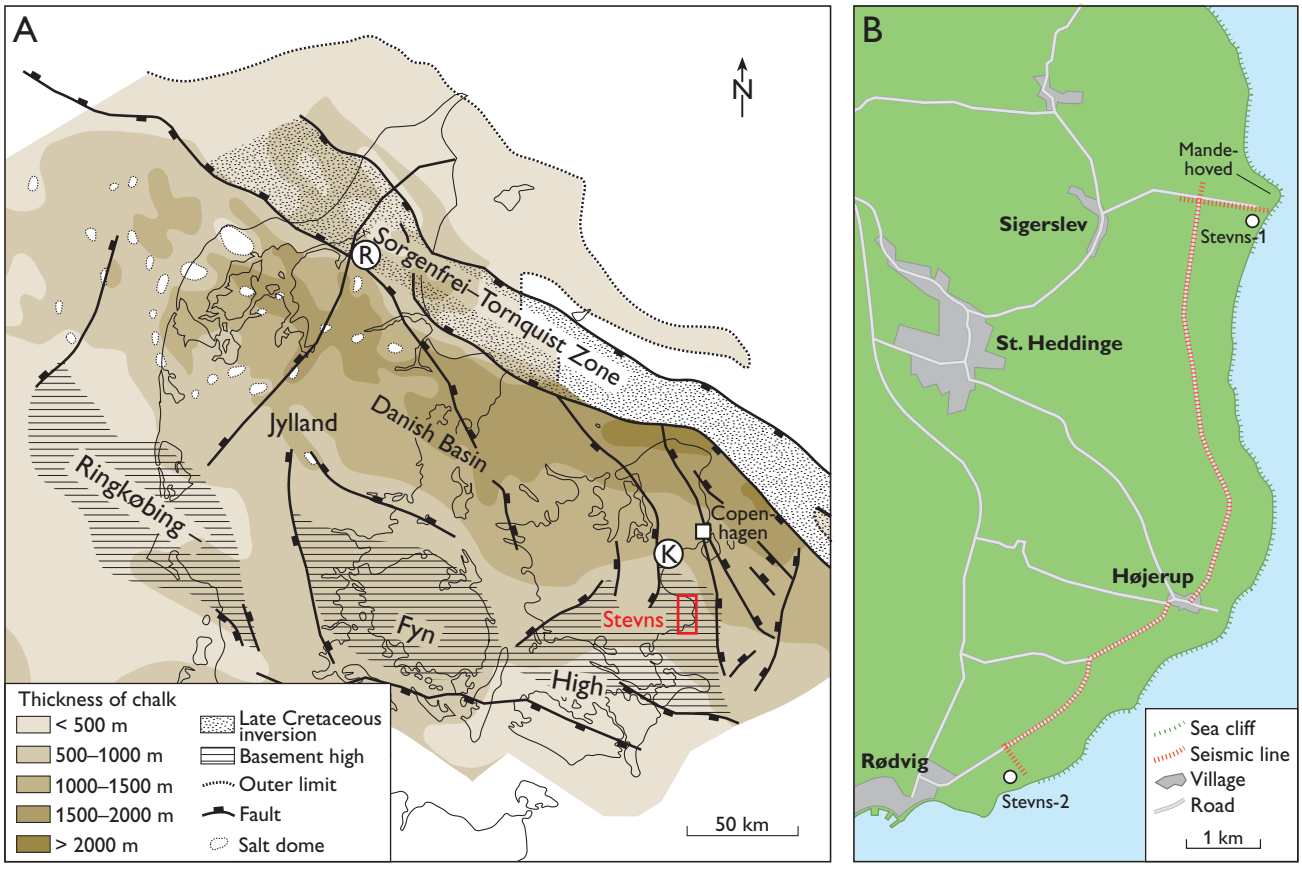

Fig. 1. **A**. Thickness of the Upper Cretaceous – Danian chalk in the Danish area. **R**: Rørdal quarry; **K**: Karlslunde-1 and Tune-1 boreholes. **B**. Map of the study area at Stevns showing the location of the Stevns-1 and Stevns-2 boreholes.

Fig. 2. The Fakse Kalk A/S Diamant Board 747 wireline rig at the site of Stevns-2 in the abandoned Boesdal quarry north-east of Rødvig.

paign at Stevns Klint, eastern Denmark (Fig. 1), where two shallow boreholes were drilled and logged from near the base of the Danian bryozoan limestone and down through the upper 350–450 m of the very thick Upper Cretaceous chalk section (Vejbæk *et al*. 2003). The cores represent the first complete sections through the Maastrichtian chalk of eastern Denmark.

Shallow core drilling

Seismic data from the offshore area immediately to the east of Stevns Klint indicate that chalk deposits in this area were modified by powerful, long-lasting bottom currents, and that the Late Cretaceous sea floor was continuously sculpted by contour-parallel bottom currents into systems of ridges and drifts, moats and valleys with amplitudes up to 150 m and widths of several kilometres (Lykke-Andersen & Surlyk 2004; Esmerode *et al*. in press). In order to investigate the lithological composition of this dynamic chalk system and to provide material for time series analysis, two shallow boreholes were drilled and cored along Stevns Klint from near the base of the Danian bryozoan limestone and 350–450 m down into the Upper Cretaceous chalk (Fig. 1). The northern borehole, Stevns-1 (DGU 218.1938) approximately 2 km east of Sigerslev was drilled near the culmination of the undulating K–T boundary surface, and is believed to penetrate a ridge succession (Fig. 1). The southern borehole, Stevns-2 (DGU 218.1945) north-east of Rødvig was drilled on a depression in the undulating K–T boundary surface, and was drilled to penetrate a valley-fill succession (Figs 1, 2).

A comprehensive logging program was subsequently carried out in the two boreholes including spectral gamma, density, sonic, induction, temperature, conductivity, porosity, magnetic susceptibility, resistivity and optic televiewer logs. Logging was carried out in open hole using standard methods.

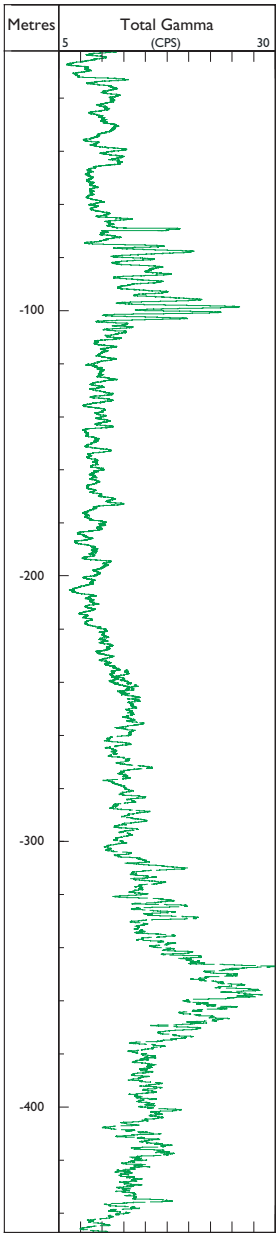

Fig. 3. Gamma-ray log of Stevns-1 showing the presence of two marl-rich intervals from *c*. 65–100 m and 345–370 m.

Stevns-1 was drilled to a depth of 456.1 m with 100% core recovery. It penetrated approximately 12 m of Danian bryozoan limestone before entering the Maastrichtian chalk succession. Preliminary nannofossil data (E. Sheldon, personal communication 2005) indicate that the Maastrichtian chalk is approximately 400 m thick and that the basal part of the drilled succession is of Late Campanian age. The drilled succession is roughly divided into an upper Campanian – lowermost Maastrichtian interval of bioturbated chalk with rare thin clay beds that gradually passes up into a 50 m thick succession of interbedded lower Maastrichtian chalk and marl. The gamma ray log indicates that marl layers become gradu-

ally less abundant upwards, and the interval from 300–100 m is composed of almost pure chalk (Fig. 3). The first flint nodules and layers appear at 135 m and flint is common in the upper part of the succession. The 100–70 m interval consists of flint-rich chalk with distinctive marly horizons while the uppermost part of the Maastrichtian succession shows an increasing content of bryozoans and other macrofossils.

Stevns-2 was drilled to a depth of 350 m with 100% core recovery. It penetrated 4 m of Danian limestone and approximately 300 m of Maastrichtian chalk before it terminated in upper Campanian chalk. The drilled succession shows the same overall changes in lithology as Stevns-1 but the thickness of the individual units seem to vary considerably. This is particularly true for the chalk-dominated succession between the two marly intervals which thins from approximately 200 m in Stevns-1 to 120–130 m in Stevns-2.

Core scanning

The 456.1 m long Stevns-1 core has been scanned at the GEUS core laboratory using a set-up which allows simultaneous spectral gamma-ray and density measurements (Fig. 4). The spectral gamma-ray analysis is carried out using two 15 cm NaI (Tl) crystals and the bulk density is determined using a caesium source. The scanning was performed using a speed of 1 cm/min., corresponding to a vertical resolution of approximately 2 cm for the density log. The scanning data thus supply high resolution data to support sedimentary and geochemical data from the core, as exemplified in Fig. 4 illustrating the cyclic nature of the succession. In this interval Uranium only shows minor variations and the high total gamma readings correspond to K- and Th-peaks. It is thus evident that these peaks correspond to marly beds with high levels of clay-bound K and Th whereas intervals with low total gamma readings correspond to purer chalk.

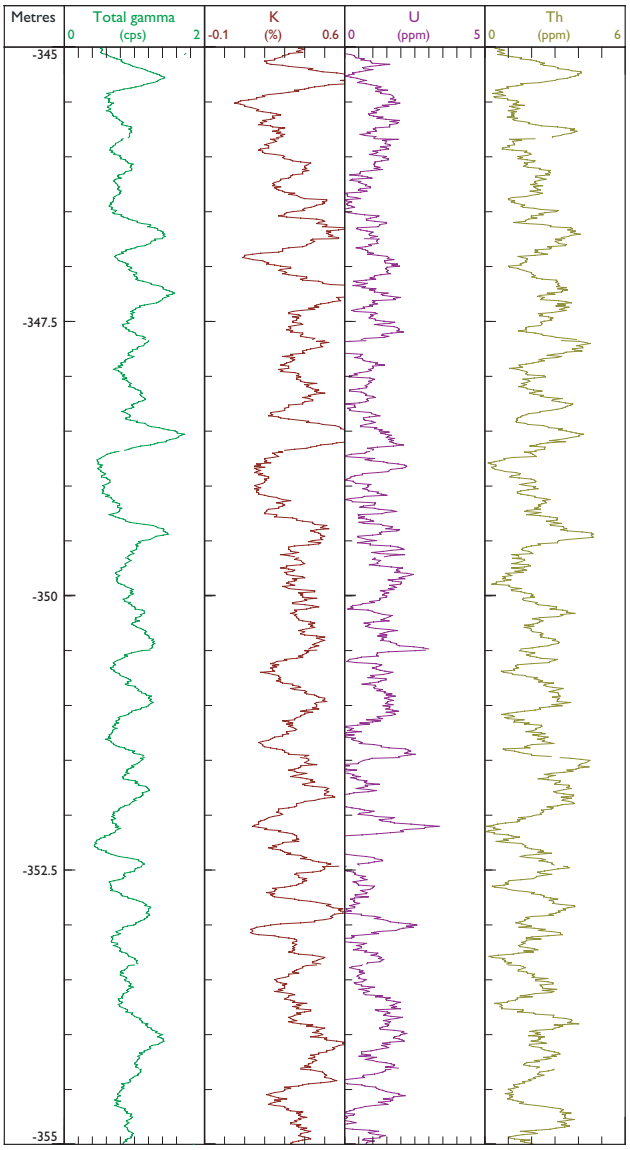

Fig. 4. Core scan log of the 345–355 m interval in Stevns-1 showing total gamma response and K, U and Th concentrations. Note that intervals with high total gamma correlate with high concentrations of K and Th, and correspond to marly beds.

Comparison with other Danish chalk sections

The Stevns-1 and Stevns-2 cores represent the first complete sections through the Maastrichtian chalk of eastern Denmark. The uppermost up to 35 m of the Maastrichtian are exposed along Stevns Klint and in quarries along the cliff. Further south, on the island of Møn, approximately 70 m of lower Maastrichtian chalk occur as glacially disturbed thrust sheets in excellent cliff exposures dominated by flint-rich bioturbated chalk with rare incipient hardgrounds; at Stevns Klint the youngest Maastrichtian deposits become gradually richer in bryozoans. The main difference between the cored section and the adjacent outcrops is the lack of flint in the deeper part of the core.

The Danian – uppermost Maastrichtian succession has been drilled by numerous water wells in the greater Copenhagen area to the north and north-west of Stevns Klint, and more recently the upper 250 m of the Maastrichtian chalk were cored in Tune-1 (DGU 207.3841) and Karlslunde-1 (DGU 207.3850; Fig. 1; Larsen *et al.* 2006). These two cores show a facies development similar to that seen in the upper part of the Stevns cores with a downward change from bryozoan-rich chalk to bioturbated chert-rich chalk interrupted in the mid-Maastrichtian by a succession of interbedded marl

and chalk layers before the core bottoms in mid-Maastrichtian chalk (Larsen *et al*. 2006). The most important difference is the presence of a distinctive 20 cm thick marl, interpreted as representing the Kjølby Gaard Marl of Troelsen (1937, 1955), 9–10 m below the K–T boundary in Tune-1. This marl has also been reported from adjacent water wells (Larsen 1997) and in quarries in northern Jylland (Troelsen 1955), and seems to be a distinctive stratigraphic marker bed in northern Denmark. The mid-Maastrichtian interval of interbedded chalk and marl drilled in Stevns-1, Stevns-2 and Karlstrup-1 also seems to represent a distinctive regional event as a similar cyclic chalk-marl succession is known from the Rørdal quarry in northern Jylland.

Future work

The Stevns cores represent the first continuous sections of the Maastrichtian chalk in NW Europe and provide a unique possibility for sedimentological, geochemical and isotope geochemical investigations as well as time series analysis and studies of reservoir properties. The Stevns area has been buried to less than 600–700 m during post-Danian time and the lack of burial diagenetic overprinting makes the carbonates ideal for isotope geochemical analyses to monitor both the global carbon cycle and to provide information on the temperature and salinity of the Late Cretaceous Boreal Ocean.

Core data will be integrated with log data to better understand the lithological significance of the log responses, and 2D depositional models of the chalk will be based on integration of core and log data with reflection seismic data along a line connecting the two boreholes. Reflection seismic data have been collected between the two boreholes in cooperation with Holger Lykke-Andersen, University of Aarhus, and refraction seismic data have been collected by Lars Nielsen, University of Copenhagen. The two data sets are still in the stage of processing but will provide important 2D data to support the information from the cores.

Acknowledgements

The Danish Natural Science Research Council is thanked for financial support. Additional funding for logging has been obtained from Geocenter Copenhagen. Fakse Kalk A/S and Rambøll A/S provided technical assistance. Stevns Kommune and Stevns Natur Center kindly allowed us to drill at their property.

References

Esmerode, E.V., Lykke-Andersen, H. & Surlyk, F. in press: Ridge and valley systems in the Upper Cretaceous chalk of the Danish Basin: contourites in an epeiric sea. Geological Society of London, Special Issue.

Klinkby, L., Kristensen, L., Nielsen, E.B., Zinck-Jørgensen, K. & Stemmerik, L. 2005: Geological characterisation of the Kraka Field chalk reservoir, Danish North Sea – integration of seismic and log data. Petroleum Geoscience **11**, 113–124.

Larsen, F., Sonnenborg, T.O., Madsen, P., Ulbak, K.A. & Klitten, K. 2006: Saltvandsgrænsen i kalkmagasinerne i Nordøstsjælland; Delrapport 6: Saltvandsudvaskning i Danienkalk og Skrivekridt – Detailundersøgelser i Karlslunde værkstedsområde. Danmarks og Grønlands Geologiske Undersøgelse Rapport **2006/21**, 103 pp.

Larsen, O. 1997: Mapping of the Maastrichtian–Danian boundary in the coastal area of Køge Bugt by gamma and resistivity logging. Bulletin of the Geological Society of Denmark **44**, 101–113.

Lykke-Andersen, H. & Surlyk, F. 2004: Topography of the Cretaceous-Palaeogene boundary at Stevns Klint, Denmark: Inversion tectonics or primary relief of the chalk sea-floor? Journal of the Geological Society (London) **161**, 343–352.

Surlyk, F. 1997: A cool-water carbonate ramp with bryozoan mounds: Late Cretaceous – Danian of the Danish Basin. In: James, N.P. & Clarke, J.A.D. (eds): Cool-water carbonates. SEPM (Society for Sedimentary Geology) Special Publication **56**, 293–307.

Surlyk, F., Dons, T., Clausen, C.K. & Higham, J. 2003: Upper Cretaceous. In: Evans, D., Graham, C., Armour, A. & Bathurst, P. (eds/coordinators): The Millennium Atlas: petroleum geology of the central and northern North Sea, 213–233. London: Geological Society.

Troelsen, J.C. 1937: Om den stratigrafiske inddeling af Skrivekridtet i Danmark. Meddelelser fra Dansk Geologisk Forening. Bulletin of the Geological Society of Denmark **9**, 260–263.

Troelsen, J.C. 1955: *Globotruncana* in the White Chalk of Denmark. Micropaleontology **1**, 76–82.

Vejbæk, O.V., Bidstrup, T., Britze, P., Erlstrøm, E., Rasmussen, E.S. & Sivhed, U. 2003: Chalk structure map of the central and eastern North Sea. Danmarks og Grønlands Geologiske Undersøgelse Rapport **2003/106**, 55 pp.

Authors' addresses

L.S., S.L.R., K.K. & N.S., *Geological Survey of Denmark and Greenland, Geocenter Copenhagen, Øster Voldgade 10, DK-1350 Copenhagen K, Denmark.*
E-mail: *ls@geus.dk*

F.S., *Geological Institute, University of Copenhagen, Geocenter Copenhagen, Øster Voldgade 10, DK-1350 Copenhagen K, Denmark.*

Spit-systems – an overlooked target in hydrocarbon exploration: the Holocene to Recent Skagen Odde, Denmark

Peter N. Johannessen and Lars Henrik Nielsen

Well-constrained depositional models are essential for successful exploration and field development. The Skagen spit-system offers a unique possibility for the establishment of a depositional model constrained by excellent outcrops, well-defined palaeogeography, good age control and detailed observations on hydrodynamics and morphology of the prograding part of the spit-system. The model offers a supplementary interpretation of shallow marine sandstones to the existing delta and linear shoreface models. The sand-dominated Skagen spit-system is *c.* 22 km long, 4 km wide and up to 35 m thick, with a sand volume of *c.* 2.2 km^3. If filled with oil, this system would contain 0.6 km^3 corresponding to 3.8 × 10^9 barrels assuming a porosity of 30% and an oil saturation of 90%. This is comparable in size with the largest Danish oil field (the Dan field), in the North Sea.

Reservoir models for isolated linear 'offshore' sandstone bodies have been controversial for many years. Their size and internal indications of palaeocurrent directions are similar to those of the spit-system model, and this model may therefore be applicable for some of these bodies.

Depositional model for the Skagen spit-system

The Skagen spit-system is part of the large triangular coastal complex termed Skagen Odde that forms the northern tip of Jylland (Fig. 1). The complex began to form at 7150 years BP, and the actual spit-system has developed within the past 5500 years (Fig. 1); (Nielsen & Johannessen 2001, 2004). The older parts of the spit-system have been raised *c.* 13 m above present-day sea-level as a result of the rate of glacial rebound has exceeded the rate of eustatic sea-level rise during the Holocene and can therefore be studied in cliff sections (Fig. 2). The distal youngest part of the spit-system is still prograding by several metres per year, and the depositional processes can be studied at the point of the spit (Fig. 3). Age relationships are well constrained by C^{14} dates of peat and shells along the 22 km long spit-system (Hauerbach 1992; Clemmensen *et al.* 2001). The possibility of direct comparison between geological sections in the older raised part of the spit and the Recent depositional processes at the point of the spit is unique, and provides a very high degree of certainty to the interpretation of the sedimentary units. The Skagen spit-

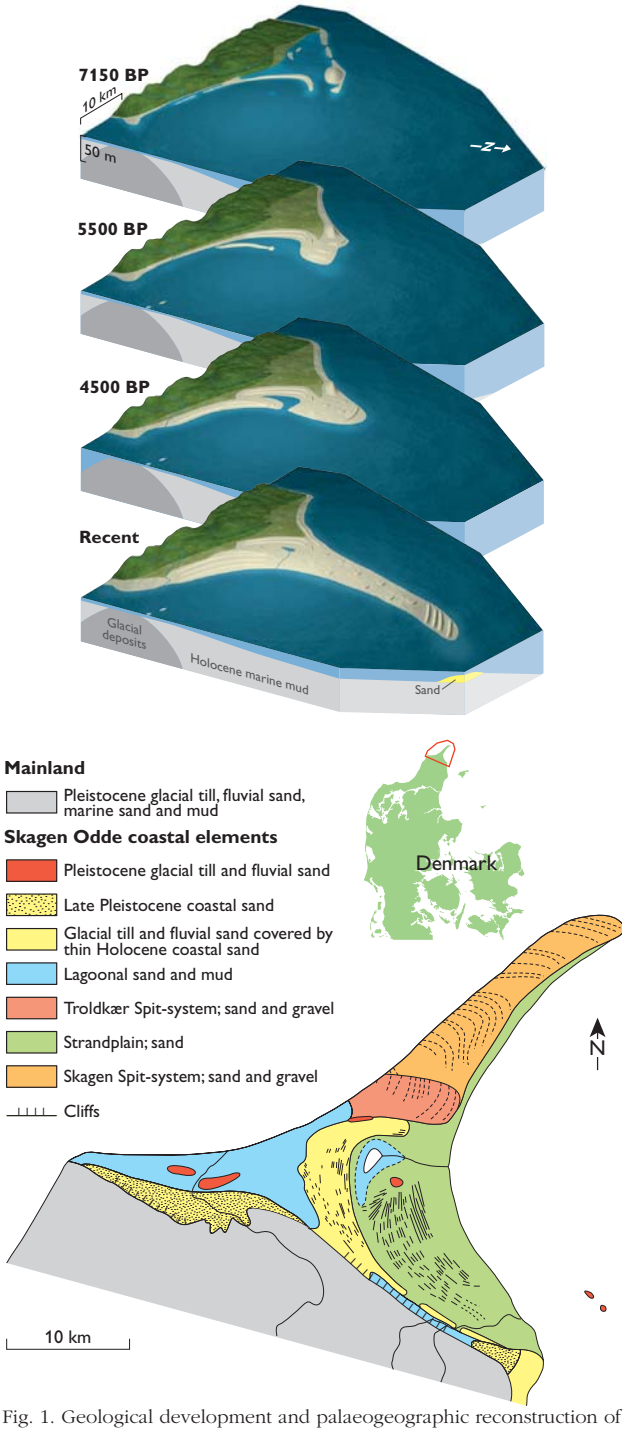

Fig. 1. Geological development and palaeogeographic reconstruction of the Skagen Odde coastal complex. The Skagen spit-system discussed here is shown in **orange** on the lowermost geomorphological map. The Skagen spit-system began to form *c.* 5500 years BP.

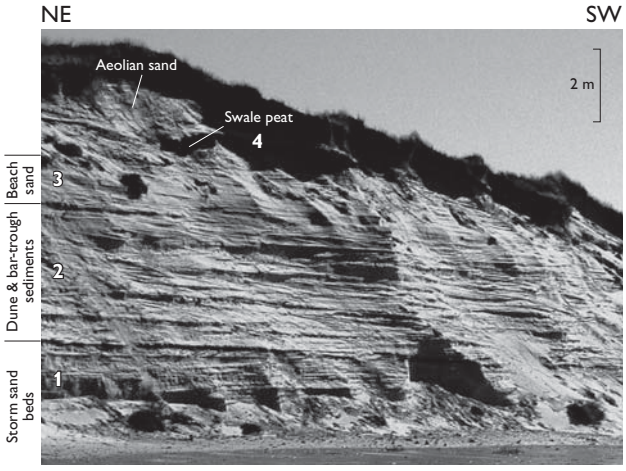

Fig. 2. Coastal cliff-section exposing the raised four depositional units of the Skagen spit-system shown in Fig. 3.

system may thus be regarded as a natural full-scale sedimentological laboratory.

The spit-system overlies offshore mud. It shows a weak coarsening-upward trend and consists of three sand-dominated units locally topped by peat. The lowest consists of up to 25 m of storm sand beds (unit 1), and is overlain by *c.* 5 m of dune and bar-trough sediments (unit 2), followed by *c.* 2 m of beach sand and 0–2 m aeolian sand (unit 3), topped by peat lenses up to 1.5 m thick (unit 4; Figs 2, 3). This spit-system succession is overlain by up to 10 m of Recent aeolian sand. In the constructive phases of the development of the spit-system, sand is transported from eroding glacial deposits more than 40 km south-west of the present tip of the spit,

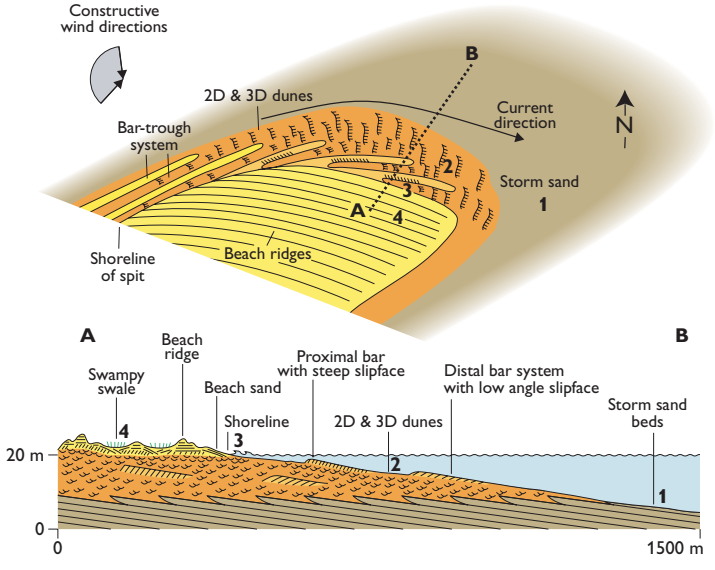

Fig. 3. Photographs of the four depositional units and the sites of their formation (1–4) on the active subaerial spit and the submarine spit-platform at the point of the spit-system (section **A**–**B**).

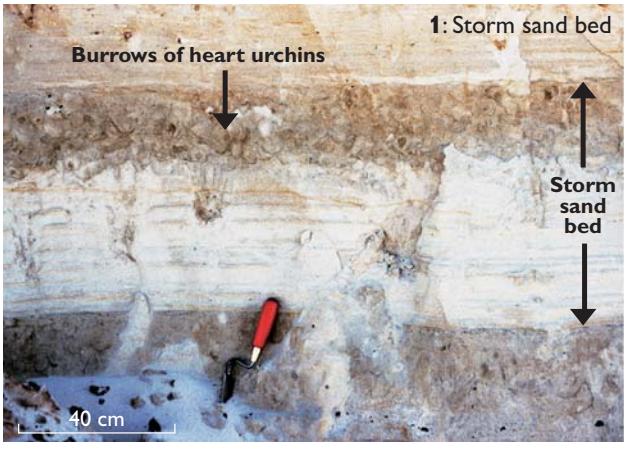

and from the older uplifted part of the spit-system. The preferential wind directions are from the south-west and west creating a strong shore-parallel northward flowing current capable of transporting large amounts of sand (up to *c.* 1.5 million m^3/year) along the coast. By far the greater part of the sediments are deposited in front of the spit point where storm sand beds are deposited from heavily loaded suspension currents in water depths of *c.* 7–30 m causing progradation (Fig. 3). Sandy 2D and 3D dunes migrate northwards along the spit coast, and pebbles are transported in the swash-backwash zone. Deposition occurs mainly where the spit coast bends and refraction of the waves results in reduction of the transport capacity. At the same time, the longshore currents expand over the area at the tip of the spit, as the controlling effect of the subaerial spit ceases and water depth increases. This combination causes high sedimentation rates on the platform at the tip of the spit. The majority of the dunes migrate obliquely basinwards on the gentle seaward dipping platform surface in front of the spit, leaving behind thick units of cross-bedded sand that is deposited in water depths of *c.* 0.3–9.5 m (Fig. 3). Occasionally, a shore-attached bar-trough system is formed in the surf zone along the front of the spit. Such bars migrate towards the coast, emerge and become swash bars with swash-backwash lamination forming on the seaward side. During severe storms from the north, pebbly beach ridges are formed on the backshore up to *c.* 1 m above average sea-level. Peat formation takes place in swales between beach ridges up to a few hundreds metres from the active spit coast. Aeolian dunes subsequently develop and migrate across the spit.

Spit-systems may be differentiated from other shallow marine sandstones by the presence of platform foresets (e.g. Nielsen *et al.* 1988), curved beach ridges showing pronounced lateral fining of grain-size, curved peat deposits, and palaeocurrent directions that differ from deltaic and linear shoreface sandstones (Fig. 3). For instance, the foresets of the 2D and 3D dune sands in unit 2 show nearly unimodal palaeocurrent directions obliquely to the accretionary spit coast and therefore show palaeocurrent directions at high angles to the long, exposed side of the spit-system (Figs 1, 3).

Preservation potential

The subaerial part and the upper marine part of the spit-system may be subject to erosion during transgression, and parts of the aeolian sand, peat lenses and beach sand may be eroded away and replaced by a thin transgressive sand. However, the remaining part of the spit-system has a high preservation potential and may be enveloped and sealed by offshore mudstones.

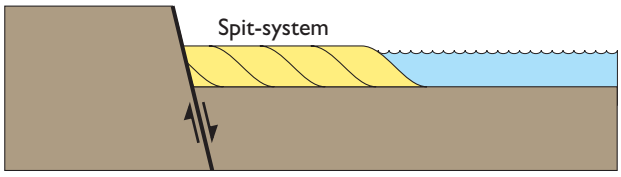

Fig. 4. Spit-system formation and preservation on a hanging-wall fault block.

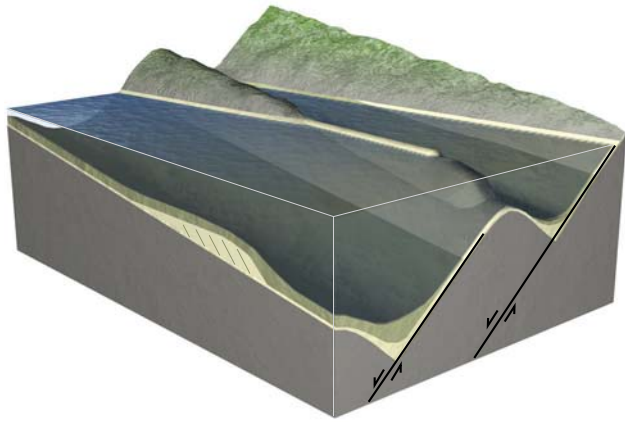

Fig. 5. Conceptual model of spit-systems attached to plunging fault block crests and prograding on the submarine part of the fault block crest.

Exploration and reservoir model for spit-systems

Headland-attached spit-systems

Linear coast and delta progradation systems depend on sediment input from rivers and distributary channels. Spit-systems, on the other hand, rely on wave erosion and longshore drift and may be found downdrift from a headland (as the Skagen spit-system) or a fault block partly submerged and exposed to waves. In the latter case spit-systems may form on a hanging-wall fault block down-drift from a footwall block (Fig. 4). The thickness of the spit-system succession depends on the water depth in which it progrades; the platform will be thick above topographic lows and thin over highs. Spit-systems have a tendency to prograde on top of elevated areas such as submarine ridges, because the progradation rate is greater at shallow water levels over the ridge than at deeper water depths on both sides of the ridge. Consequently, spit-systems preferentially prograde on the plunging crest of fault blocks. A potential reservoir is therefore situated on the elevated crests rather than lying in the deep parts of the hanging-wall blocks (Fig. 5).

Detached spit-systems – a model for offshore sand bars?

During progradation of a spit-system the headland and the proximal part of the spit may be eroded by wave activity and

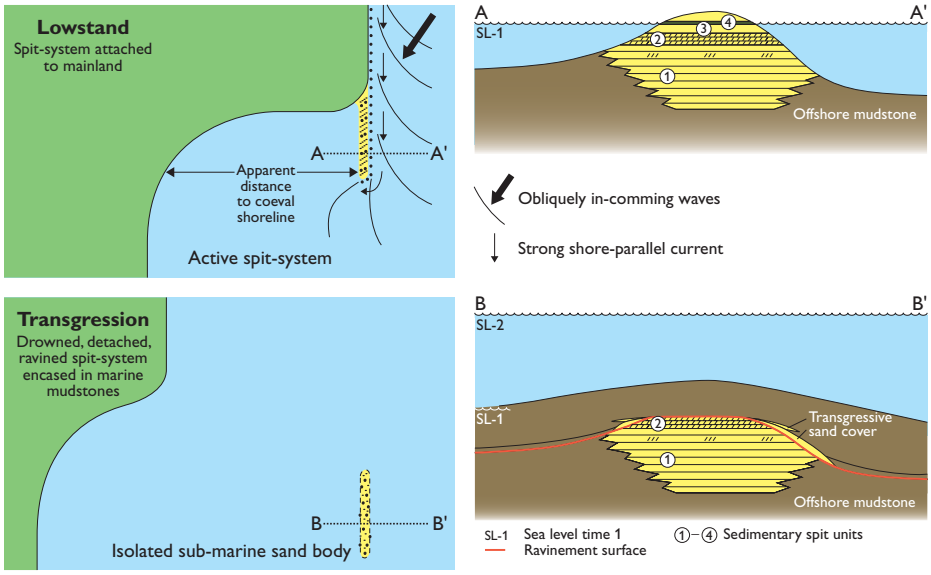

Fig. 6. Conceptual model of detached spit-systems. Isolated, elongated sandstone bars in the Western Interior Seaway (USA) may originally have been spit-systems prograding from a headland (**A–A'**). Later they became detached from the headland due to erosion of the headland and the proximal part of the spit-system. During subsequent transgression the headland became submerged and upper parts of the spit-system was eroded (**B–B'**) and the preserved sandstone bars may appear to have formed at great distance from the mainland.

longshore currents, and the spit-system may eventually be detached and become an isolated sand body (Fig. 6). The upper part of the sand body will be exposed to erosion, and only the lower part of the former spit-system may be preserved. Elongated, isolated sandstone bars (up to 35 km long, 2–4 km wide and 30 m thick) encased in offshore mudstones and apparently deposited some distance from land are common hydrocarbon exploration targets in the Western Interior Seaway of the USA (e.g. Suter & Clifton 1999). However, their genesis has been controversial for decades, and the reservoir models are poorly constrained. Some of these sandstone bodies contain unimodal cross-bedded units which indicate palaeocurrents at an acute angle to the length of the bars. Their size, facies and palaeocurrent directions are similar to those of the spit-system model.

Concluding remarks

The Middle and Upper Jurassic in the North Sea rift basins are characterised by heavily block-faulted areas subjected to transgressions. As extensive spit-systems can develop within a few thousand years under the right conditions, it is likely that spit-systems were locally formed on partly submerged, fault block crests and on hanging-wall fault blocks. Aspects of the Skagen spit-system model have been applied in the mapping of reservoirs in the Troll Field in the Norwegian North Sea (Dreyer *et al.* 2005).

Acknowledgements

Norsk Hydro and the Carlsberg Research Foundation (ans-0881/10) provided financial support to the studies of the Skagen spit-system.

References

Clemmensen, L.B., Richardt, N. & Andersen, C. 2001: Holocene sea-level variation and spit development: data from Skagen Odde, Denmark. The Holocene **11**, 323–331.

Dreyer, T., Whitaker, M., Dexter, J., Flesche, H. & Larsen, E. 2005: From spit systems to tide-dominated delta: integrated reservoir model of the Upper Jurassic Sognefjord Formation on the Troll West Field. In: Doré, A.G. & Vining, B. (eds): Petroleum geology: north-west Europe and global perspectives. Proceedings of the 6th Petroleum Geology Conference, 423–448. London: Geological Society.

Hauerbach, P. 1992: Skagen Odde – Skaw Spit. An area of land created between two seas. Folia Geographica Danica **20**, 119 pp.

Nielsen, L.H. & Johannessen, P.N. 2001: Accretionary, forced regressive shoreface sands of the Holocene–Recent Skagen Odde spit complex, Denmark – a possible analogue to fault-attached shoreface sandstone reservoirs. In: Martinsen, O. & Dreyer, T. (eds): Sedimentary environments offshore Norway – Palaeozoic to Recent. Norwegian Petroleum Society (NPF) Special Publications **10**, 457–472.

Nielsen, L.H. & Johannessen, P.N. 2004: Skagen Odde – et fuldskala, naturligt laboratorium. Geologi – Nyt fra GEUS **1**, 1–12.

Nielsen, L.H., Johannessen, P.N. & Surlyk, F. 1988: A Late Pleistocene coarse-grained spit-platform sequence in northern Jylland, Denmark. Sedimentology **35**, 915–937.

Suter, J.R. & Clifton, H.E. 1999: The Shannon Sandstone and isolated linear sand bodies: interpretations and realizations. In: Bergman, K.M. & Snedden, J.W. (eds): Isolated shallow marine sand bodies: sequence stratigraphic analysis and sedimentologic interpretation. SEPM (Society for Sedimentary Geology) Special Publication **64**, 321–356.

Author's address

Geological Survey of Denmark and Greenland (GEUS), Øster Voldgade 10, DK-1350 Copenhagen K, Denmark. E-mail: *pjo@geus.dk*

Construction of 3D geological models in glacial deposits to characterise migration of pollution

Knud E.S. Klint, Frants von Platen-Hallermund and Mette Christophersen

The National geological database at the Geological Survey of Denmark and Greenland (GEUS) is based on an extensive well database *Jupiter*, a geophysical database *Gerda* (Tulstrup 2003) and a recently established database for various types of geological models. These databases are integrated in a GIS system. The integration of this data enables new possibilities of constructing improved geological models. GIS systems offer a powerful tool for the geologist not only in combining multiple data, but also in visualising the model and hence presenting the final product in a simple and understandable way. 3D geological models will become increasingly important for the execution of improved cost-benefit analysis and risk assessment of contaminated sites, as well as strategic evaluation of groundwater and raw material resources in general. The possibility of storing such models on a public platform will be a major advance for future users of geological databases.

The primary goal of this paper is to demonstrate the potential of an integrated GIS system, with an example of how traditional geological information may be combined in new ways in order to improve the correlation of well data in multiple directions. The application is demonstrated for a highly contaminated industrial site in the town of Ringe, Denmark (Fig. 1).

Data analysis

Basically two methods exist for constructing 3D models from borehole data. Using the *vertical approach*, information from the nearest boreholes is projected onto an array of vertical sections (Fig. 2), thus guiding the drawing of lines separating the interpreted units. The boundaries separating the geological units from all cross-sections are then converted into a 3D surface through interpolation. Using the *horizontal approach*, information from all boreholes is projected onto an array of horizontal sections covering the relevant area (Fig. 3). The

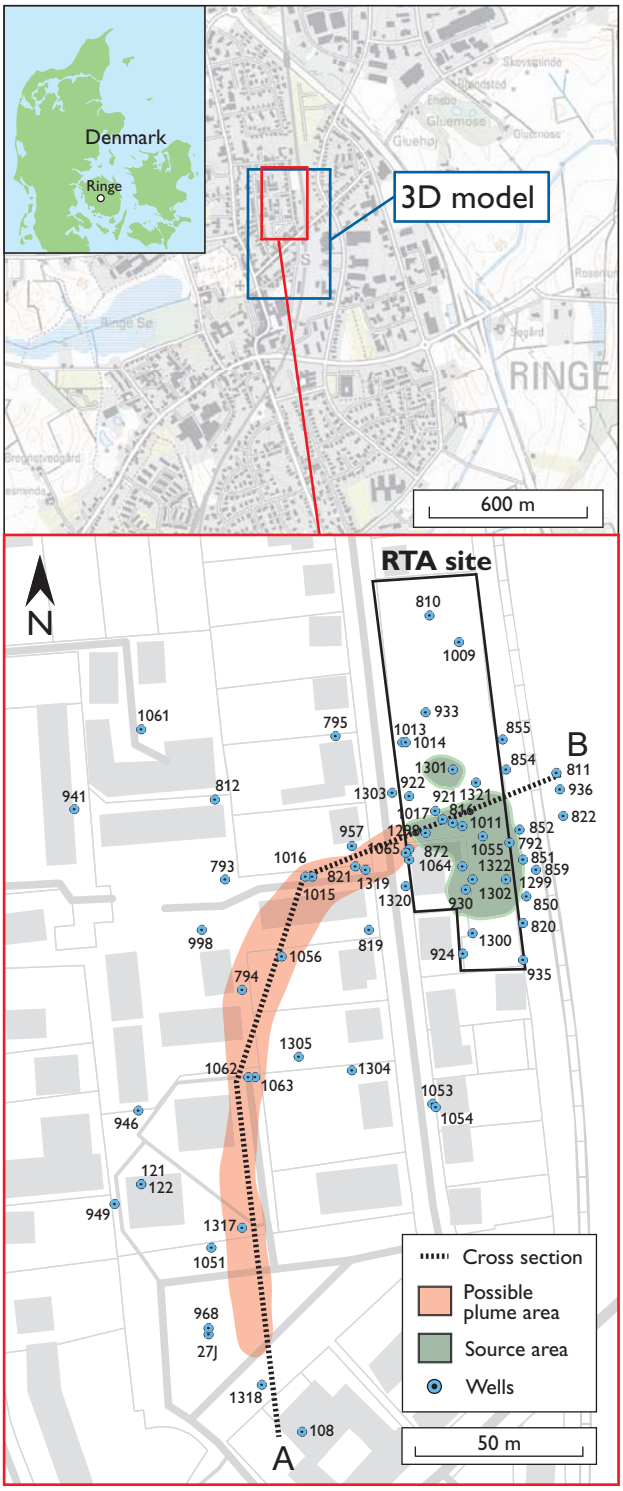

Fig. 1. Location of the former tar and asphalt factory in Ringe (RTA site) with the distribution of wells inside the source area and in a wider zone around the site. The site is situated on map sheet 155, and all well numbers have the prefix '155.' in the *Jupiter* well database. Vertical section **A–B** shown in Fig. 2; a horizontal slice diagram and 3D model are shown in Figs 3–4.

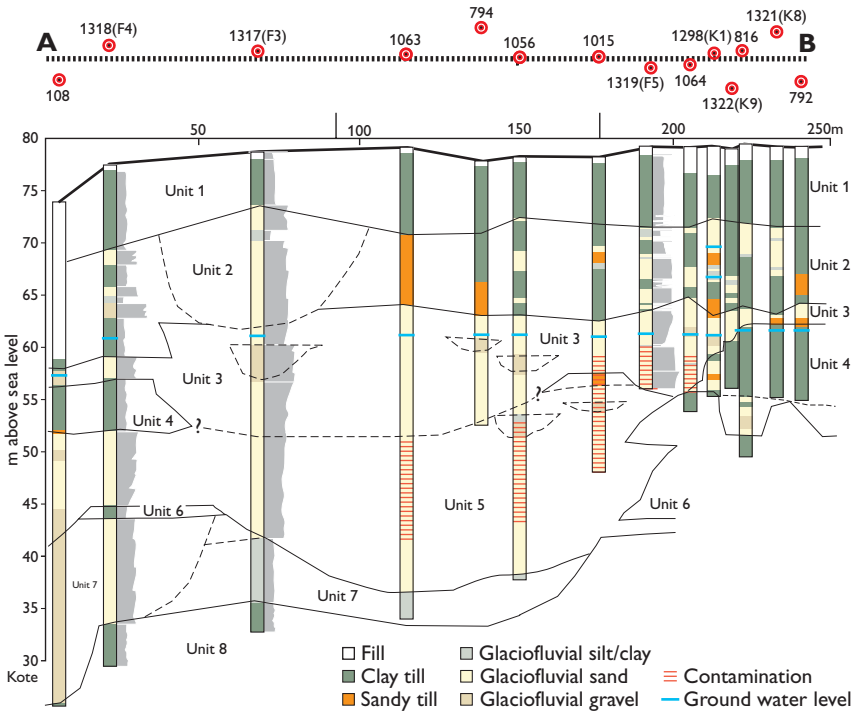

Fig. 2. Vertical correlation approach. Cross-section **A–B** (Fig. 1) showing the distribution of the eight primary geological units. Three new wells display grain size distributions in **grey shading**. All well numbers are prefixed '155.'.

distance between the sections is determined by the geological complexity. The lithological and hydraulic information from the boreholes penetrating the sections is used to guide drawing of unit boundaries at the relevant level. Finally, the 3D model is constructed by stacking all the horizontal sections (Fig. 4).

In this study both methods are used, but with emphasis on the horizontal sections because current knowledge of the glaciodynamic history and position of the local geological units are better utilised in this way. A general geomorphological analysis and thorough description of the depositional environment is included in the interpretation of the different geological units in the area (Klint & von Platen-Hallermund 2006). Database procedures for extracting borehole data from a series of horizons, as well as GIS procedures for producing a collection of maps based on borehole information or interpreted unit boundaries in the same intervals have been developed as a tool for the construction of improved geological models. The 3D display of the GIS system is used for viewing the final model.

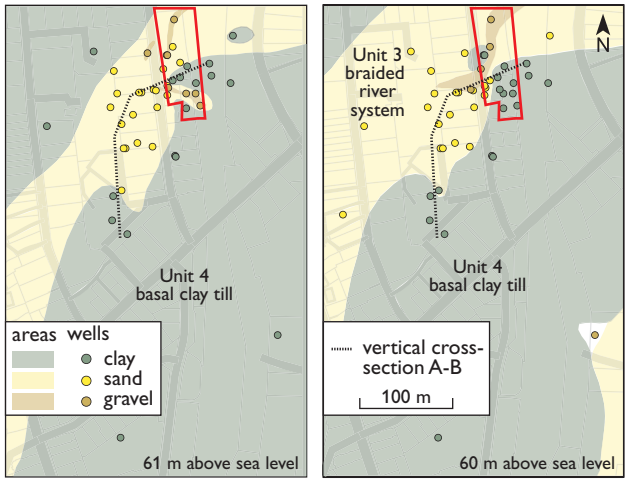

Fig. 3. Horizontal correlation approach. Slice diagram showing the distribution of clay, sand and gravel in wells at two depth intervals. **Red frame** indicates location of the Ringe tar and asphalt factory site. Position of section **A–B** in Fig. 2 is indicated.

Site history

The Ringe tar and asphalt factory site (RTA site) is located in the centre of Ringe (Fig. 1). Asphalt and creosote production took place from 1929 to 1962, and during that period storage tanks were placed all over the area. In 1987 it was discovered that the factory site subsurface was strongly contaminated with creosote, and in 1988 remediation of the site was commenced. Old buildings and storage tanks were removed and some of the most heavily contaminated soil was excavated and removed. The site has been used extensively for contamination investigations for several years (e.g. Broholm *et al.* 2000; Klint & Tsakiroglou 2000). A large number of wells have been drilled during these projects, and four open pits were excavated.

Geological framework

The Ringe tar and asphalt factory site is situated on top of an elongated hill approximately 80 m above sea level. Several small hills and depressions without runoff indicate that the sediments in the hilly area were probably deposited from a stagnating glacier (dead-ice relief) and overridden during a later ice advance. During the earlier research projects a local geological model was established for the upper 22 m of the Ringe site (Sidle *et al.* 1998, Nilsson *et al.* 2001). The investigations showed that the site is dominated by sediments deposited during the Late Weichselian Glaciation 25 000 – 11 500 years ago. During 2005 nine wells were drilled in the source area to *c.* 20 m below ground surface, and five deep wells were drilled downstream for locating the contamination plume (Fig. 2). The wells were described in terms of matrix texture, structures, colour, fractures, consolidation and contamination. Hydraulic tests and groundwater table measurements in both secondary and primary aquifers supported the interpretation of the depositional environment. The conceptual geological model is well constrained near the surface, but becomes more speculative at greater depth due to the decreasing amount of well data. The eight geological units described below were deduced from the cross-sections and log descriptions (Fig. 2), and slice diagrams produced with a 1 m interval from 26 to 80 m above sea level (Fig 3). Finally, a 3D geological model was constructed to outline the spatial distribution of the geological units (Fig. 4).

Unit 1 is basal till. The upper 4–8 m are dominated by a continuous, massive, undulating ground moraine with occasional minor sand lenses which covers most of the area. This till may be classified as a basal till deposited below a glacier that transgressed the area from the east-south-east during the *c.* 16 kyr Young Baltic Ice advance (Nilsson *et al.* 2001; Houmark-Nielsen & Kjær 2003). The till is penetrated by fractures, and there is generally good hydraulic contact to the underlying beds through the fracture network and embedded sand lenses.

Unit 2 comprises mixed fluvial and diamict deposits. From 4–16 m below the ground surface, a heterogeneous glacial complex dominated by glaciofluvial silty, sandy and gravelly deposits is interbedded with clayey and sandy diamict sediments. The sediments are partly deformed by glaciotectonic processes, and isolated sand lenses form small secondary water reservoirs especially in the central part of the RTA site, at *c.* 8–9 m below ground surface. Other lenses are unsaturated and hence in hydraulic contact with the primary aquifer. Approximately 12 m below ground surface a more widespread, 3–4 m thick layer of unconsolidated clayey till covers most of the area, though it may be mixed with larger sand bodies in places. The till is fractured locally and contains numerous thin sand lenses. It is classified predominantly as flow till. The general topography in the area includes several small depressions with the characteristics of dead-ice holes, and the whole unit is interpreted to represent a dead-ice landscape overridden by a glacier.

Unit 3 consists of braided river valley deposits. Between 14–21 m depth a widespread sand/gravel layer 2–7 m thick covers most of the area and probably represents a braided river system with minor channels eroded into an underlying ground moraine. The channels are generally dominated by coarse glaciofluvial sand/gravel and boulders. Unit 3 truncates the underlying clay till (Unit 4) locally, thus creating a good hydraulic contact with a major sandy aquifer below, which dominates the western and northern parts of the site (Unit 5). Unit 3 is partly saturated, as the water table is here located approximately 18 m below ground surface. Accordingly, the deepest, saturated parts of the channels act as hydraulic avenues for infiltration of groundwater and contaminants from the upper units. The general groundwater and contamination flow is directed towards the west-south-west at the RTA site, but turns southwards approximately 30 m west of the site, thus indicating preferential flow controlled by channels (Fig. 1).

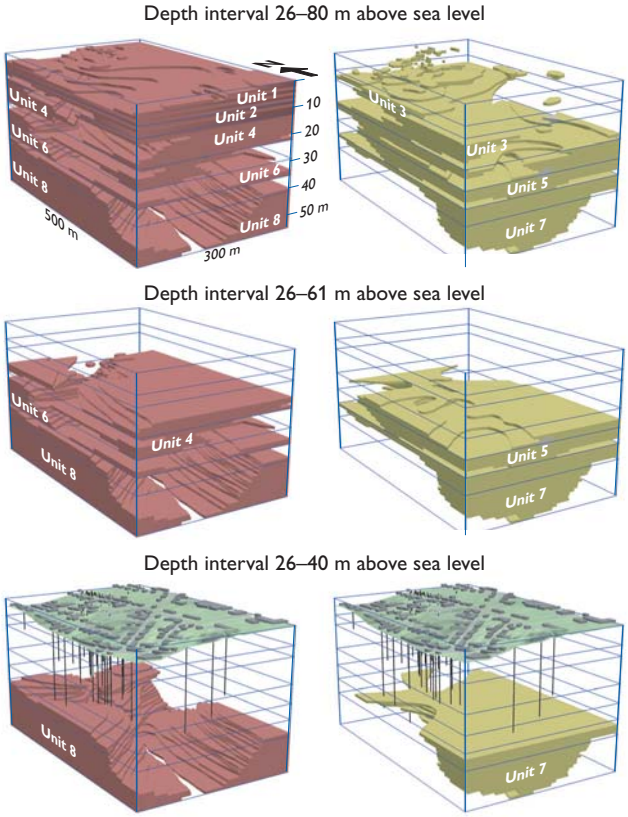

Fig. 4. 3D geological model of the Ringe site showing the distribution of clayey deposits (**left**) and sandy deposits (**right**) at different depth intervals (note vertical exaggeration). Ground surface with buildings and position of wells shown in lower model.

Unit 4 is basal till. A massive basal till 4–8 m thick covers most of the south-eastern area 17–22 m below ground surface. Its surface is situated above groundwater level in some areas. It is completely eroded by Unit 3 just west of the RTA site, where Unit 3 is resting directly on Unit 5 (Fig. 3).

Unit 5 consists of sandy and silty melt-water river deposits. Unit 5 constitutes a more widely distributed occurrence of glaciofluvial sand, occurring between 24–45 m depth, with a generally finer grain size than Unit 3. The sand becomes very fine in the lowest parts, and is dominated by glaciofluvial silt and clay below 37–40 m depth. Unit 5 is deeply incised into the underlying units, and is thought to represent a well-defined river valley filled with generally finer material than Unit 3. The contaminant plume seems to follow this unit in a narrow south-directed fan.

Unit 6 is clay till. A thin clay till unit locally separates the two sandy units 5 and 7 (Fig 4). This unit probably represents erosional remnants of a previously more widespread clay till unit located 33–36 m below ground surface. The lithological and structural information is, however, sparse and any interpretation of its origin is therefore highly speculative.

Unit 7 comprises river valley deposits. At least 14 m of sand and gravel have been encountered in wells 155.108 and 155.1318 between 35–49 m below ground surface (Fig. 2). The water-supply well 155.108 has produced 45 m3 of water per hour and is considered to be located within an extensive sand/gravel body representing a major buried river valley incised in the clay till of Unit 8. Well 155.1318 has much smaller capacity and hence must be related to a somehow smaller sand reservoir although hydraulically connected to 155.108.

Unit 8 is basal till. Generally little information exists on the lowest clay till unit below 40 m depth. The till is generally massive and well consolidated, with a medium to high content of boulders. It has the nature and appearance of a basal till and is locally more than 10 m thick. Only six wells reach this unit, and its distribution is consequently largely unknown.

Conclusions

The combination of correlating multiple geological horizontal sections with traditional vertical geological cross-sections using GIS has facilitated the construction of a detailed 3D geological model of the contaminated tar and asphalt factory site in Ringe, which outlines the spatial distribution of primarily sandy and clayey sediments. Detailed descriptions of the sediment properties were used to interpret the depositional processes and hence the depositional environment. This interpretation was included in the separation of the different deposits into units related to distinct glacial environments. The model will be used for assessing the risk of polluting nearby groundwater reservoirs and for designing an optimal remediation programme.

Acknowledgements

The work was financed by Fyns Amt and carried out in cooperation with Orbicon.

References

Broholm, M.M., Rügge, K., Tuxen, N., Mosbæk, H. & Bjerg, P.L. 2000: Migration and degradation of pesticides in an aerobic groundwater aquifer: field injection experiments. In: Bjerg, P.L., Engesgaard, P. & Krom, T.D. (eds): Proceedings of the International Conference on Groundwater Research, Copenhagen, Denmark, 6–8 June, 2000, 169–170. Rotterdam: Balkema.

Houmark-Nielsen, M. & Kjær, K.H. 2003: Southwest Scandinavia, 40–15 kyr BP: palaeogeography and environmental changes. Journal of Quaternary Science **18**, 765–786.

Klint, K.E.S. & Tsakiroglou, C.D. 2000: A new method of fracture aperture characterisation. In: Tsihrintzis, V.A. *et al*. (eds): Proceedings of the 5th International Conference on Restoration and Protection of the Environment 1, Thassos, Greece, 3–6 July, 2000, 127–136.

Klint, K.E.S. & von Platen-Hallermund, F. 2006: Geologisk model af RTA-grunden ved Villavej i Ringe. En 3-D geologisk model af kildeområde og faneområde ved den tidligere Ringe Tjære Asfalt fabrik på Villavej i Ringe. Danmarks og Grønlands Geologiske Undersøgelse Rapport **2006/9**, 18 pp.

Nilsson, B., Sidle, R.C., Klint, K.E.S., Bøggild, C.E. & Broholm, K. 2001: Mass transport and scale-dependent hydraulic tests in a heterogeneous glacial till – sandy aquifer system. Journal of Hydrology **243**, 162–179.

Sidle, R.C., Nilsson, B., Hansen, M. & Fredericia, J. 1998: Spatially varying hydraulic and solute transport characteristics of a fractured till determined by field tracer tests, Funen, Denmark. Water Resources Research **34**, 2515–2527.

Tulstrup, J. 2003: Environmental data and the Internet: openness and digital data management. Geological Survey of Denmark and Greenland Bulletin **4**, 45–48.

Authors' addresses

K.E.S.K. & F.v.P.-H., *Geological Survey of Denmark and Greenland, Øster Voldgade 10, DK-1350 Copenhagen K, Denmark,* E-mail: *kesk@geus.dk*

M.C., *Fyns Amt, Ørbækvej 100, DK-5220 Odense SØ, Denmark.*

Advanced *in situ* geochronological and trace element microanalysis by laser ablation techniques

Dirk Frei, Julie A. Hollis, Axel Gerdes, Dan Harlov, Christine Karlsson, Paulina Vasquez, Gerhard Franz, Leif Johansson and Christian Knudsen

Laser ablation inductively coupled plasma mass spectrometry (LA-ICP-MS) was developed in 1985 and the first commercial laser ablation systems were introduced in the mid 1990s. Since then, LA-ICP-MS has become an important analytical tool in the earth sciences. Initially, the main interest for geologists was in its ability to quantitatively determine the contents of a wide range of elements in many minerals at very low concentrations (a few ppm and below) with relatively high spatial resolution (spot diameters of typically 30–100 µm). The potential of LA-ICP-MS for rapid *in situ* U–Th–Pb geochronology was already realised in the early to mid 1990s. However, the full potential of LA-ICP-MS as the low-cost alternative to ion-microprobe techniques for highly precise and accurate *in situ* U–Th–Pb age dating was not realised until the relatively recent advances in laser technologies and the introduction of magnetic sectorfield ICP-MS (SF-ICP-MS) instruments. In March 2005, the Geological Survey of Denmark and Greenland (GEUS) commissioned a new laser ablation magnetic sectorfield inductively coupled plasma mass spectrometry (LA-SF-ICP-MS) facility employing a ThermoFinnigan Element2 high resolution magnetic sectorfield ICP-MS and a Merchantek New Wave 213 nm UV laser ablation system. The new GEUS LA-SF-ICP-MS facility is widely used on Survey research projects in Denmark and Greenland, as well as in collaborative research and contract projects conducted with partners from academia and industry worldwide. Here, we present examples from some of the these ongoing studies that highlight the application of the new facility for advanced geochronological and trace element *in situ* microanalysis of geomaterials. The application of LA-SF-ICP-MS based *in situ* zircon geochronology to regional studies addressing the Archaean geology of southern West Greenland is presented by Hollis *et al.* (2006, this volume).

Zircon U–Pb geochronology using LA-SF-ICP-MS

In situ U–Th–Pb geochronology was developed in the mid-80s with the introduction of ion-microprobe techniques, most commonly referred to as secondary ion mass spectrometry (SIMS) and sensitive high resolution ion microprobe (SHRIMP). The advantage of *in situ* U–Th–Pb geochronology over conventional chemical dating by isotope dilution thermal ionisation mass spectrometry (ID-TIMS) is the capability to analyse different domains in heterogeneous single zircons with high spatial resolution (spot diameters of typically 10–30 µm). This allows resolution of igneous and metamorphic events separated by intervals of only a few tens of million years from polychronic zircons. The disadvantages of ion-microprobe techniques are the very high purchasing and operating costs for the instrument. The rapid improvements in laser based U–Th–Pb geochronology makes it now possible to obtain *in situ* U–Th–Pb geochronological data with comparable spatial resolution as well as analytical precision and accuracy at only a fraction of the costs of ion-microprobe techniques (e.g. Jackson *et al.* 2004; Janoušek *et al.* 2006).

Dating of magmatic and metamorphic events

The capabilities of LA-SF-ICP-MS for the precise and accurate U–Pb age dating of relatively young igneous zircons are demonstrated by the analysis of a population of 40 zircons extracted from a gabbro from the Coastal Cordillera at Tregualemu, central Southern Chile. The gabbro is believed to have been formed by regional extension during the late Triassic to early Jurassic (Charrier 1979). Three zircons proved to be too small for analysis (< 30 µm). The results for the remaining 37 zircons (Fig. 1) define a highly precise igneous concordia age of 203 ± 2 Ma (2σ; MSWD = 1.7) and indicate a Late Triassic (Rhaetian) intrusion age of the gabbro. An even

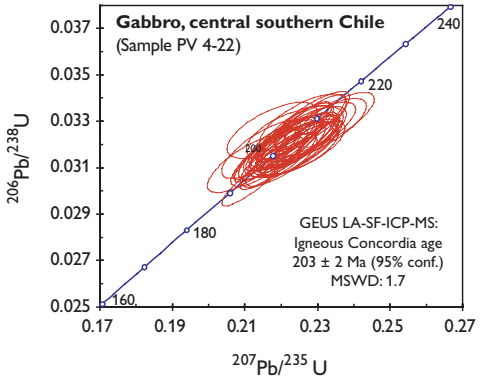

Fig. 1. Concordia diagram for igneous zircons from a gabbro from the Coastal Cordillera in central Southern Chile.

younger igneous age of 158 ± 2 Ma was recently obtained for a zircon xeno- or phenocryst derived from a newly discovered carbonatite in southern West Greenland (Steenfelt *et al.* 2006, this volume).

The high sensitivity of the Element2 SF-ICP-MS allows U–Pb zircon age dating with a laser spotsize of 30 µm or less, depending on the Pb content of the zircons. This makes it feasible to analyse different age domains in polychronic zircons, e.g. igneous cores and metamorphic rims. For example, zircons from an orthogneiss from the Nuuk region, southern West Greenland, display characteristic textures in back-scattered electron (BSE) and cathodoluminescence (CL) pictures that are interpreted as igneous cores surrounded by rims grown during a metamorphic event (see inset in Fig. 2). The U–Pb age data of the cores suggest an emplacement of the igneous protolith at *c.* 3660 Ma, while the rim data indicate metamorphism close to 2700 Ma (Fig. 2).

Dating of detrital zircons

Analyses of the crystallisation ages of detrital zircons in clastic sediments are a powerful tool in sedimentary provenance analysis. Accurate and precise U–Pb ages of >100 detrital zircon grains in a sample are needed to detect all major sedimentary source components with statistical confidence (cf. Vermeesch 2004; and references therein). The relatively high costs and the limited capacities of ion microprobe techniques (*c.* 75 zircon age analyses per day) impose restrictions on the number of samples that can be studied. Because LA-SF-ICP-MS provides very high capacities (in excess of 300 zircon age analyses per day) without compromising accuracy and precision, it constitutes the economic method of choice for provenance studies based on detrital zircon U–Pb ages.

An example for detrital zircon age data obtained by LA-SF-ICP-MS is shown in Fig. 3, where the ^{207}Pb–^{206}Pb age distribution for a population of 100 zircon grains separated from a Cambrian sandstone from Torekov, southern Sweden, are shown in a combined histogram and probability density distribution (PPD) diagram. The concordance filtered zircons (dark shaded area; 90–110% concordance, defined as 100* [^{206}Pb–^{238}U age / ^{207}Pb–^{206}Pb age]) show a polymodal age distribution with a minor peak at ~1000 Ma and two major peaks at *c.* 1150 Ma and 1650 Ma. The presence of two older sedimentary sources (*c.* 2150 Ma and *c.* 3050 Ma) is indicated by discordant grains (lighter shaded grey areas) that most likely suffered lead loss during their petrogenetic evolution.

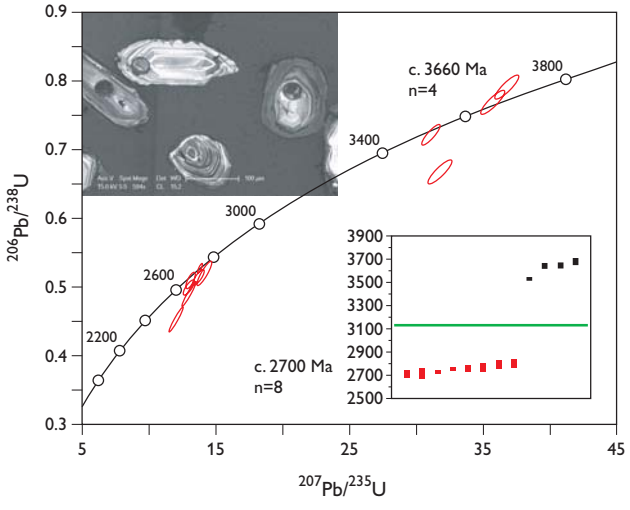

Fig. 2. Concordia diagram and inset of $^{207}Pb/^{206}Pb$ age plot for polychronic zircons from an orthogneiss in the Nuuk region, southern West Greenland. **Inset** CL image shows laser ablation pits (pit diameter = 30 µm) in igneous cores and metamorphic rims of polychronic zircons. Note the shallow depth (usually < 20 µm) of the laser ablation pits.

Figures of merit

The short and long term precision and accuracy of LA-SF-ICP-MS for U–Pb zircon age dating has been assessed using two zircon reference materials, Plesovice (with an ID-TIMS age of 338 ± 1 Ma; Aftalion *et al.* 1989; provided by Jan Kosler, University of Bergen) and 91500 (ID-TIMS age = 1065 ± 0.4 Ma; Wiedenbeck *et al.* 1995). The PL zircon is routinely analysed as unknown for quality control purposes in every analytical session in the GEUS laboratory. The results for 16 analyses of the zircon from a typical single analytical session are shown in Fig. 4A. They define a concordia age that is in excellent agreement with the ID-TIMS age reported by Aftalion *et al.* (1989). Long-term precision (2σ) based on 109 analyses of the Plesovice zircon by two different operators was 2%, 2.3% and 1.1% for the $^{206}Pb/^{238}U$, $^{207}Pb/^{235}U$ and $^{207}Pb/^{206}Pb$ ratios, respectively. The widely used 91500 zircon has so far only been analysed during one analytical session. The results for all seven analyses carried out

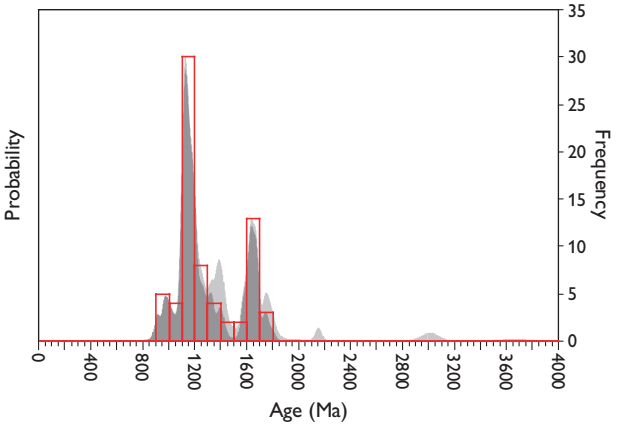

Fig. 3. Combined display of histogram and probability density distribution (PPD) diagram for zircons from a Cambrian sandstone from Torekov, south-western Sweden. See text for explanations.

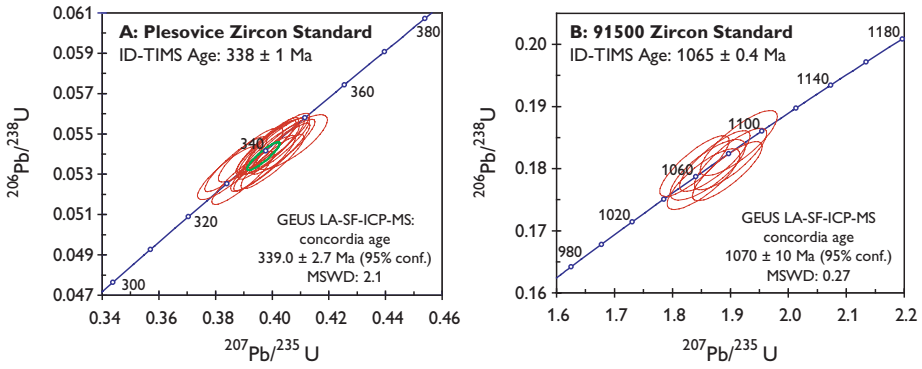

Fig. 4. Concordia diagrams for 16 analysis of the Plesovice zircon reference material obtained during a single analytical session (**A**); and 7 analysis of the 91500 zircon reference material obtained during a single analytical session (**B**).

during this session (Fig. 4B) define a concordia age which is in excellent agreement with the ID-TIMS age reported by Wiedenbeck *et al.* (1995).

Trace element analysis using LA-SF-ICP-MS

Due mainly to the introduction of LA-ICP-MS techniques, the trace element signatures of individual minerals (e.g. garnet, clinopyroxene, epidote, rutile, calcite) are now frequently being used to deduce the petrogenetic evolution of magmatic rocks, unravel water–rock interactions, identify geotectonic settings and sediment sources, track down the pathways of potentially health-damaging pollutants, and to unravel the change of seasurface and atmospheric temperatures. Furthermore, LA-ICP-MS is an important tool for the characterisation of synthetically produced geomaterials.

Water–rock interaction

Fluid-mediated mass transfer during metamorphism and metasomatism is a hotly debated issue. Mobility of geochemically important trace elements during fluid flow has far-reaching implications for e.g. ore-forming processes and mass transfer during subduction. Detailed investigation of the mechanisms of element mobility during fluid–rock interaction on a grain-scale are pivotal for an understanding of the processes that lead to the characteristic element enrichments and depletions observed in nature.

In the Söndrum stone quarry in Sweden, a localised dehydration zone of 2.5 to 3 m width occurs in garnet-bearing granitic gneiss around an approximately 1 m wide pegmatoid dyke. Whole-rock chemistry suggests that the solid-state dehydration of the granitic gneiss to charnokite via low H_2O activity fluids consisting principally of CO_2 and a minor brine component was predominantly isochemical (Harlov *et al.* 2006). Exceptions include Y and the heavy rare earth elements (HREE), which are markedly depleted throughout the dehydration zone. In order to assess the mechanism of Y and HREE depletion, the trace element geochemistry of garnet was studied in a traverse across the dehydration zone. Garnets from the pristine, unaltered granitic gneiss are characterised by a strong negative Eu-anomaly and the steep, HREE enriched pattern typical for garnet (sample SD45-600 in Fig. 5). In contrast, garnets from within the dehydration zone show a less pronounced Eu-anomaly and are characterised by dramatic Y and HREE depletions, leading to almost flat REE pattern (sample SD9-120 in Fig. 5). This observation provides direct evidence for massive release of Y and HREE from garnets, the principal hosts of these elements in the granitic gneiss, via solid-state fluid–rock interaction which was also accompanied by dehydration of hornblende and biotite to ortho- and clinopyroxene.

Analysis of synthetic geomaterials

Another application of LA-ICP-MS is the trace element analysis of synthetic geomaterials, e.g. products of experiments carried out for petrogenetical purposes. Since the experimentally produced mineral phases are usually very small, *in situ* microanalysis with high spatial resolution is needed. This was traditionally achieved by SIMS techniques. Because LA-ICP-MS analyses are much cheaper and facilities are much

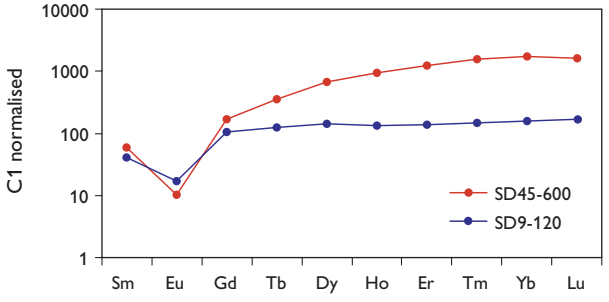

Fig. 5. Average chondrite-normalised REE-pattern of garnets from the unaffected granitic gneiss (SD45-600) and the dehydration zone (SD9-120). Note the depletion in HREE of garnets from the dehydration zone.

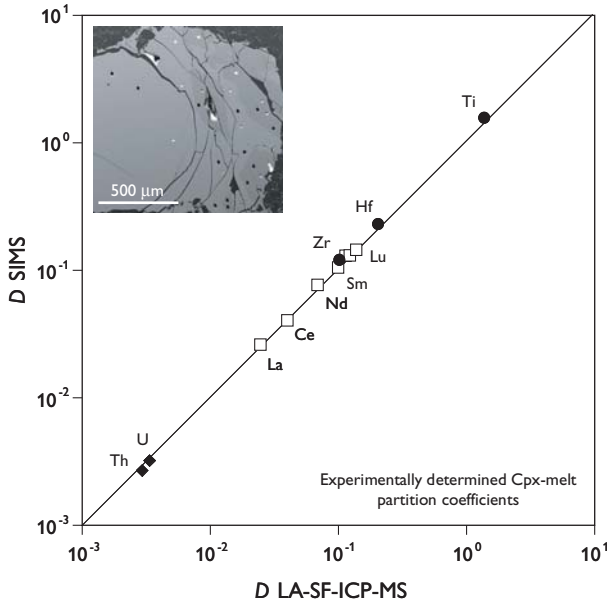

Fig. 6. Comparison of clinopyroxene-melt trace element partition coefficients (**open symbols**: REE; **solid symbols**: HFSE) determined from synthetic run products by SIMS and LA-SF-ICP-MS. **Inset** shows a BSE photomicrograph of synthetic, euhedral clinopyroxene coexisting with a glassy melt produced experimentally at high pressure and temperature. Shallow, bright spots are SIMS ablation pits (*c.* 20 µm diameter), while deeper, dark spots are laser ablation pits (*c.* 30 µm in diameter).

more widely available, LA-ICP-MS is increasingly used for the trace element analysis of synthetic geomaterials.

The inset in Fig. 6, for example, shows a back-scattered electron photomicrograph of an experimental charge containing euhedral clinopyroxene and a coexisting anhydrous silicate melt. The experimental charge was synthesised in order to determine the clinopyroxene-melt trace element partition coefficients D_i (defined as D_i = [concentration of i]$_{cpx}$/[concentration of i]$_{melt}$), knowledge of which is important for geochemical melt modelling purposes (Landwehr *et al.* 2001). In order to test the ability of laser ablation techniques to correctly determine partition coefficients from such experimental charges, we have analysed clinopyroxenes and coexisting silicate melts from a number of experiments with both SIMS (at the NERC ion-microprobe facility in Edinburgh) and LA-SF-ICP-MS (at GEUS). The resulting partition coefficients determined by SIMS and LA-SF-ICP-MS are graphically compared in Fig. 6 for a representative sample. For all investigated samples, the partition coefficients determined by SIMS and LA-SF-ICP-MS are in excellent agreement, clearly demonstrating the reliability of laser ablation techniques for the characterisation of synthetic geomaterials.

Acknowledgements

The establishment of the new LA-SF-ICP-MS facility was funded with a grant of the Danish Ministry of Education and Technology to the Geocenter Copenhagen ('Geocenterbevilling') and financial support by GEUS. PV thanks the DAAD for awarding a PhD scholarship.

References

Aftalion, M., Bowes, D.R. & Vrána, S. 1989: Early Carboniferous U–Pb zircon age of garnetiferous, perpotassic granulites, Blanský les massif, Czechoslovakia. Neues Jahrbuch für Mineralogie, Monatsheft 4, 145–152.

Charrier, R. 1979: El Triásico en Chile y regiones adyacentes de Argentina: Una reconstrucción paleogeográfica y paleoclimática. Comunicaciones **26**, 1–37.

Harlov, D.E., Johansson, L., Van Den Kerkhof, A. & Förster, H.-J. 2006: The role of fluid flow and diffusion during localised, solid-state dehydration: Söndrum Stenhuggeriet, Halmstad, SW Sweden. Journal of Petrology **47**, 3–33.

Hollis, J.A., Frei, D., van Gool, J.A.M., Garde, A.A. & Persson, M. 2006: Using zircon geochronology to resolve the Achaean geology of southern West Greenland. Geological Survey of Denmark and Greenland Bulletin **10**, 49–52.

Jackson, S., Pearson, N.J., Griffin, W.L. & Belousova, E.A. 2004: The application of laser ablation – inductively coupled plasma – mass spectrometry to *in situ* U–Pb zircon geochronology. Chemical Geology **211**, 47–69.

Janoušek, V., Gerdes, A., Vrána, S., Finger, F., Erban, V., Friedl, G. & Braithwaite, C.J.R. 2006: Low-pressure granulites of the Lišov massif, Southern Bohemia: Viséan metamorphism of late Devonian plutonic arc rocks. Journal of Petrology **47**, 705–744.

Landwehr, D., Blundy, J.D., Chamorro-Perez, E.M., Hill, E. & Wood, B.J. 2001: U-Series disequilibria generated by partial melting of spinel lherzolite. Earth and Planetary Science Letters **188**, 329–348.

Steenfelt, A., Hollis, J.A. & Secher, K. 2006: The Tikiusaaq carbonatite and associated kimberlites: a new alkaline magmatic province in the Nuuk region, southern West Greenland. Geological Survey of Denmark and Greenland Bulletin **10**, 41–44.

Wiedenbeck, M., Allé, P., Corfu, F., Griffin, W.L., Meier, M., Oberli, F., von Quadt, A., Roddick, J.C. & Spiegel, W. 1995: Three natural zircon standards for U–Th–Pb, Lu–Hf, trace element and REE analysis. Geostandards Newsletters **19**, 1–23.

Vermeesch, P. 2004: How many grains are needed for a provenance study? Earth and Planetary Science Letters **224**, 441–451.

Authors' addresses

D.F., J.H. & C.Kn., *Geological Survey of Denmark and Greenland, Øster Voldgade 10, DK-1350 Copenhagen K, Denmark.* E-mail: *df@geus.dk*

A.G., *Institute of Mineralogy, Johan-Wolfgang-Goethe University, Senckenberganlage 28, D-60054 Frankfurt, Germany.*

D.H., *GeoForschungsZentrum Potsdam, Section 4.1 Experimental Geochemistry and Mineral Physics, Telegrafenberg, D-14473 Potsdam, Germany.*

C.Ka. & L.F., *Department of Geology, University of Lund, Sölvegatan 12, S-22362 Lund, Sweden.*

P.V. & G.F., *Institut für Angewandte Geowissenschaften, Technische Universität Berlin, Ernst-Reuter-Platz 1, D-10587 Berlin, Germany.*

East Greenland and Faroe–Shetland sediment provenance and Palaeogene sand dispersal systems

Michael Larsen, Christian Knudsen, Dirk Frei, Martina Frei, Thomas Rasmussen and Andrew G. Whitham

The sedimentation and basin evolution of the Kangerlussuaq Basin, southern East Greenland has gained renewed interest with the licensing rounds offshore the Faroe Islands in 2000 and 2005, as it forms an important analogy to the Faroese geological setting. The Faroes frontier area is in part covered by basalts and is a high-risk area with poorly known plays and sedimentary basins. It is therefore essential to obtain as much information as possible on the evolution of sedimentary basins on the rifted volcanic margins closest to the Faroese Islands margin. Plate reconstructions of the North Atlantic region indicate the former close proximity of East Greenland to the Faroe Islands region (Fig. 1), and the Kangerlussuaq Basin thus constitutes the most important field analogue with respect to stratigraphy, major unconformities and basin evolution. The study of the sedimentary succession in the Kangerlussuaq Basin, and the provenance of the sandstones in particular, will provide constraints on exploration models and may help to predict the distribution of potential reservoir sandstones in the Faroese offshore basins, and eventually lead to development of play types that are new to this frontier region.

This paper presents the main conclusions from two research projects: *Stratigraphy of the pre-basaltic sedimentary succession of the Kangerlussuaq Basin -Volcanic basin of the North Atlantic* and *An innovative sedimentary provenance analysis*, jointly undertaken by the Geological Survey of Denmark and Greenland (GEUS) and CASP (formerly Cambridge Arctic Shelf Programme). Both projects were initiated in October 2002 and concluded in September 2005. They form part of *Future Exploration Issues Programme of the Faroese Continental Shelf* (*SINDRI programme*), established by the Faroese Ministry of Petroleum and financed by the partners of the Sindri Group (see Acknowledgements).

Cretaceous–Palaeogene stratigraphy

Field work in the 1990s and results from the present projects require revision of the existing lithostratigraphic schemes for the pre-basaltic succession in the Kangerlussuaq Basin. Several hitherto unknown units have been discovered, and a new detailed biostratigraphy has been established incorporating

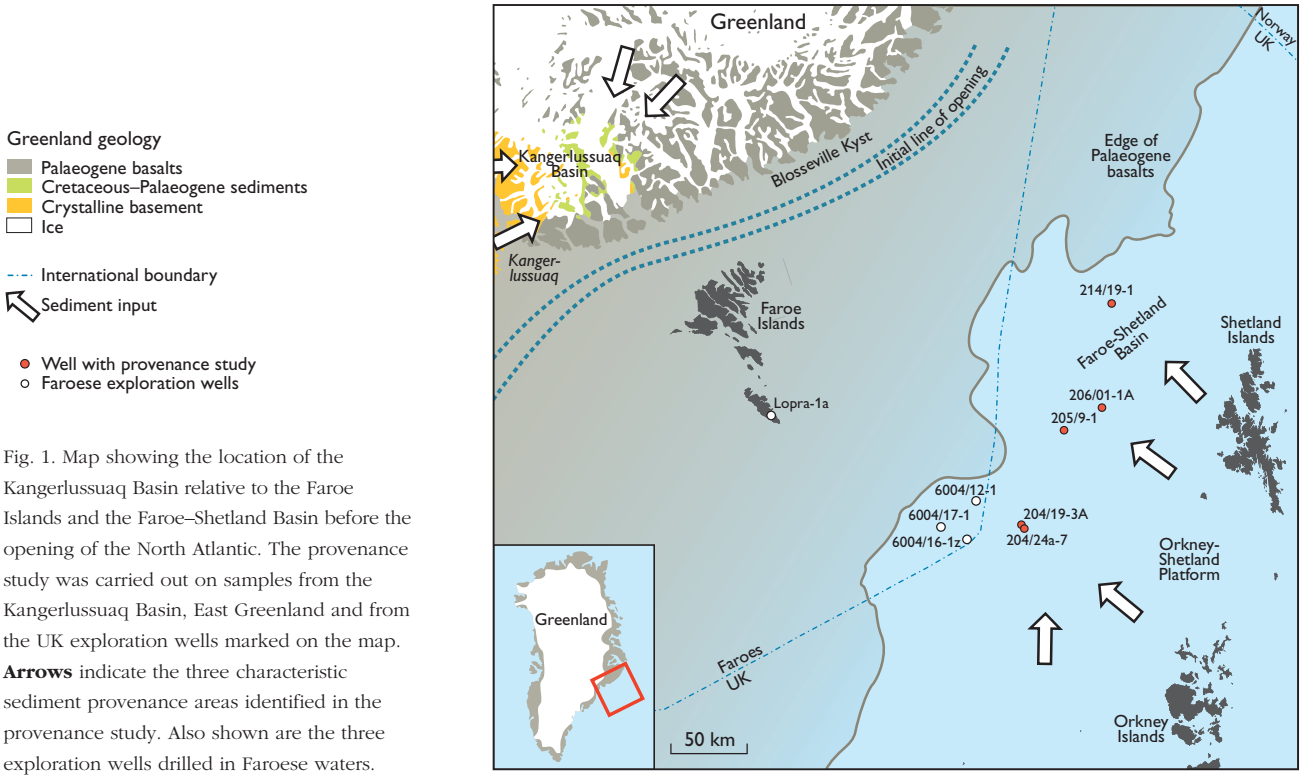

Fig. 1. Map showing the location of the Kangerlussuaq Basin relative to the Faroe Islands and the Faroe–Shetland Basin before the opening of the North Atlantic. The provenance study was carried out on samples from the Kangerlussuaq Basin, East Greenland and from the UK exploration wells marked on the map. **Arrows** indicate the three characteristic sediment provenance areas identified in the provenance study. Also shown are the three exploration wells drilled in Faroese waters.

age revisions based on both macrofossils and palynomorphs (Fig. 2; Larsen *et al.* 1999, 2001). The new biostratigraphy allows close correlation with the sub-basaltic successions in the offshore basins west of Shetland and in the Faroe Islands region. Most striking is the presence in both the Kangerlussuaq Basin and the Faroe–Shetland Basin of a Lower Cretaceous shallow marine sandstone unit as well as a number of thick Paleocene units dominated by sandstones. For the provenance study six sedimentary units were established (Fig. 2). The first four of these are Cretaceous; the Palaeogene units 5 and 6 are discussed below.

In the Kangerlussuaq Basin several regional subaerial unconformities representing sequence boundaries indicate times of sediment erosion and bypass. Based on field work a depositional model for the Kangerlussuaq Basin has been established and prediction of reservoir sandstones in offshore basins can be carried out.

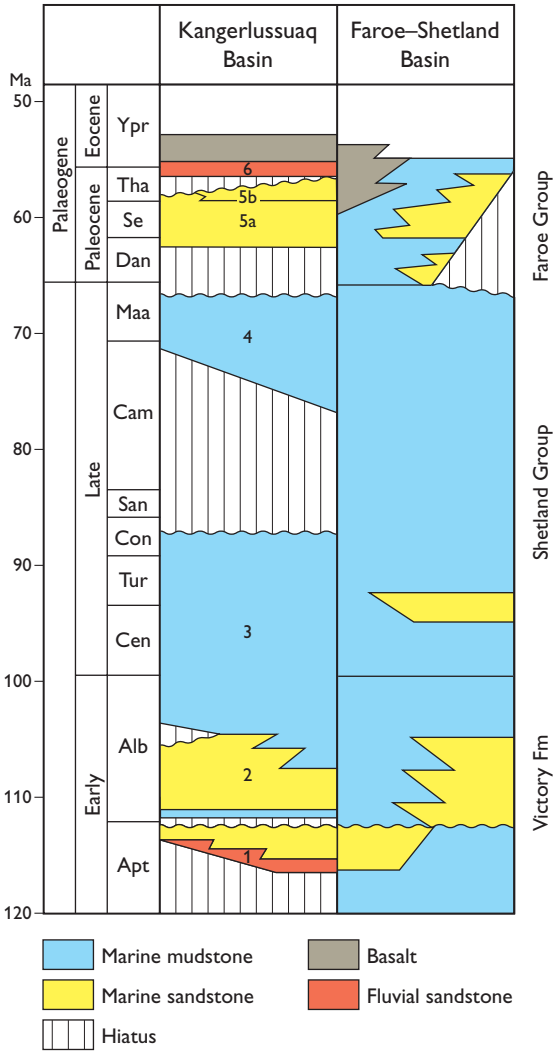

Fig. 2. Revised stratigraphy of the pre-basaltic succession in the Kangerlussuaq Basin. A formal lithostratigraphic scheme including names for new formations and members is in preparation. A composite stratigraphy of the Faroe–Shetland Basin is shown for comparison (from Grant *et al.* 1999; Ellis *et al.* 2002). Numbers **1–6** refer to units samples for detrital zircon studies (see Fig. 4).

Palaeogene sandstones of the Kangerlussuaq Basin

The Early Palaeogene succession in the Kangerlussuaq Basin consists of three distinct sandy units labelled 5a, 5b and 6 (Fig. 2), which represent different depositional environments. Graded thin-bedded sandstones dominate the lowest unit (5a); the sandstones are laterally consistent and may form amalgamated units up to 20 m thick. They were deposited in a deep marine environment and represent Selandian turbidite channel-fill and distal submarine fan lobes (Larsen *et al.* 1999). The next unit (5b) consists of well-sorted fine- to medium-grained sandstones showing hummocky cross-stratification and wave ripples. The sandstones are bioturbated showing traces of *Ophimorpha isp*. and *Thallasoinoides isp*. The unit forms an overall coarsening upward succession and is interpreted as deposited by shallow marine sand-bars and deltaic mouth-bars. A major erosional unconformity separates the second unit from coarse-grained and pebbly sandstones of the overlying unit 6. The sandstones show large-scale trough cross-bedding and contain fragments of coal and coalified wood. Unit 6 represents fluvial sandstones deposited in a proximal braided river system (Fig. 3).

Sandstone provenance

Provenance studies of sediments in the Faroe–Shetland Basin, on the Orkney–Shetland Platform and in the Kangerlussuaq Basin, East Greenland have been carried out using both analysis of bulk geochemical composition of the sediments and age determinations of detrital zircons.

Bulk geochemical analysis was carried out at GEUS on a total of 440 samples. Of these, 171 samples were collected from the Cretaceous, Paleocene and Eocene sedimentary rocks in the Kangerlussuaq Basin, while 269 represent Paleocene and Eocene sediments selected from cutting samples from wells in the Faroe–Shetland Basin. In each sample, major elements were analysed by fusion wavelength dispersive X-ray fluorescence (WD-XRF) and 33 trace elements by fusion inductively coupled plasma mass spectroscopy (ICP-MS). The analytical results provide distinctive geochemical signatures for the various units of the Kangerlussuaq Basin and the Faroe–Shetland Basin. Thus, Selandian marine turbiditic sandstones in the Kangerlussuaq Basin can be shown to be derived from beach placer deposits; their high Zr contents and characteristic U/REE ratios are indicative of a high heavy mineral content. This is in contrast to marine Selan-

dian sediments of the Faroe–Shetland Basin, where comparable Zr and U/REE patterns are lacking, suggesting that the Selandian marine sandstones in the Kangerlussuaq Basin and the Faroe–Shetland Basin have different sources.

Age determinations of detrital zircon

During the present study a total of 4347 detrital zircon grains from 47 samples were dated. The samples were from three locations: 25 from the Kangerlussuaq Basin, 20 from the Faroe–Shetland Basin and two from outcrops of Old Red Sandstone on the Orkney Islands. The analyses were carried out at GEUS using a laser ablation inductively coupled plasma mass spectrometer (LA-ICP-MS, Quadrupole), with *in situ* determination of the $^{207}Pb/^{206}Pb$ isotopic ratios. Frei *et al.* (2006, this volume) have compared ages obtained by U-Pb dating using both conventional SHRIMP and high resolution sector field LA-ICP-MS (HR-SF-LA-ICP-MS) methods and demonstrated that the Pb/Pb dating based on $^{207}Pb/^{206}Pb$ isotopic ratios determined by LA-ICP-MS is a reliable method for determining detrital zircon age distributions.

The observed distribution of zircon ages clearly shows that there are two distinct sources of detrital grains in the Kangerlussuaq Basin (Fig. 1). The Lower Cretaceous sedimentary rocks in the basin (units 1–3, Figs 2, 4) contain dominantly Neoarchaean and Mesoarchaean detrital zircons. The Upper Cretaceous sediments, however, contain a significant proportion of Proterozoic detrital zircons (unit 4, Figs 2, 4). The Paleocene marine sandstones are characterised by a large proportion of Archaean grains and variable proportions of Proterozoic zircons (unit 5, Figs 2, 4). The fluvial deposits of unit 6 (Figs 2, 4) contain mainly Archaean detrital zircons and very few Proterozoic detrital zircons.

Known possible sources of Archaean zircons are the Archaean basement gneisses south and south-west of Kangerlussuaq. The most probable sources of Proterozoic zircons are to the north, where the Caledonian orogenic belt exposes extensive areas of Proterozoic granites and gneisses, as well as Archaean gneiss complexes. It can be argued that units 1–3 and 6 received their main sediment input from the south, unit 4 from the north, while unit 5 may have had input from both north and south.

The samples analysed from the Faroe–Shetland Basin range in age from Early Paleocene to Early Eocene. The detrital zircon age distributions are similar in all analysed samples (not illustrated here), and include both Proterozoic and Archaean zircons. The Proterozoic zircons exhibit a wide age distribution from Neo- to Palaeoproterozoic, whereas the Archaean zircons all fall in a narrow cluster from 2550 to 2950 Ma, with a peak around 2800 Ma. The almost complete absence of Mesoarchaean zircons compared to the

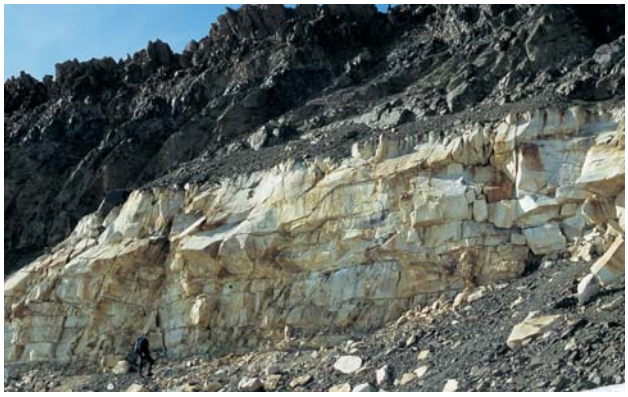

Fig. 3. The Paleocene of the Kangerlussuaq area is characterised by siliciclastic sandstone units deposited by prograding shallow marine and deltaic systems. The photograph shows fine-grained, pale sandstones (unit 6, Fig. 2) overlain by dark brown volcanic deposits (tuffs and lavas). Person (lower left) for scale.

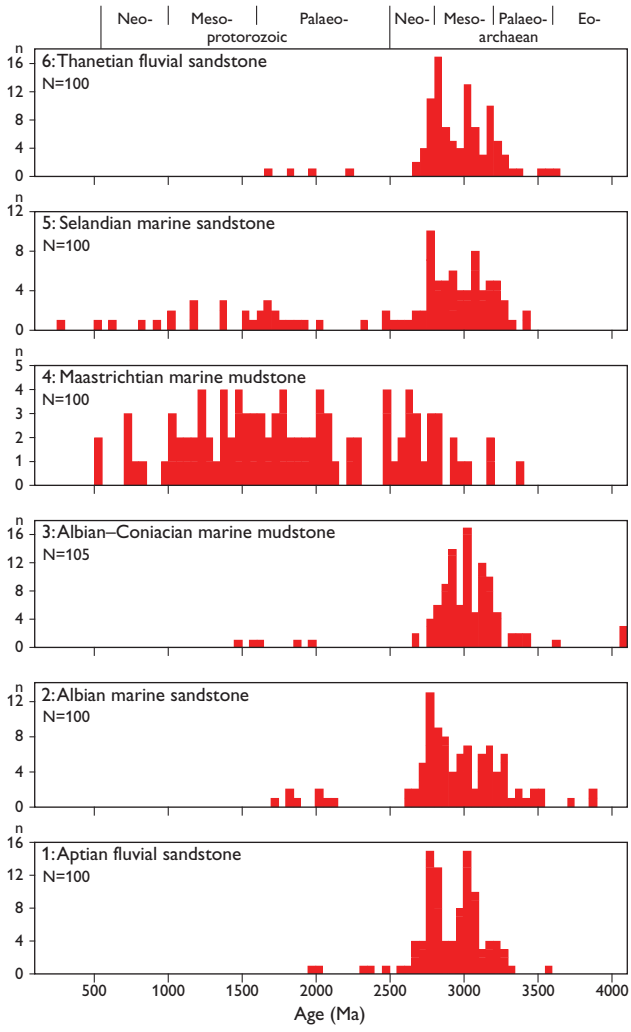

Fig. 4. Age distribution of detrital zircons from six units of the Kangerlussuaq Basin. **N**, number of analyses; **n**, sample frequency. Note vertical scale varies from unit to unit. For stratigraphic position of samples, see Fig. 2.

Kangerlussuaq Basin suggests that the sandstones from the Kangerlussuaq basin and the wells we have studied in the Faroe–Shetland Basin were sourced from different areas.

Greenland sands in offshore basins?

It was noted by Larsen *et al.* (1999) that the Cretaceous – Early Palaeogene evolution of the Kangerlussuaq Basin is similar to the eastern margin of the Faroe–Shetland Basin (Fig. 2). Ziska & Andersen (2005) stressed the apparent symmetrical development of the Faroe–Shetland Basin and thus the possibility of locating reservoir units below the basalts on the Faroe Islands side of the basin, similar to those already identified on the United Kingdom side. Sandstone provenance studies provide a possible means of testing the hypothesis that the Kangerlussuaq region provided sediment to the south-western end of the Faroe–Shetland Basin. The only Paleocene sand units in the basin so far recognised as having a western source are found in well 205/9-1 (Lamers & Carmichael 1999), but these units do not have heavy mineral characteristics compatible with an origin from the Kangerlussuaq region (Whitham *et al.* 2004). Recent studies by Jolley *et al.* (2005), based on pollen frequency data, suggest that sediments derived from Greenland are present in several wells of the Faroe–Shetland Basin. Sediment input from Greenland is related to periods of low relative sea level in the Palaeogene and appear to be focused along sediment transfer zones, e.g. the Westray and Judd transfer zones (Larsen & Whitham 2005). The provenance study of sandstones from the Kangerlussuaq Basin demonstrates that sandstones and mudstones show stratigraphic variations that are related to major sequence boundaries. Furthermore, these sands show distinctive characteristics, particularly in the age distribution of detrital zircons, suggesting that they may be differentiated from sands derived from the north-west European margin (Whitham *et al.* 2004). Further studies from wells on the western part of the Faroe–Shetland Basin and newer, not yet released data from wells drilled in Faroese waters may provide the final evidence for the Palaeogene sand dispersal systems discussed here.

Acknowledgements

The companies of the Sindri Group are gratefully acknowledged for their financial support of the two projects and field work in the Kangerlussuaq Basin, southern East Greenland in 2004. The Sindri Group comprises Agip Denmark BV, Amerada Hess (Faroes) Ltd., Anadarko Faroes Company, P/F Atlantic Petroleum, BP Amoco Exploration Faroes Ltd., British Gas International BV, DONG Føroyar P/F, Enterprise Oil Exploration Ltd., Føroya Kolvetni P/F, Petro-Canada Faroes GmbH, Phillips Petroleum Europe Exploration Ltd., Shell (UK) Ltd. and Statoil Færøyene AS.

References

Ellis, D., Bell, B.R., Jolley, D.W. & O'Callaghan, M. 2002: The stratigraphy, environment of eruption and age of the Faroes Lava Group, NE Atlantic: In: Jolley, D.W. & Bell, B.R. (eds): The North Atlantic Igneous Province. Stratigraphy, tectonic, volcanic and magmatic processes. Geological Society (London) Special Publications **197**, 253–269.

Frei, D., Hollis, J.A., Gerdes, A., Harlov, D., Karlsson, C., Vasquez, P., Franz, G., Johansson, L. & Knudsen, C. 2006: Advanced *in situ* geochronological and trace element microanalysis by laser ablation techniques. Geological Survey of Denmark and Greenland Bulletin **10**, 25–28.

Grant, N., Bouma, N. & McIntyre, A. 1999: The Turonian play in the Faeroe–Shetland Basin. In: Fleet, A.J. & Boldy, S.A.R. (eds): Petroleum geology of Northwest Europe: Proceedings of the 5th Conference, 661–673. London: Geological Society.

Jolley, D.W., Morton, A. & Prince, I. 2005: Volcanogenic impact on phytogeography and sediment dispersal patterns in the northeast Atlantic. In: Doré, A.G. & Vining, B. (eds): Petroleum geology: North-West Europe and global perspectives – Proceedings of the 6th Petroleum Geology Conference, 969–975. London: Geological Society.

Lamers, E. & Carmichael, S.M.M. 1999: The Paleocene deepwater sandstone play West of Shetland. In: Fleet, A.J. & Boldy, S.A.R. (eds): Petroleum geology of Northwest Europe: Proceedings of the 5th Conference, 645–659. London: Geological Society.

Larsen, M. & Whitham, A.G. 2005: Evidence for a major sediment input point into the Faroe–Shetland Basin from the Kangerlussuaq region of southern East Greenland. In: Doré, A. & Vining, B. (eds): Petroleum geology: North-West Europe and global perspectives – Proceedings of the 6th Petroleum Geology Conference, 913–922. London: Geological Society.

Larsen, M., Hamberg, L., Olaussen, S., Nørgaard-Pedersen, N. & Stemmerik, L. 1999: Basin evolution in southern East Greenland: an outcrop analog for the Cretaceous–Paleogene basins on the North Atlantic volcanic margin. American Association of Petroleum Geologists Bulletin **83**, 1236–1261.

Larsen, M., Bjerager, M., Nedkvitne, T., Olaussen, S. & Preuss, T. 2001: Pre-basaltic sediments (Aptian–Paleocene) of the Kangerlussuaq Basin, southern East Greenland. Geology of Greenland Survey Bulletin **189**, 99–106.

Whitham, A.G., Morton, A.C. & Fanning, C.M. 2004: Insights into Cretaceous–Paleocene sediment transport paths and basin evolution in the North Atlantic from a heavy mineral study of sandstones from southern East Greenland. Petroleum Geoscience **10**, 61–72.

Ziska, H. & Andersen, C. 2005: Exploration opportunities in the Faroe Islands. In: Ziska, H., Warming, T. & Bloch, D. (eds): Faroe Islands exploration conference: Proceedings of the 1st conference. Annales Societatis Scientiarum Færoensis Supplementum **43**, 146–162.

Authors' address

M.L.,*Geological Survey of Denmark and Greenland, Øster Voldgade 10, DK-1350 Copenhagen K, Denmark.* Present address: *DONG Energy, Agern Alle 24–26, DK-2970 Hørsholm, Denmark.*

C.K., D.F., M.F. & T.R., *Geological Survey of Denmark and Greenland, Øster Voldgade 10, DK-1350 Copenhagen K, Denmark.* E-mail: *ckn@geus.dk*

A.G.W., *CASP, Department of Earth Sciences, University of Cambridge, West Building, 181a Huntingdon Road, Cambridge, CB3 ODH, UK.*

Continental crust in the Davis Strait: new evidence from seabed sampling

Finn Dalhoff, Lotte M. Larsen, Jon R. Ineson, Svend Stouge, Jørgen A. Bojesen-Koefoed, Susanne Lassen, Antoon Kuijpers, Jan A. Rasmussen and Henrik Nøhr-Hansen

Although the structural framework of the subsurface offshore West Greenland has been well documented based on comprehensive seismic analysis (cf. Dalhoff *et al.* 2003), the stratigraphy of the region is less well known. The oldest documented sedimentary rocks drilled offshore West Greenland are Santonian sandstones reached at TD in the 6354/4-1 well (Fig. 1) although reworked palynomorphs of Carboniferous, Triassic and Jurassic (Kimmeridgian) age have been reported from a number of wells in the region. In order to obtain better constraints on the pre-Upper Cretaceous stratigraphy, a preliminary screening was undertaken to identify inversion structures and erosional canyons where such deeper stratigraphic levels crop out at the seabed (Nielsen et al. 2001). Sea-floor sampling at selected sites between 62° and 67°N (Fig. 1) was undertaken during the summers of 2003 and 2004. Other objectives of these cruises were to seek direct evidence of active petroleum systems, to establish further constraints on tectonic and stratigraphic models, and to obtain a better understanding of the Neogene and Pleistocene history of the region (Dalhoff *et al.* 2005).

The most promising seabed features identified by Nielsen *et al.* (2001) were investigated in more detail using a wide range of techniques in order to optimise sampling positions. In 2003, these techniques included echo sounder, side-scan sonar, single-channel seismic and video inspection before sampling either by dredge, gravity corer, or by video-controlled grab. In 2004, comprehensive data acquisition with a deep-water sparker system was undertaken before sampling by dredge or gravity corer, supplemented by grab samples at selected stations.

Sampling

A total of 19 dredges and five gravity cores, together with three grab samples, were recovered from the eastern and western flank of canyon C_1 (Fig. 1). On the Davis Strait High, four dredge and four grab stations were located on the eastern flank and one gravity core was recovered from the western flank (Fig. 1). Sampling at the seamounts was carried out by dredge on the flanks (six stations) with one grab station at the top of seamount S_3 (Fig. 1). Twenty-six gravity core stations and one piston core station were located in the areas with shallow Direct Hydrocarbon Indications (DHI), inferred from seismic anomalies or from sea-surface slicks recognised on satellite data; the majority were taken within D_1 and D_2 with the remaining five stations covering D3 and D_4 (Fig. 1). However, none of the samples produced significant hydrocarbon readings.

From a survey on the Labrador Shelf, McMillan (1973) reported a positive correlation between sea-floor outcrop and debris composition and concluded that only a small proportion of the recovered rock samples are ice rafted debris (IRD). In this study, differentiation between in situ samples and IRD

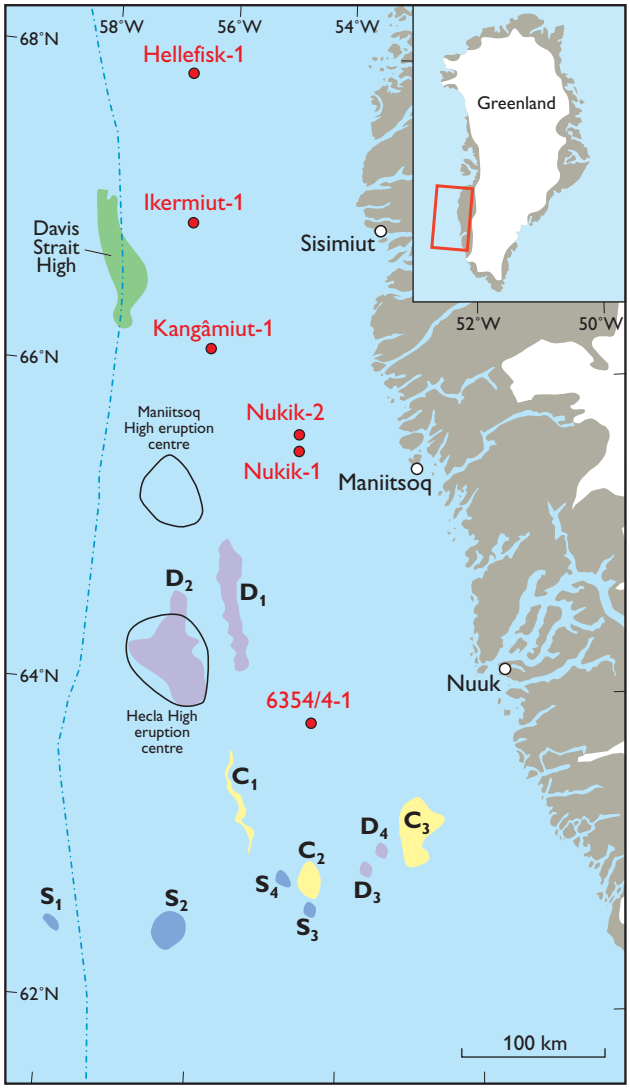

Fig. 1. Map of Labrador Sea and Davis Strait showing sample objectives of the 2003 and 2004 seabed sampling programme referred to in the text.

is based on the number of samples and the lithological homogeneity of the rock types collected at each station. For each dredge and grab station, the samples were classified into three groups: sedimentary rocks (siliciclastic and carbonates), igneous rocks, and Precambrian crystalline rocks.

Quaternary sedimentation

Understanding of Quaternary sedimentation patterns offshore West Greenland has greatly improved based on these surveys. Gravity cores from the site survey acquired prior to drilling the 6354/4-1 well (Fig. 1) and the 37 cores from the seabed sampling programme between 62°N–67°N have formed the basis for a detailed stratigraphic study of the uppermost sediment package (Lassen *et al.* 2005). Based on magnetic susceptibility profiles, ^{14}C accelerator-mass-spectrometry (AMS^{14}C) dates and core descriptions, it has been possible to relate the succession in the study areas to published event stratigraphic schemes. In general, cores from intermediate water depths (all areas except D_2 and the Davis Strait High, see Fig. 1) contain hemipelagic sediments alternating with IRD-rich layers. Since this pattern is found in all of the studied areas, it is concluded that no resedimentation of the upper sediments has occurred.

Ordovician and Jurassic sediments

The identification of dipping reflectors extending up to or near the seabed on conventional seismic lines presented the possibility of sampling sedimentary successions of unknown age at several stations. Test sampling (one gravity core) on the eastern flank of canyon C_1 (Fig. 1) in 2002 revealed reworked Middle–Upper Jurassic and Lower Cretaceous palynomorphs (H. Nøhr-Hansen, unpublished data 2004). Extensive sampling at this locality was undertaken and a pseudo stratigraphy has been established with the Danian–Selandian boundary identified on the western flank and the presence of Archaean crystalline basement overlain by Upper Ordovician – Lower Silurian carbonates and marine Mesozoic sediments on the eastern flank.

At the Davis Strait High sampling was undertaken together with a wide range of geophysical investigations indicating the presence of a possible inverted Palaeozoic carbonate platform. The assemblage of sedimentary rock types dredged up from the eastern side of the high (Fig. 1) is characterised in particular by marine carbonates, which form over 60% of the dredge clasts. Other rock types include fragments of sandstone, Precambrian crystalline rocks and igneous rocks. The carbonates comprise a range of lithofacies from biomottled lime mudstones and skeletal wackestones (about half of the carbonate clasts from both Davis Strait High sites) through skeletal, peloidal and intraclastic packstones and grainstones to rare microbial carbonates, including oncolitic and stromatolitic carbonates. Partially and wholly dolomitised representatives of these lithofacies are also present. Quartz silt and sand are common within the carbonates and fine-grained calcareous or dolomitic sandstones in the sample set are thought to form part of the facies spectrum. The bioclasts within these carbonates include crinoid, brachiopod, mollusc, bryozoan, coral, stromatoporoid, ostracod and trilobite fragments, testifying to the open marine, Palaeozoic affinity of the sediments; the facies represented record primarily a low-energy subtidal setting, although high-energy subtidal and lagoonal/intertidal settings are also indicated.

Organic geochemical analyses of the sedimentary rocks have only revealed two samples with promising results. One sample from canyon C_1 and one sample from the Davis Strait High (Fig. 1). The sample from canyon C_1 is a laminated Upper Ordovician mudstone, showing Hydrogen Index ~400, Total Organic Carbon = 1.3–4% and generative potential (S_2-value) that indicates a type 2 source rock with good to excellent potential for oil generation. For a marine carbonate, the biomarker signature shows unusually high proportions of gammacerane, 28-nor-spergulanes (Nytoft *et al.* 2006) and tetracyclic polyprenoids (TPP) and very high proportions of C_{29} regular steranes. Similar characteristics are found in samples of the Aleqatsiaq Fjord Formation in North Greenland (Christiansen 1989) and in Ordovician carbonates from Hudson Bay and around Foxe Basin, Canada (M.G. Fowler, personal communication 2004). The sample from the Davis Strait High is an Ordovician carbonate with oil staining of same age as seen in the source rock from canyon C_1.

Biostratigraphic studies indicate a Late Ordovician age (Maysvillian to Richmondian) for Davis Strait High sample suite, suggesting correlation with Lower Palaeozoic carbonate successions of the south-east Arctic Platform and the Hudson Platform in eastern and north-eastern Canada (Sanford & Grant 2000) and North Greenland, and 'Fossilik' in West Greenland (Stouge & Peel 1979). The correlation with Canada and North Greenland is supported by the geochemical data.

Igneous rocks

Igneous rocks constitute 10–20% of the clast population in most of the dredges, which is a much larger proportion than in the onshore areas. The clasts are typically 5–25 cm in size, rarely > 30 cm across. The majority are massive or vesiculated, fine-grained plagioclase-phyric or aphyric basalts. There are a few oxidised and brecciated samples interpreted as flow tops, and some picrites and gabbros. The clasts vary from angular to rounded and nearly all show abrasion indicative of transportation. Notable exceptions are two irregular,

very friable rock fragments from seamount S_2 (Fig. 1) which must be very local.

Of the total of 195 igneous rock samples, 95 were selected for geochemical analysis. Of these, 12 are interpreted to be of Precambrian age based on petrography (alteration) and geochemistry, and they are considered to be IRD; these include the gabbro samples. The remaining 83 samples can be grouped into relatively few geochemical groups (Fig. 2).

All the analysed samples from the Davis Strait High are tholeiitic basalts showing moderate to strong depletion in the most incompatible elements, with REE patterns sloping down to the left (Fig. 2A) and low Nb/La and Nb/Lu ratios mostly < 1 (Fig. 2B). Four samples have increased contents of a number of elements notably Si, K, Rb, Ba, Th and Pb, and are depleted in Nb indicating contamination by continental crustal material (Fig. 2B).

In the region south of 64°N the majority of samples belong to one geochemical type (the 'main group'). These rocks are tholeiitic basalts with moderate contents of incompatible elements, REE patterns sloping down to the right (Fig. 2A), and Nb/La and Nb/Lu ratios > 1 (Fig. 2B). A group of eight samples have relatively flat REE patterns and Nb/La and Nb/Lu ratios close to one. Two of these samples show signs of crustal contamination (Fig. 2B). A group of six samples are enriched tholeiitic basalts with steeper REE patterns and higher Nb contents than the main group. Two friable samples of obvious local origin from seamount S_2 are alkaline; they are basanites with steep REE patterns and high Nb/Lu ratios > 10 (Fig. 2). Other samples include two probably crustally contaminated basaltic andesites and two different rhyolites.

Radiometric ages have been obtained by the $^{40}Ar/^{39}Ar$ step-heating technique for 12 samples. One sample from the flat-patterned group yielded 119 ± 1 Ma (Early Cretaceous), one sample from the Davis Strait High yielded 63.0 ± 0.7 Ma (Early Paleocene), whereas ten samples from the region south of 64°N yielded ages ranging from 58.0 ± 0.4 Ma to 48.1 ± 0.9 Ma (Late Paleocene – Early Eocene).

Several lines of evidence support a relatively local derivation for the Palaeogene igneous rocks. The high abundance of igneous clasts in the dredges is incompatible with the absence of such rocks in the neighbouring onshore areas. If the basalts in the dredges in the southern region were ice-rafted from the northern onshore volcanic areas in West Greenland and Baffin Island, they should have the same composition and be more frequent in the northern dredges, but this was not observed.

The geochemically depleted rocks from the Davis Strait High are compositionally similar to lava flows outcropping on the sea floor in the same area and sampled in short drill cores (Srivastava *et al.* 1982; M.-C. Williamson, unpublished data), making a strong argument for local derivation of these

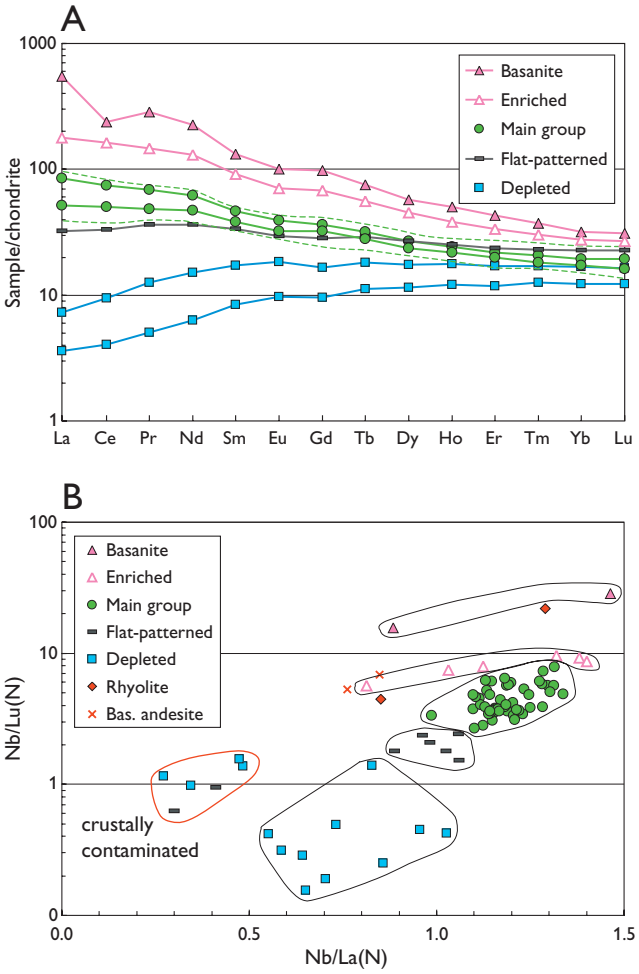

Fig. 2. Geochemistry of the dredged igneous rocks. **A**: Rare earth element (REE) patterns for representative samples, chondrite normalised data. The dotted green lines indicate the compositional range of the 'main group'. **B**: Nb/Lu vs Nb/La, N means primitive mantle normalised data. Normalisation values for both plots from McDonough & Sun (1995).

samples. The crustally contaminated samples support the presence of continental crust in the Davis Strait High, as suggested by Keen *et al.* (1974).

The stations south of 64°N are situated immediately south of the large volcanic complexes of the Hecla High Eruption Centre (Fig. 1). The lava succession of the Hecla High is dated as Eocene, and seismic sections show that an eroded and tilted cuesta landscape of lava flows has been exposed subaerially until some time during the Pleistocene (Sørensen 2005). It is therefore considered most likely that the dredged volcanic rocks from south of 64°N are derived from the Hecla High.

Seamount S_2 (Fig. 1) is flat-topped with a number of small volcanic cones rising from the platform. The cones probably consist of strongly alkaline rocks as judged from the occurrence of very local samples of basanite.

The slopes of the REE patterns indicate that the geochemically depleted basalts from the Davis Strait High were produced by melting to relatively shallow levels in the spinel stability field in the mantle, i.e. beneath a relatively thin (< 80 km) lithospheric lid. However, the contaminated samples show that they also came into contact with continental crust. The non-depleted and enriched basalts from the Hecla High were produced by melting at deeper levels in the garnet stability field in the mantle beneath a thicker lithospheric lid, and the basanites from seamount S_2 were produced by the smallest degrees of melting at the deepest levels. The mantle source could in all cases be the proto-Icelandic mantle plume. For a more detailed discussion of the igneous rocks see Larsen & Dalhoff (2006).

Archaean gneiss

Two dredges on the eastern side of canyon C_1 yielded Precambrian gneisses that are considered to be of local origin because of the uniform lithology and unabraded angular morphologies. Dating of a gneiss sample by the $^{206}Pb/^{207}Pb$ method yielded a well-defined Archaean age (2740 ± 150 Ma) with no indications of later thermal events. This is compatible with ages derived from the gneisses of the central Archaean craton of West Greenland, suggesting that the basement gneisses exposed in canyon C_1 represent the offshore continuation of this cratonic basement complex. This would extend the known occurrence of Archaean basement to nearly 200 km offshore, well into areas that were previously interpreted to comprise oceanic crust (Srivastava 1978; Roest & Srivastava 1989).

Conclusion and future work

The seabed sampling programme has yielded much new information on the Early Palaeozoic, Mesozoic and Palaeogene history of the Davis Strait and Labrador Sea including the extension of the continental crust into areas earlier described as oceanic crust. Continuation of the project with extension of the sampling region to 71°N, west of Disko, is planned for the summer of 2006 with collection of additional geophysical data and samples in selected areas.

Acknowledgement

The Bureau of Minerals and Petroleum, Nunaoil A/S and EnCana Corporation are thanked for financial support.

References

Christiansen, F.G. 1989: Petroleum geology of North Greenland. Bulletin Grønlands Geologiske Undersøgelse **158**, 92 pp.

Dalhoff, F., Chalmers, J.A., Gregersen, U., Nøhr-Hansen, H., Rasmussen, J.A. & Sheldon, E. 2003: Mapping and facies analysis of Paleocene – Mid-Eocene seismic sequences, offshore southern West Greenland. Marine and Petroleum Geology **20**, 935–986.

Dalhoff, F., Kuijpers, A., Nielsen, T., Lassen, S., Bojesen-Koefoed, J.A., Larsen, L.M., Stouge, S., Rasmussen, J.A. & Nøhr-Hansen, H. 2005: Seabed sampling offshore West Greenland – new information of inverted Palaeozoic and Mesozoic basins. GAC-MAC-CSPG-CSSS Joint Meeting , Halifax, Nova Scotia, Canada, 15–18 May, 2005, Abstracts **30**, 39 only.

Keen, C.E., Keen, M.J., Ross, D.I. & Lack, M. 1974: Baffin Bay: small ocean basin formed by seafloor spreading. American Association of Petroleum Geologists Bulletin **58**, 1098–1108.

Larsen, L.M. & Dalhoff, F. 2006: Composition, age, and geological and geotectonic significance of igneous rocks dredge from the Labrador Sea and the Davis Strait. Danmarks og Grønlands Geologiske Undersøgelse Rapport **2006/43**, 73 pp.

Lassen, S.J., Dalhoff, F., Kuijpers, A. & Nielsen, T. 2005: Late Quaternary sedimentation patters offshore West Greenland based on magnetic susceptibility profiles. Danmarks og Grønlands Geologiske Undersøgelse Rapport **2005/71**, 12 pp.

McDonough, W.F. & Sun, S.-S. 1995: The composition of the Earth. In: McDonough, W.F. *et al.* (eds): Chemical evolution of the mantle. Chemical Geology **120**, 223–253.

McMillan, N.J. 1973: Surficial geology of Labrador and Baffin Island shelves. In: Hood, P.J. (ed.): Earth science symposium on offshore eastern Canada. Geological Survey of Canada, Paper **71-23**, 451–469.

Nielsen, T., Andersen, C., Jensen, J.B., Kuijpers, A., Marcussen, C., Piasecki, S., Sønderholm, M. & Rasmussen, R. 2001: Geohazard 2001 study offshore West Greenland. Danmarks og Grønlands Geologiske Undersøgelse Rapport **2001/127**, 64 pp.

Nytoft, H.P., Lutnæs, B.F. & Johansen, J.E. 2006: 28-Nor-spergulanes, a novel series of rearranged hopanes. Organic Geochemistry 37, 772–786.

Roest, W.R. & Srivastava, S.P. 1989: Sea-floor spreading in the Labrador Sea; a new reconstruction. Geology **17**, 1000–1003.

Sanford, B.V. & Grant, A.C. 2000: Geological framework of the Ordovician system in the Southeast Arctic Platform, Nunavut. In: McCracken, A.D. & Bolton, T.E. (eds): Geology and paleontology of the Southeast Arctic Platform and southern Baffin Island, Nunavut. Geological Survey of Canada Bulletin **557**, 13–38.

Sørensen, A.B. 2006: Stratigraphy, structure and petroleum potential of the Lady Franklin and Maniitsoq Basins, offshore southern West Greenland. Petroleum Geoscience **12**, 221–234.

Srivastava, S.P. 1978: Evolution of the Labrador Sea and its bearing on the early evolution of the North Atlantic. Geophysical Journal of the Royal Astronomical Society **52**, 313–357.

Srivastava, S.P., Maclean, B., Macnab, R.F. & Jackson, H.R. 1982: Davis Strait: Structure and evolution as obtained from a systematic geophysical survey. In: Embry, A.F. & Balkwill, H.R. (eds): Arctic geology and geophysics. Canadian Society of Petroleum Geologists Memoir **8**, 267–278.

Stouge, S. & Peel, J.S. 1979: Ordovician conodonts from the Precambrian Shield of southern West Greenland. Rapport Grønlands Geologiske Undersøgelse **91**, 105–109.

Authors' addresses

F.D., L.M.L., J.R.I., S.S., J.B.-K., A.K. & H.N.-H., *Geological Survey of Denmark and Greenland, Øster Voldgade 10, DK-1350 Copenhagen K, Denmark.*
E-mail: *fd@geus.dk*

S.L., *96 Settrington Road, London SW6 3BA, UK.*

J.A.R., *Geological Museum, University of Copenhagen, Øster Voldgade 5–7, DK-1350 Copenhagen K, Denmark.*

An integrative and quantitative assessment of the gold potential of the Nuuk region, West Greenland

Bo Møller Stensgaard, Thorkild M. Rasmussen and Agnete Steenfelt

Visual inspection and comparison of lithological, topographical, geochemical and geophysical maps is a necessary (and often successful) way of interpreting geological features across poorly exposed or poorly explored areas. In mineral exploration, geochemical and geophysical maps are used to visually identify anomalies believed to reflect mineral occurrences. Outcropping mineral occurrences of a certain size can produce elevated concentrations of elements in stream sediment samples, or create magnetic or radioactive signals retrievable by airborne surveys. However, if the regional data are widely spaced, and if the occurrences are small or poorly exposed, the anomalies created may be too subtle to be recognised visually. In such cases, statistical data analyses may help identify deviations from background variations and trends in the data. Furthermore, visually based correlation between distribution patterns on maps is often limited to a few parameters, and multi-variable relationships are easily overlooked or not possible to deduce.

Gold occurrences in Greenland occur in specific host rocks as a result of mineralising processes, e.g. hydrothermal activity, that have affected a larger area. Thus, the favourable environment for a gold occurrence may be reflected in regional scale survey data as subtle changes in certain geochemical and geophysical properties. If such changes, i.e. a multi-parameter signature for gold mineralisation, can be identified, the regional data can be searched for areas that might hold the same signature.

This paper presents results gained in the application of a statistical spatial analysis method to investigate how known gold showings are expressed in a range of regional datasets from the Nuuk region, southern West Greenland. The main objective is to identify new areas with gold potential, and to

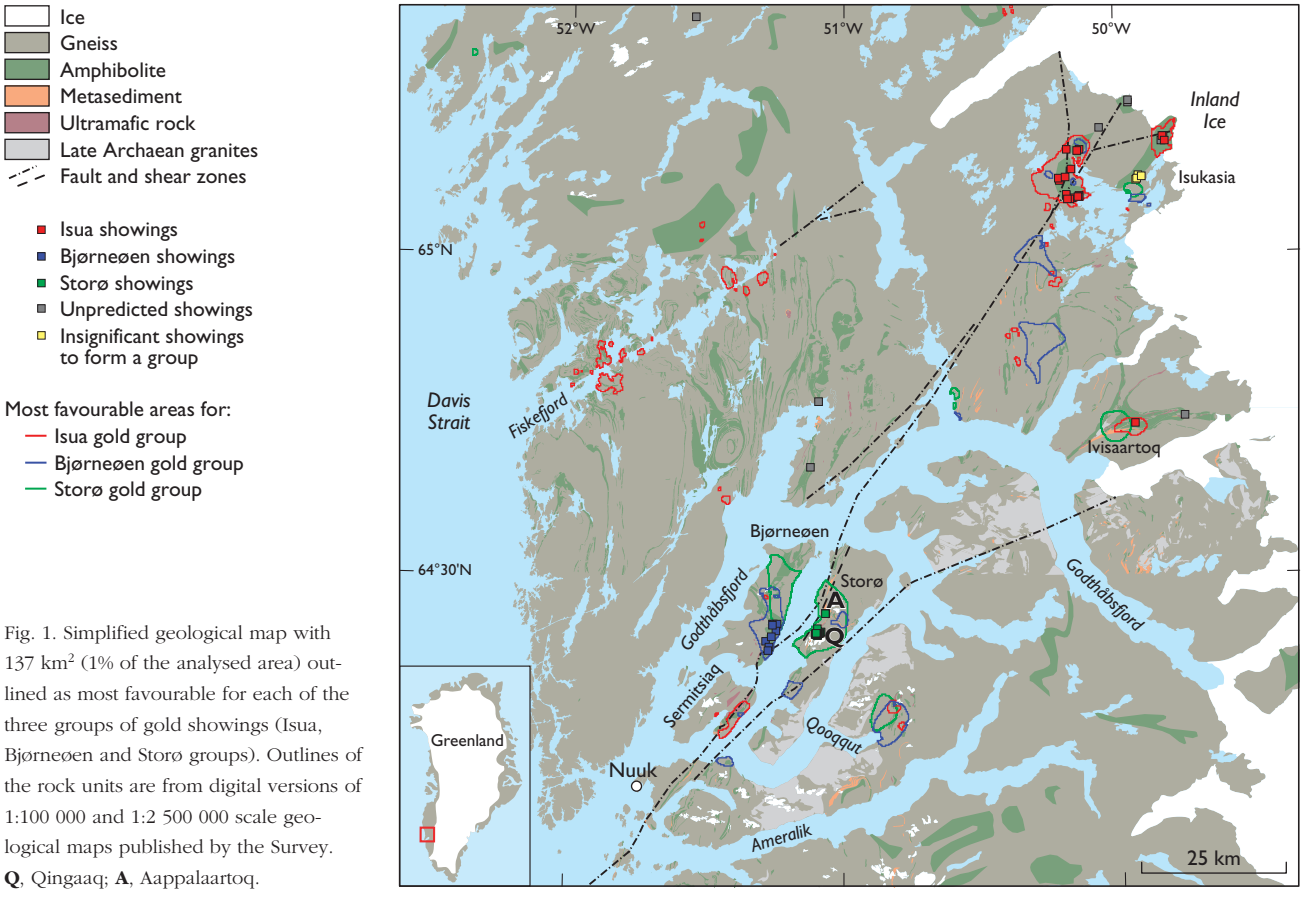

Fig. 1. Simplified geological map with 137 km^2 (1% of the analysed area) outlined as most favourable for each of the three groups of gold showings (Isua, Bjørneøen and Storø groups). Outlines of the rock units are from digital versions of 1:100 000 and 1:2 500 000 scale geological maps published by the Survey. **Q**, Qingaaq; **A**, Aappalaartoq.

quantify the signatures of the showings. The first tests based on this approach were reported in Nielsen *et al.* (2004) and Steensgaard *et al.* (2006).

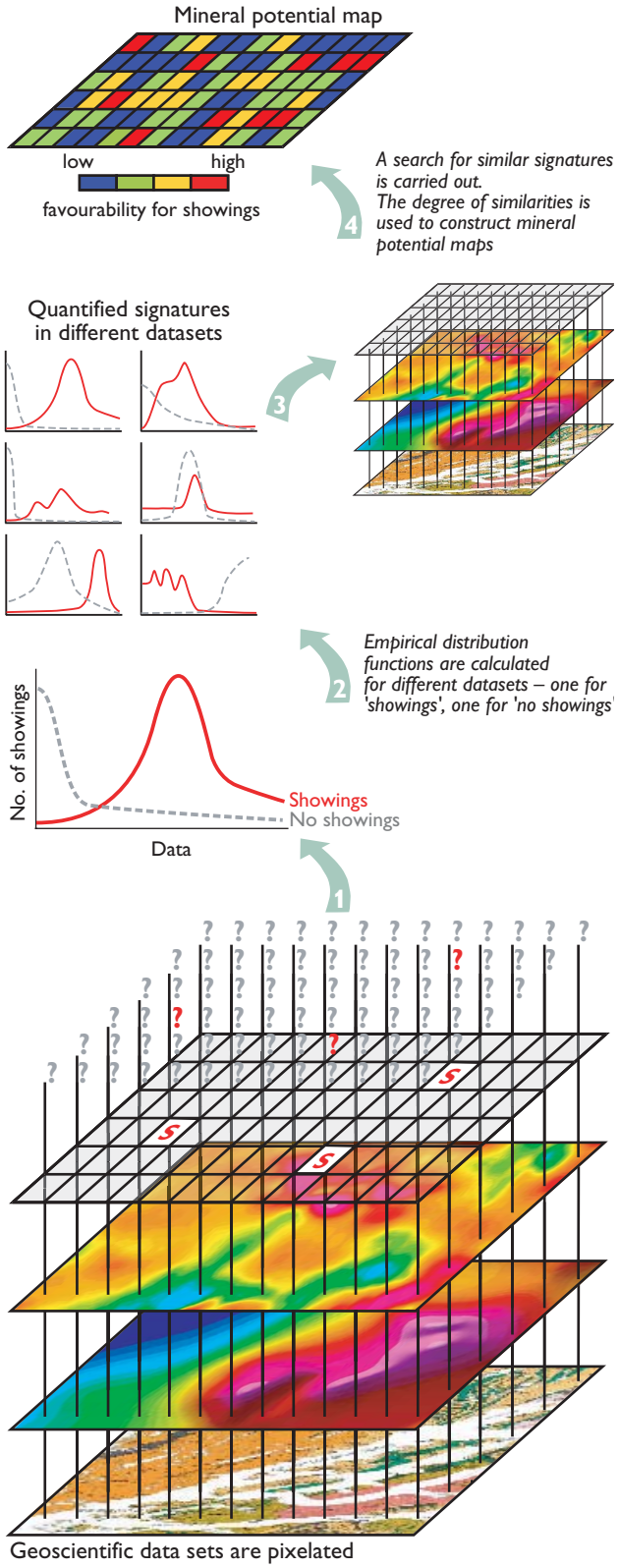

Compilation of available information in databases and company reports

The Nuuk region is underlain by early to late Archaean rocks dominated by quartzofeldspathic orthogneisses, but with a significant proportion of supracrustal belts, some of which contain greenstones (Fig. 1). The belts represent remnants of Archaean volcanic and associated intrusive rocks, with subordinate chemical and clastic sediments. Recent studies have revealed that the belts represent a number of individual successions formed at different locations and ages. The most common rock type is amphibolite of tholeiitic to komatiitic composition, but andesitic compositions have also been recognised in some belts (Hollis *et al.* 2005, 2006, this volume). Metasedimentary rocks are mostly garnet-biotite schist. The supracrustal rocks host several gold occurrences in association with hydrothermal alteration (Fig. 1; Appel *et al.* 2005). Two of these, at Qingaaq and Aappalaartoq on Storø (Q and A, Fig. 1) are currently targets for commercial drilling by NunaMinerals A/S.

Datasets analysed

Twenty-nine datasets have so far been included in the statistical analysis. The data are derived from regional scale surveys, and comprise stream sediment geochemistry and aeromagnetic data. The geochemical data include concentrations of Al_2O_3, As, Au, CaO, Cs, Fe_2O_3, K_2O, La, MgO, Na_2O, P_2O_5, Rb, Sb, SiO_2, Th, TiO_2, V, Zr, Zn, U, Ni/MgO and Ni + Cr in the < 0.1 mm grain size fraction of stream sediments. The magnetic data include the total magnetic field intensity (TMI), and derivatives of the total field, i.e. vertical gradient of TMI, horizontal gradients of TMI in various directions (HGTMI), and the amplitude of the HGTMI. A search through available non-confidential data reported by exploration companies, as well as Survey databases, provided

Fig. 2. Illustration of the statistical approach. 1: Regional datasets and gold showings (S) are referred to a common grid with fixed cell size. 2: Empirical distribution functions for cells with and without known gold showings are used to establish the signatures of the showings in each dataset. 3: Likelihood ratio functions for all datasets are calculated as the ratio of the two previous functions, expressing the likeliness of a showing to be present,. Groupings of gold showings are based on constructed mineral potential maps for each showing. Pixel by pixel, these maps outline the predicted favourability for data signatures similar to the selected showing, i.e., the potential for a similar showing to be present. In this way the mutual prediction capability amongst different showings can be compared. 4: Finally, mineral potential maps are calculated for each identified group of showings. These maps are based on the signatures found to be indicative for each of the different groups.

all known localities from which gold-bearing rock samples had been collected.

Methodology

The principles of the methodology are illustrated in Fig. 2. All spatial datasets must be converted into a form where they can be compared and subjected to statistical analysis. Each dataset is presented as a regular grid, using a common cell size of 200 m × 200 m, and a gridding procedure based on principles of minimum curvature. Note that the resulting grid values for geochemical and geophysical data are obtained by interpolation, as most measured points of the original datasets have a larger spacing than 200 m. There is therefore a risk that interpolated values in some areas misrepresent the data. Grid cells with and without gold showings are registered. In this study, a gold showing is defined as a cell in which rock samples with ≥ 1 ppm Au have been collected. In total, 52 gold showings were identified.

The data were analysed using statistical methodologies based on Chung (2003, and references therein). In summary, analysing the integrated data signature of cells with gold showings, and using this information to calculate for each cell the probability that it contains a similar gold showing, can be used to construct mineral potential maps. A mineral potential map defines zones or classes of different favourability for a certain mineralisation type. The methodologies involve calculation of empirical distribution functions (EDFs) for cells with and without gold showings, which can be regarded as the signature of the gold showings and the regional background (Fig. 3). The ratio between the two EDFs is used to calculate likelihood ratio functions (LFs) for each dataset. A joint likelihood ratio function (JLF) is then calculated as the product of the LFs. This JLF is then used to construct the mineral potential map.

Grouping of gold showings

In our first simple approach, we treated all known gold showings as one group (Nielsen *et al.* 2004). However, the results suggested that some gold showings had different signatures, and statistical methods were subsequently used to test whether the showings could be grouped according to their signatures. A gold potential map was then made for each single showing, based on the datasets that are characteristic of all showings. Then, the capability of the selected showing to predict the remaining showings was evaluated. As a result, a group defined this way consists of showings that have mutual prediction capabilities. The analysis resulted in the identification of three main groups of gold showings (Fig. 1): the Storø group (11 showings in a discrete area at Qingaaq and Aappalaartoq), the Bjørneøen group (10 showings located around central Bjørneøen), and the Isua group (19 widely spread showings at Isukasia and one showing at Ivisaartoq). Two other groups shown on Fig. 1 are not treated further here, namely a group of eight showings without mutual prediction capabilities with other showings, and another group of four showings which is considered too small to be statistically significant.

Gold potential maps

Figure 1 displays a gold potential map, where red, blue and green boundaries outline the most favourable areas for finding gold occurrences according to the criteria established for each of the three main groups.

It is not surprising that areas immediately surrounding known gold showings are predicted as favourable, but more interestingly, a number of favourable areas are also predicted outside known gold showings. Many of the latter areas are within or adjacent to supracrustal rocks, that may otherwise be regarded as potential hosts to gold. Some of the most notable favourable areas are east of the fjord Qooqqut, areas on Storø favourable for Bjørneøen group gold showings, and areas on south-eastern Sermitsiaq and farther to the southwest. Finally, several favourable areas are outlined along Fiskefjord (Fig. 1). This area has hardly been prospected for gold, but comprises both supracrustal rocks and structures that are similar to the hosts of some of the known gold showings.

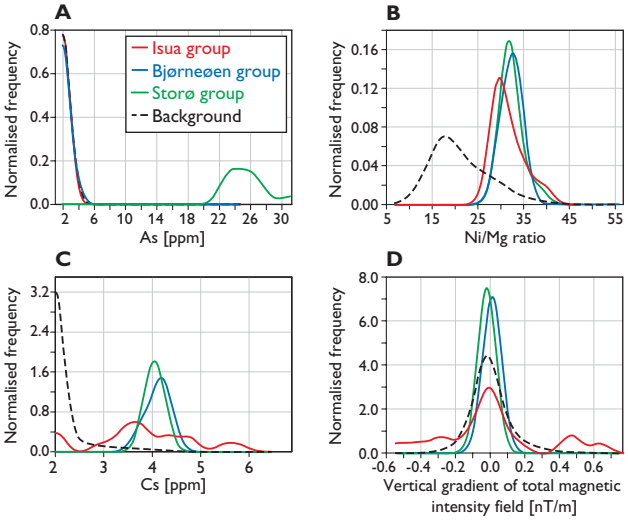

Fig. 3. Single-parameter signatures of three groups of gold showings and the background. **A**: Arsenic (As), based on concentrations in the fine fraction of stream sediment. **B**: Nickel/magnesium (Ni/Mg) ratio, based on concentrations in the fine fraction of stream sediment. **C**: Caesium (Cs), based on concentrations in the fine fraction of stream sediment. **D**: Vertical gradient (VGTMI), based on airborne measurements of total magnetic field intensity.

When a mineral potential map for gold is evaluated, it is important to keep in mind that areas outlined as having a low favourability need not necessarily be discarded as targets for gold since the constructed maps only reflect the data and known gold occurrences included in the analysis.

Signatures of gold showings

The systematic construction of signatures of showings and background (EDFs) draw attention to the significance of parameters that are not immediately or traditionally regarded as indicative of gold mineralisation. This is illustrated in Fig. 3 by four examples of single-parameter empirical distribution functions for each of the three groups of gold showings, together with the background variation.

It has previously been established that the combination of elevated As in stream sediment and gold mineralisation has not been found outside Storø (Fig. 3A). However, the possible significance of the Ni/Mg ratio (Fig. 3B) in relation to gold has not previously been substantiated in a quantitative way. This observation is an incentive to conduct further studies of host rock properties in terms of their Ni and Mg behaviour.

The rare and unique As signature of the Storø group poses a problem in the search for areas holding a potential for new showings. Since this signature only exists on Storø, only this area will be outlined as favourable for the Storø group. Consequently, the As data are omitted in the calculation of cells with a potential for Storø-type showings. Steenfelt (2000) has argued that Cs may be considered a pathfinder element for gold mineralisation associated with granite-related hydrothermal alteration. The signature for Cs in stream sediment confirms that the gold at Storø and Bjørneøen is indeed located in a Cs-rich environment (Fig. 3C), but also suggests that the mineralisation at Isua has a different nature.

The last example (Fig. 3D) illustrates the indicated significance of the vertical gradient of the total magnetic field intensity (denoted VGTMI). This signature for the Storø and Bjørneøen groups (–0.2 to 0.1 nT/m) is identical to the background signature, and is consequently regarded as non-indicative for these groups. The Isua group has a more dispersed signature (–0.5 to 0.8 nT/m), with a more highly indicative positive and negative VGTMI than the other groups. This probably reflects local scale changes in lithology. Other datasets, which yield a characteristic signature of one or more of the three groups of gold showings, are the Au, Cs, Rb, La, Th, and U concentrations in stream sediment geochemistry.

Further work and perspectives

The results obtained in the first tests of the applied statistical method have been positive in the sense that areas with high probability for new gold occurrences were outlined in geological settings that would otherwise be regarded as prospective for gold. In the next phase of the study additional datasets will be included, such as airborne gamma-ray spectrometry, digital topography, lithology and structure; the gridding procedure will be refined, and the influence of changing the cell size and the use of other statistical methods will be tested.

This kind of statistical approach has a potential for a range of applications, such as the prediction of other types of mineral occurrences, and identification and mapping of specific rock units in poorly exposed or poorly known terrain. Multivariate statistical analysis seems inevitable as a way to optimise the use of geoscientific data. However, it is important that geoscientists critically evaluate the results of any statistical analysis in order to reveal misleading effects of interpolation and other ways of standardising parameters that by their nature are very variable.

Acknowledgement

The Bureau of Minerals and Petroleum, Government of Greenland, financially supported the project.

References

Appel, P.W.U., Coller, D., Coller, V., Heijlen, W., Moberg, E., Polat, A., Raith, J., Schjøth, F., Stendal, H. & Thomassen, B. 2005: Is there a gold province in the Nuuk region? Danmarks og Grønlands Geologiske Undersøgelse Rapport **2005/27**, 79 pp., 1 CD-ROM.

Chung, C.F. 2003: Use of airborne geophysical surveys for constructing mineral potential maps. Economic Geology Monograph **11**, 879–891.

Hollis, J.A., van Gool, J.A.M., Steenfelt, A. & Garde, A.A. 2005: Greenstone belts in the central Godthåbsfjord region, southern West Greenland. Geological Survey of Denmark and Greenland Bulletin **7**, 65–68.

Hollis, J.A., Frei, D., van Gool, J.A.M., Garde, A.A. & Persson, M. 2006: Using zircon geochronology to resolve the Archaean geology of southern West Greenland. Geological Survey of Denmark and Greenland Bulletin **10**, 25–28.

Nielsen, B.M., Rasmussen, T.M. & Steenfelt, A. 2004: Gold potential of the Nuuk region based on multi-parameter spatial modelling of known gold showings. Danmarks og Grønlands Geologiske Undersøgelse Rapport **2004/121**, 155 pp.

Steenfelt, A. 2001: Geochemical atlas of Greenland – West and South Greenland. Danmarks og Grønlands Geologiske Undersøgelse Rapport **2001/46**, 39 pp.

Steensgaard, B.M., Steenfelt, A. & Rasmussen, T.M. 2006: Gold potential of the Nuuk region based on multi-parameter spatial modelling. Progress 2005. Danmarks og Grønlands Geologiske Undersøgelse Rapport **2006/27**, 207 pp.

Authors' address

Geological Survey of Denmark and Greenland, Øster Voldgade 10, DK-1350 Copenhagen K, Denmark. E-mail: *bmst@geus.dk*

The Tikiusaaq carbonatite: a new Mesozoic intrusive complex in southern West Greenland

Agnete Steenfelt, Julie A. Hollis and Karsten Secher

Ultrabasic alkaline magmatic rocks are products of melts generated deep within or at the base of the lithospheric mantle. The magmas may reach the surface to form lavas and pyroclastic deposits; alternatively they crystallise at depth to form dykes or central complexes. The rocks are chemically distinct and may contain high concentrations of economically interesting minerals and chemical elements, such as diamonds, niobium, tantalum, rare earth elements, phosphorus, iron, uranium, thorium, and zirconium. Ultrabasic alkaline rocks are known from several provinces in Greenland, but extrusive facies have only been preserved at a few places; e.g. at Qassiarsuk in South Greenland where pyroclastic rocks occur, and in the Maniitsoq region, where a small volcanic breccia ('Fossilik') contains fragments of Palaeozoic limestone. Ultramafic lamprophyre and kimberlite are mainly emplaced as dykes, whereas carbonatite forms large intrusive bodies as well as dykes. The ultrabasic alkaline magmas that have been emplaced at certain times during the geological evolution of Greenland can be related to major episodes of continental break-up (Larsen & Rex 1992). The oldest are Archaean and the youngest dated so far are Palaeogene. Figure 1 shows the distribution of known ultrabasic alkaline rocks in West Greenland.

The large and well-exposed bodies of alkaline rocks and carbonatites in the Gardar Province were discovered already in the early 1800s (Ussing 1912), while less conspicuous bodies were discovered much later during geological mapping and mineral exploration. Many alkaline rock bodies, particularly dykes, are difficult to identify in the field because they weather more extensively than the country rock gneisses and form vegetated depressions in the landscape. However, their distinct chemistry and mineralogy render alkaline rocks identifiable in geochemical and geophysical survey data. Thus, the Sarfartôq carbonatite complex was discovered during regional airborne gamma-spectrometric surveying owing to its elevated uranium and thorium contents (Secher 1986).

The use of kimberlite indicator minerals has led to the discovery of alkaline rocks such as kimberlites and ultramafic lamprophyres that carry fragments of deep lithospheric mantle.

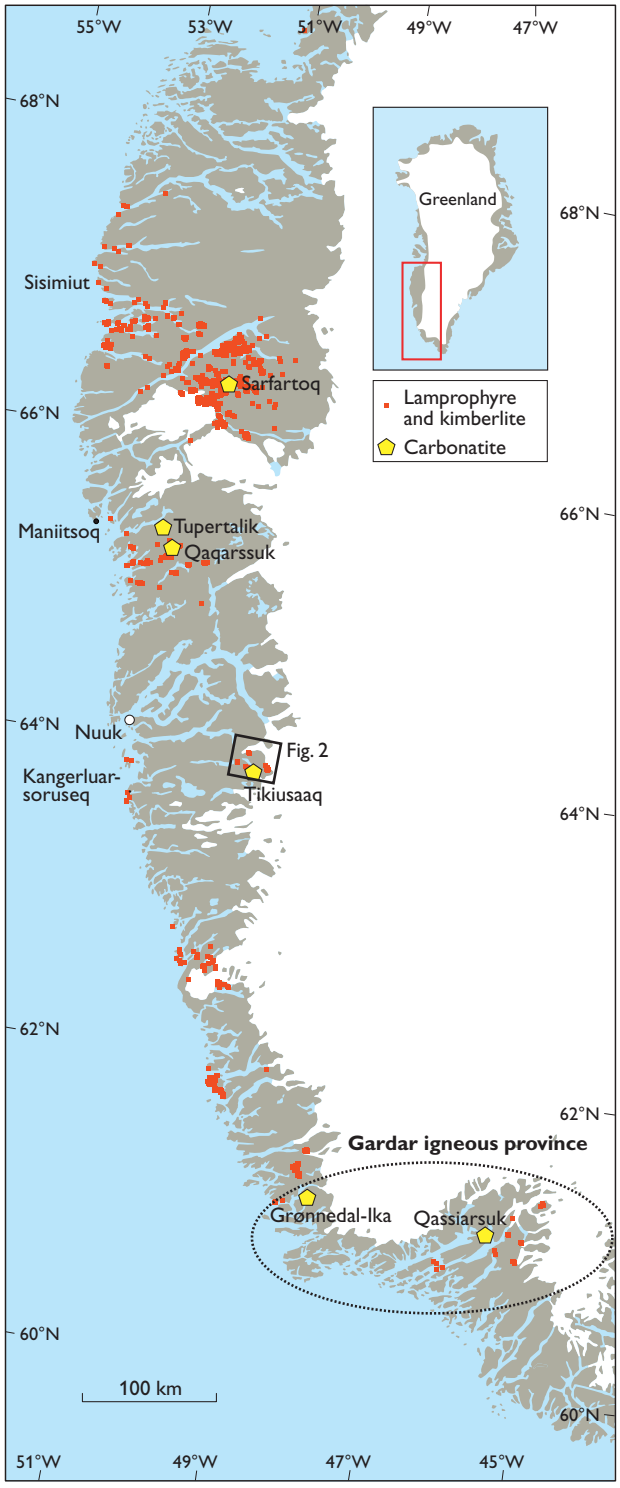

Fig. 1. Occurrences of lamprophyre, kimberlite and carbonatite in the southern part of West Greenland.

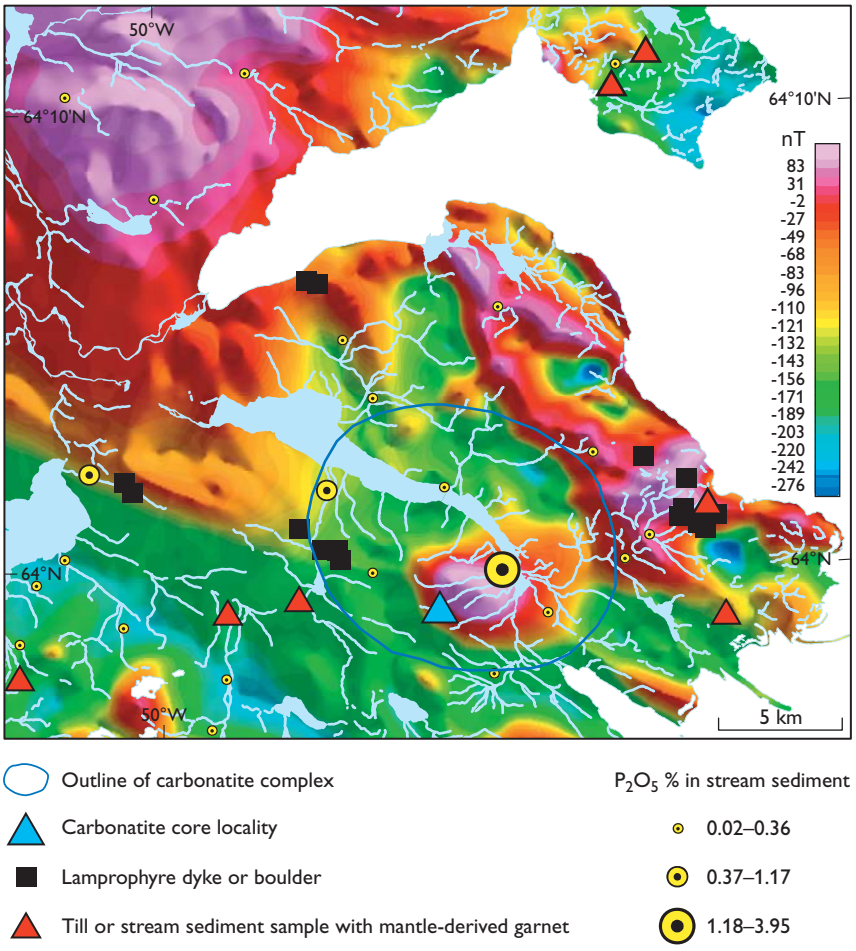

Fig. 2. Close-up of the area, where the new carbonatite was found. The map shows a shaded image of the total magnetic field with large lakes and streams (**light blue**), and the Inland Ice (**white**) superposed on the image. Symbols illustrate the concentration of phosphorus (P_2O_5) in stream sediment and localities where mantle-derived garnet grains have been identified in till or stream sediment. The occurrence of a distinct positive magnetic ano-maly in combination with anomalous stream sediment composition downstream was a strong indication of the presence of alkaline or carbonatitic rocks. The fieldwork confirmed solid carbonatite sheets (**dark blue triangle**), lamprophyre dykes (**black squares**), and an area (**ringed**) of fracturing and veining related to the intrusion of the carbonatite magma.

Such rocks may also contain diamonds. Kimberlite indicator minerals are high-pressure varieties of minerals, such as garnet, clinopyroxene, chromite and ilmenite that were formed in the lithospheric mantle. Exploration companies have processed thousands of till samples from southern West Greenland for kimberlite indicator minerals and found many new dykes.

A new carbonatite complex and associated lamprophyre dykes

A new carbonatite complex, named Tikiusaaq, was discovered in 2005 approximately 100 km east of Nuuk, as a result of a field-check of a combined stream sediment geochemical and aeromagnetic anomaly (Figs 1, 2). A stream sediment sample collected during the geochemical mapping of West Greenland (Steenfelt 2001) had a chemical composition that strongly indicated the presence of carbonatitic rocks similar to those at Sarfartoq (Secher & Larsen 1980) and Qaqarssuk (Knudsen 1991). A small-sized but strong magnetic anomaly (Fig. 2) displayed by the aeromagnetic map of West Greenland (see e.g. Rasmussen 2002) upstream of the anomalous sample also favoured the presence of carbonatite, as large magnetite accumulations are characteristic features of carbonatite complexes. The field work confirmed the presence of the new carbonatite complex. The complex appears to be centred at the position 64°N, 49°46′W, where *in situ* massive carbonatite was found in the walls of a creek cutting through a gentle slope covered by gravel and vegetation.

The preliminary field observations have determined that the emplacement of the carbonatite has affected an area of more than 100 km^2 within highly metamorphosed and strongly deformed Archaean basement comprising granite, dioritic and tonalitic orthogneiss, amphibolite, and anorthosite. Centrally in the area (Fig. 2), closely spaced, near-vertical massive carbonatite sheets are up to several metres wide (Fig. 3). In their surroundings, the host rocks have been chemically altered (fenitised), and further away the host rocks are fractured and contain numerous small veins (< 1 mm to 20 cm) of carbonatite. The brittle fracturing together with the observation of carbonate-rich breccia indicates that the intrusion was explosive. The dimensions and internal structure of the core zone have not yet been established. However, by analogy with other carbonatite complexes in West Green-

Fig. 3. View northwards along creek with exposed near-vertical sheets of carbonatite emplaced into mafic host rock. Intense fracturing with yellow-brown coating of fracture surfaces characterises both the core zone and its surroundings.

land, it is expected that the core zone is in the order of 1–2 km wide.

In addition to the main carbonatite body, many boulders and a few outcropping ultramafic alkaline dykes were discovered in the area north and north-east of the Tikiusaaq carbonatite, and these are the likely source of the kimberlite indicator minerals previously recorded in till samples from this area (Fig. 2). The observed dykes were only exposed over a few metres, are between 1 and 4 m wide, and have strikes that vary between E–W and NE–SW.

Mineralogy, chemistry and age

Carbonatite

Preliminary field work has identified at least two carbonatite varieties, one pale, creamy white in colour and one brownish grey (Fig. 4). The white variety is calcite carbonatite containing disseminated grains or bands of pale green mica, magnetite and apatite. Barite and monazite have been found in small amounts. The grey variety is dolomite carbonatite with occasional tiny brown spots suggesting an ankeritic component.

Boulders of carbonate-rich breccia have abundant xenoliths of the host orthogneiss and garnet-clinopyroxene aggregates (up to 1 cm diameter), along with xenocrysts of phlogopite, olivine, and rare garnet. The matrix of the breccia is similar to that of *in situ* brown-weathering thin carbonatite dykes within the complex; hence it seems likely that the boulders are derived from a certain phase within the carbonatite.

A preliminary age determination of 158 ± 2 Ma suggests that the carbonatite is Late Jurassic. This age was determined by means of U-Pb isotope analysis by Laser Ablation-Sector Field-Inductively Coupled Plasma Mass Spectrometry of a zircon crystal from the breccia described above (see also Frei *et al.* 2006, this volume). The age makes the new carbonatite near-coeval with the Qaqarssuk carbonatite (173 Ma, Larsen & Rex 1992). Further age determinations based on Rb-Sr isotope chemistry of mica grains from the carbonatite and from one of the lamprophyre dykes are underway.

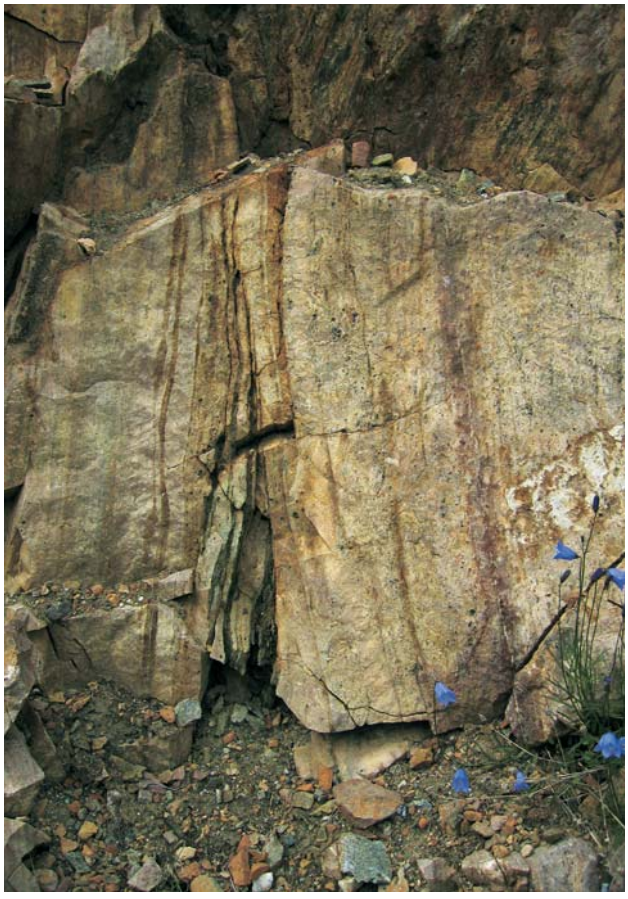

Fig. 4. Cream-coloured banded calcitic carbonatite with veins of brown ankeritic carbonatite. The faint banding is caused by variable amounts of disseminated green mica and greyish green apatite.

Ultramafic dykes

Boulders and *in situ* dykes of ultramafic lamprophyres vary in appearance and mineralogy. One widespread type has an olivine-rich groundmass and variable amounts of phlogopite crystals, 2 to 20 mm in size, together with phenocrysts of olivine and magnetite (Fig. 5). Other occurrences have variable additional carbonate and mica contents in the groundmass. The rocks are possible kimberlites. Mantle-derived xenocrysts or xenoliths were not observed macroscopically with certainty, but the presence of mantle-derived minerals will be further tested by means of microscopy and processing of large samples.

Fig. 5. Boulder of ultramafic lamprophyre with olivine rich groundmass and phenocrysts of olivine and magnetite.

Significance of discovery

The discovery of the carbonatite in the Nuuk region was made in a part of West Greenland where alkaline rocks have not hitherto been recorded. The nearest other occurrences are ultramafic lamprophyre dykes recorded at Kangerluarsoruseq (formerly Færingehavn) on the coast some 100 km west-south-west of the Tikiusaaq carbonatite, and the southernmost of the Maniitsoq kimberlites at least 150 km to the north-west. The ultramafic lamprophyre dykes at Kangerluarsoruseq yielded ages of 175±7, 185±7 and 196±8 Ma (K-Ar dating; Larsen & Rex 1992), and are thus likely to be part of related intrusive events.

Carbonatites and kimberlites commonly intrude into weakened zones through the crust, such as large rifts and sutures between former continents. Thus, the 560 to 580 Ma old Sarfartôq carbonatite and associated kimberlites occupy the northern margin of the stable Archaean block, and the *c.* 1300 to 1100 Ma old Gardar magmas, including the carbonatite within the Grønnedal-Ika alkaline complex, were emplaced in major rift zones close to the southern margin of the Archaean block.

The Tikiusaaq carbonatite and the nearby lamprophyre dykes, together with the lamprophyre dykes at Kangerluarsoruseq are situated near the proposed collision zone between the northern margin of an Archaean continent (the Tasiusarsuaq terrane) and another continent (Friend *et al.* 1988; McGregor *et al.* 1991). This suggests that the newly discovered occurrences of alkaline rocks could be the eastern part of a tract extending along the continent margin, and that more alkaline dykes could be found in this tract. Furthermore, the existence of ultramafic lamprophyres in this area opens a possibility of obtaining xenocrystic material from a part of the mantle below Greenland that is presently unknown. Finally, the discovery of the carbonatite and ultramafic lamprophyres adds to the mineral potential of this part of Greenland.

References

Frei, D., Hollis, J.A., Gerdes, A., Karlsson, C., Vasquez, P., Franz, G., Harlov, D., Johansson, L. & Knudsen, C. 2006: Advanced *in situ* trace element and geochronological microanalysis of geomaterials by laser ablation techniques. Geological Survey of Denmark and Greenland Bulletin **10**, 25–28.

Friend, C.R.L., Nutman, A.P. & McGregor, V.R. 1988: Late Archaean terrane accretion in the Godthåb region, southern West Greenland. Nature **335**, 535–538.

Knudsen, C. 1991: Petrology, geochemistry and economic geology of the Qaqarssuk carbonatite complex, southern West Greenland. Monograph Series of Mineral Deposits **29**, 110 pp.

Larsen, L.M. & Rex, D.C. 1992: A review of the 2500 Ma span of alkaline-ultramafic, potassic and carbonatitic magmatism in West Greenland. Lithos **28**, 367–402.

McGregor, V.R., Friend, C.R.L. & Nutman, A.P. 1991: The late Archaean mobile belt through Godthåbsfjord, southern West Greenland: a continent–continent collision zone? Bulletin of the Geological Society of Denmark **39**, 179–197.

Rasmussen, T.M. 2002: Aeromagnetic survey in central West Greenland: project Aeromag 2001. Geology of Greenland Survey Bulletin **191**, 67–72.

Secher, K. & Larsen, L.M. 1980: Geology and mineralogy of the Sarfartôq carbonatite complex, southern West Greenland. Lithos **13**, 199–212.

Secher, K. 1986: Exploration of the Sarfartôq carbonatite complex, southern West Greenland. Rapport Grønlands Geologiske Undersøgelse **128**, 89–101.

Steenfelt, A. 2001: Geochemical atlas of Greenland – West and South Greenland. Danmarks og Grønlands Geologiske Undersøgelse Rapport **2001/46**, 39 pp. (1 CD-ROM).

Ussing, N.V. 1912: The geology of the country around Julianehaab, Greenland. Meddelelser om Grønland **38**, 1–426.

Author's address

Geological Survey of Denmark and Greenland, Øster Voldgade 10, DK-1350 Copenhagen K, Denmark. E-mail: *ast@geus.dk*

Archetypal kimberlite from the Maniitsoq region, southern West Greenland and analogy to South Africa

Troels F.D. Nielsen, Martin Jebens, Sven M. Jensen & Karsten Secher

Ultramafic dyke rocks with kimberlitic megacrysts and mantle nodules have been known for decades from the northern part of the Archaean block and adjacent Proterozoic terranes in southern West Greenland (Fig. 1; Escher & Watterson 1973; Goff 1973; Scott 1981; Larsen & Rex 1992; Mitchell *et al.* 1999). Some of the dykes have proved to be diamondiferous (see Jensen *et al.* 2004a, b, for exploration results, diamond contents, and references). The *c.* 600 Ma old dykes were called 'kimberlitic' by Larsen & Rex (1992), but Mitchell *et al.* (1999) concluded that they were best referred to a 'carbonatite-ultramafic lamprophyre' suite (aillikites or melnoites). Mitchell *et al.* (1999) further suggested that the West Greenland province represents "one of the few *bona fide* examples of ultramafic lamprophyre which contain diamonds".

Reports on indicator mineral assemblages (Jensen *et al.* 2004b) and diamond contents (e.g. Hudson Resources Inc. 2005) have re-opened the discussion on the classification of the dykes. The results of an investigation of the Majuagaa dyke (Nielsen & Jensen 2005) are summarised below, together with the preliminary results of a regional investigation of the groundmass minerals of the dykes. It is concluded that dykes in the Maniitsoq region are similar to archetypal, South African, on-craton, Type 1 kimberlites, and that all regions of the West Greenland province of ultramafic magmatism are favourable for diamond exploration.

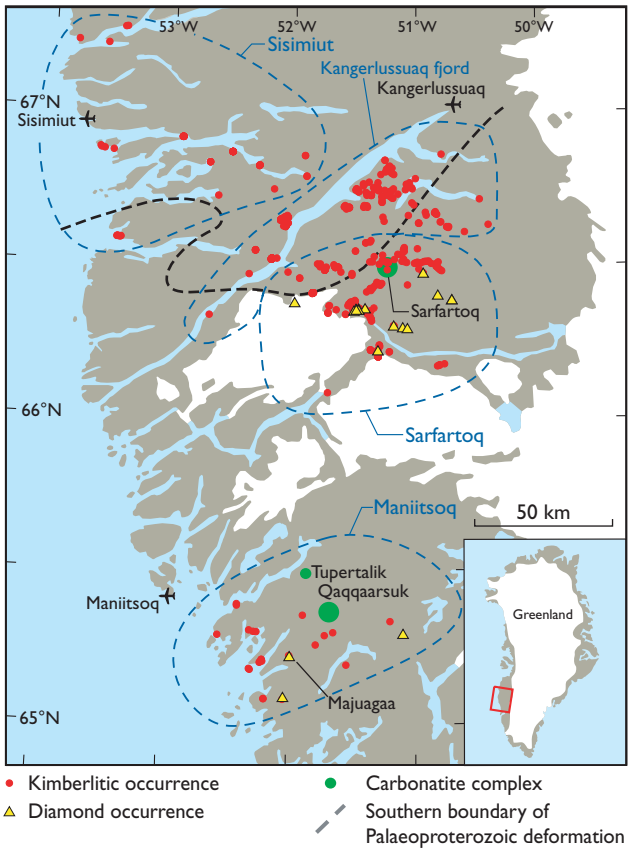

Fig. 1. Kimberlites and ultramafic lamprophyres (kimberlitic occurrences), carbonatite complexes and diamond occurrences in southern West Greenland (after Jensen & Secher 2004). Regions are indicated.

The Majuagaa dyke

The Majuagaa dyke (Jensen *et al.* 2004a) is 2.5 km long and up to 2 m wide. It is located *c.* 50 km SSE of Maniitsoq (Fig. 1) and strikes WSW–ENE. The dyke is dark grey with many olivine-rich fragments (up to 10 cm) and rounded megacrysts of ilmenite (up to 4 cm). It contains the classic kimberlitic suites of megacrysts and mantle nodules, including eclogite (Jensen & Secher 2004, fig. 5). The groundmass is fine-grained and composed of olivine fragments, calcite, serpentine, ilmenite and minor Mg-rich spinel. Phlogopite and apatite are rare. The dyke is diamondiferous (Jensen *et al.* 2004a).

Samples were collected along the length of the dyke. Sixty thin sections (Fig. 2) were examined and a number selected for an electron microprobe study. All mineral data from groundmass, megacysts and nodules, the bulk chemistry, and analytical techniques are reported in Nielsen & Jensen (2005).

Classification of the Majuagaa dyke

Mitchell (1995) and Tappe *et al.* (2005) use the following criteria for the classification of kimberlite (*s.s.*): (1) the groundmass contains no clinopyroxene; (2) groundmass spinel belongs to the Magmatic Trend 1 (Mg-rich titanomagnetite); (3) phlogopite is zoned towards the Al_2O_3- and BaO-rich kinoshitalite endmember and (4) ilmenite has a high geikilite component (> 40 mol.% $MgTiO_3$) and little pyrophanite ($MnTiO_3$). Mitchell *et al.* (1999) found that these criteria were not met by the West Greenland dykes and concluded they were ultramafic lamprophyres (aillikites or melnoites) rather than kimberlites.

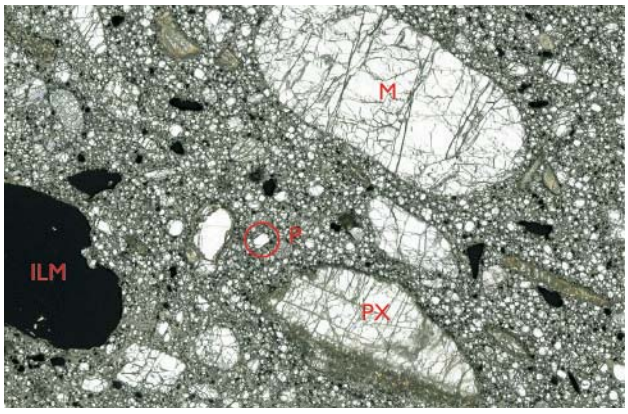

Fig. 2. Plain polarised photograph of thin section (22 x 40 mm) from the Majuagaa kimberlite. The rock is composed of fragments of olivine, ilmenite and pyroxene from disintegrated megacrysts and nodules in a groundmass of calcite, serpentine, spinel and ilmenite and rare phlogopite and apatite. Only a single olivine microphenocryst is observed (**P**). **M**: olivine megacryst; **PX**: fragment of clinopyroxene megacryst and **ILM**: ilmenite megacryst.

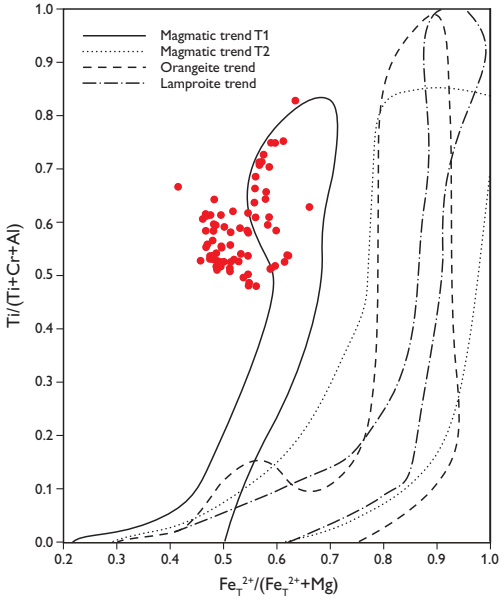

Fig. 3. Cores of groundmass spinels plot in the field of the Magmatic Trend 1 spinels of archetypal kimberlites (after Nielsen & Jensen 2005). Rim compositions to the left of the field are characteristic of calcite kimberlites (Mitchell 1995). All other fields after Mitchell (1995).

Nielsen & Jensen (2005) made the following observations in the Majuagaa dyke:

- *The clinopyroxene criteria:* No clinopyroxene was found in the groundmass.
- *The Magmatic Trend 1 spinel criteria:* The cores of euhedral spinel grains (< 0.1 mm across) have compositions in the Magmatic Trend 1 field (Fig. 3). Mg-rich rims compare with spinels of South African calcite-kimberlite (Mitchell *et al.* 1999).
- *The ilmenite criteria:* Groundmass grains conform with the compositions from archetypal kimberlite (Fig. 4), whereas megacrysts appear to be xenocrystic (Nielsen & Jensen 2005).
- *The phlogopite criteria:* Tiny, euhedral, clear to weakly greenish flakes are rich in Al_2O_3 and BaO (Fig. 5), poor in TiO_2 and FeO (total) and rich in the kinoshitalite end member. They conform with phlogopite of archetypal kimberlite (see Mitchell 1995).

Majuagaa bulk composition

The bulk composition of the Majuagaa dyke is kimberlitic (see Nielsen & Jensen 2005). The average REE (Fig. 6) and trace element (Fig. 7) compositions of the Majuagaa dyke folow the base of the fields of Kimberley (South Africa), on-craton, Type 1 kimberlites (Le Roex *et al.* 2003). The Majuagaa dyke shows positive Ti-, Nb- and Ta-anomalies. They are caused by a high proportion of ilmenite megacrysts. In mineralogy (see above) as well as bulk chemistry the Majuagaa dyke is best compared to classic South African, on-craton, Type 1 kimberlite.

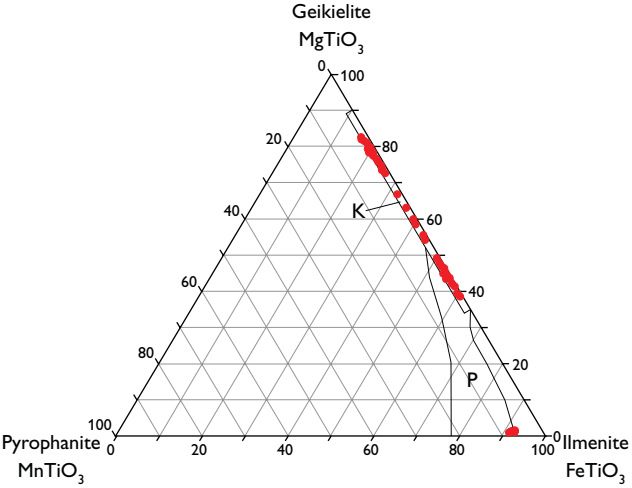

Fig. 4. Proportions of ilmenite endmembers of the Majuagaa dyke. Fields for kimberlite and Premier Mine kimberlite (**P**) from South Africa are shown (after Nielsen & Jensen 2005).

Regional variations

The West Greenland province is part of the *c.* 600 Ma old North Atlantic province of carbonatite and ultramafic alkaline magmatism, from the Torngat region (Canada) to the Archaean of West Greenland (Tappe *et al.* 2004). The compositions of groundmass phlogopite reflect the compositions of the melts (Mitchell 1995). The preliminary results of a regional investigation (Fig. 8) suggest a gradual evolution from on-craton, South African Type 1 kimberlite in the West Greenland Archaean craton (Maniitsoq), through a kimberlite/ultramafic lamprophyre (kimberlite/aillikite) zone at the border between Archaean and Proterozoic terranes (Sarfartoq and along the Kangerlussuaq fjord, Fig. 1) to ultramafic lamprophyre (aillikite/melnoite) magmatism in the Proterozoic terranes of Sisimiut (Greenland; Scott 1977) and Torngat (Canada; Tappe *et al.* 2004).

The diamond potential

Results of Hudson Resources Inc. (2005) suggest that stones of gem quality and size may be found in West Greenland. Nevertheless, it appears to be an issue for some exploration companies and investors that Mitchell *et al.* (1999) classified the West Greenland dykes as ultramafic lamprophyres and implied that true kimberlite was not found.

However, the Majuagaa dyke documents that diamondiferous, archetypal Type 1 kimberlite occurs in the West Greenland province. Hutchison (2005) describes the best investigated and most promising West Greenland diamond occurrence at 'Garnet Lake' (border zone; Sarfartoq region, Fig. 1). The 'Garnet Lake' dykes have characteristics of both kimberlite and ultramafic lamprophyre and have features reminiscent of South African orangeite. Finally, the ultramafic lamprophyres (aillikites/melnoites) of the Proterozoic Sisimuit region compare with diamondiferous ultramafic lamprophyres (aillikites) of the Torngat region (Fig. 8; Tappe *et al.* 2004), and a diamond potential is also indicated in the little prospected Sisimiut region.

Conclusions

The *c.* 600 Ma old ultramafic magmatism of the West Greenland province shows – from the Archaean craton to the Proterozoic terranes – a transition from classic South African, on-craton Type 1 kimberlite to ultramafic lamprophyre (aillikite/melnoite). Diamonds are recovered from the entire range and a diamond potential thus exists throughout the West Greenland province.

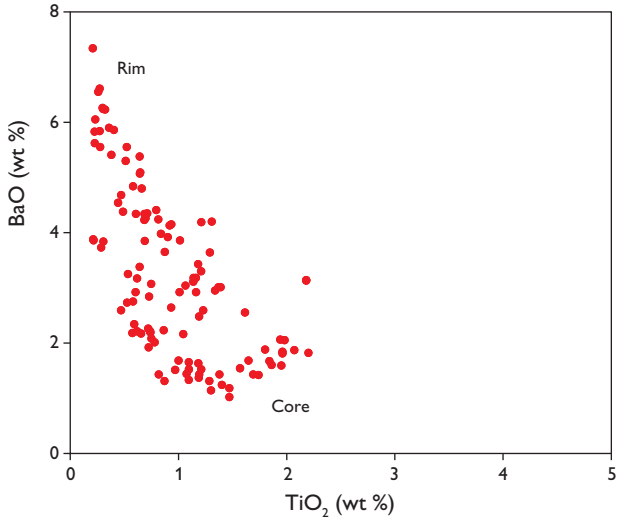

Fig. 5: BaO vs. TiO_2 in groundmass phlogopite of the Majuagaa dyke showing the general increase in BaO and decrease in TiO_2 in the margins of the grains (after Nielsen & Jensen 2005).

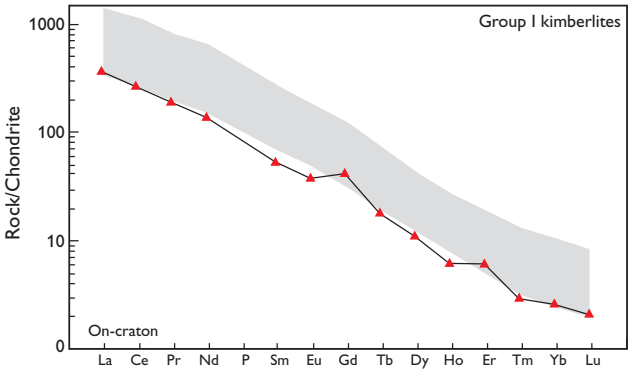

Fig. 6. Chondrite normalised bulk REE concentrations of the Majuagaa dyke (after Nielsen & Jensen 2005). **Grey field**: Kimberley (South Africa), Type 1 kimberlites (Le Roex *et al.* 2003).

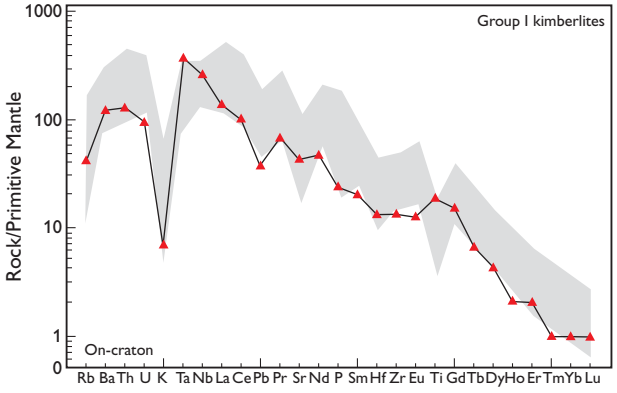

Fig. 7. Trace element concentrations of the Majuagaa dyke normalised to primitive mantle (after Nielsen & Jensen 2005). **Grey field**: Kimberley (South Africa), Type 1 kimberlites (Le Roex *et al.* 2003).

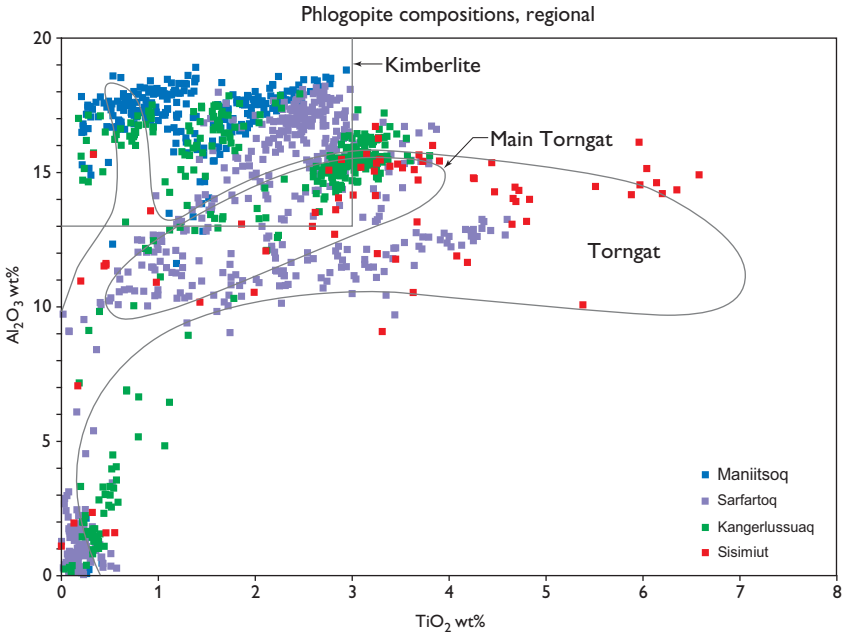

Fig. 8. Al_2O_3 vs. TiO_2 of groundmass phlogopites from the Maniitsoq (Archaean craton), Sarfartoq and Kangerlussuaq fjord (border zone to the Proterozoic) and Sisimiut (Proterozoic) regions. The Sisimiut data (Scott 1977) includes one locality referred to the border zone. Kimberlite box in top-left corner after Mitchell (1995). Torngat field after Tappe *et al.* (2004).

Acknowledgements

The investigation was carried out under contract with the Bureau of Minerals and Petroleum (BMP), Nuuk, Greenland.

References

Escher, A. & Watterson, J. 1973: Kimberlites and associated rocks in the Holsteinsborg – Søndre Strømfjord region, central West Greenland. Rapport Grønlands Geologiske Undersøgelse **55**, 26–27.

Goff, S.P. 1973: The mineralogy and mineral chemistry of a kimberlite dike from Søndre Isortoq fjord, south-west Greenland, 103 pp. Unpublished Ph.D. thesis, University of Leicester, United Kingdom.

Hudson Resources Inc. 2005: Hudson finds larger diamonds at Garnet Lake and confirms new diamond area. Web release, December 1, 2005 (info@hudsonresources.ca).

Hutchison, M.T. 2005: Diamondiferous kimberlites from the Garnet Lake area, West Greenland: exploration, methologies and petrochemistry. In: Secher, K. & Nielsen, M.N. (eds): Workshop on Greenland´s diamond potential, 7–9 November 2005, in Copenhagen. Danmarks og Grønlands Geologiske Undersøgelse Rapport **2005/68**, 33–42.

Jensen, S.M. & Secher, K. 2004: Investigating the diamond potential of southern West Greenland. Geological Survey of Denmark and Greenland Bulletin **4**, 69–72.

Jensen, S.M., Secher, K. & Rasmussen, T.M. 2004a: Diamond content of three kimberlitic occurrences in southern West Greenland. Diamond identification results, field description and magnetic profiling. Danmarks og Grønlands Geologiske Undersøgelse Rapport **2004/19**, 41 pp.

Jensen, S.M., Secher, K., Rasmussen, T.M. & Schjøth, F. 2004b: Diamond exploration data from West Greenland: 2004 update and revision. Danmarks og Grønlands Geologiske Undersøgelse Rapport **2004/117**, 90 pp. (1 DVD enclosed).

Larsen, L.M. & Rex, D.C. 1992: A review of 2500 Ma span of alkaline, ultramafic, potassic and carbonatitic magmatism in West Greenland. Lithos **28**, 367–402.

Le Roex, A.P., Bell, D.R. & Davis, P. 2003: Petrogenesis of group 1 kimberlites from Kimberley, South Africa: evidence from bulk-rock geochemistry. Journal of Petrology **31**, 779–812.

McDonough, W.F. & Sun, S.-S. 1995: The composition of the Earth. Chemical Geology **120**, 223–253.

Mitchell, R.H. 1995: Kimberlites, orangeites and relates rocks, 410 pp. New York / London: Plenum Press.

Mitchell, R.H., Scott Smith, B.H. & Larsen, L.M. 1999: Mineralogy of ultramafic dikes from the Sarfartoq, Sisimiut and Maniitsoq areas, West Greenland. In: Gurney, J.J. *et al.* (eds): Proceedings of the Vita International Kimberlite Conference **2**, 574–583. Cape Town: Red Roof Design.

Nielsen, T.F.D. & Jensen, S.M. 2005: The Majuagaa calcite-kimberlite dyke, Maniitsoq, southern West Greenland. Danmarks og Grønlands Geologiske Undersøgelse Rapport **2005/43**, 59 pp.

Scott, B.H. 1977: Petrogenesis of kimberlites and associated potassic lamprophyres from central West Greenland, 133 pp., + 6 appendices. Unpublished Ph.D. thesis, University of Edinburgh, United Kingdom.

Scott, B.H. 1981: Kimberlite and lamprophyre dykes from Holsteinsborg, West Greenland. Meddelelser om Grønland. Geoscience **4**, 24 pp.

Tappe, S., Jenner, G.A., Foley, S.F., Heaman, L.M., Besserer, D., Kjarsgaard, B.A. & Ryan, A.B. 2004: Torngat ultramafic lamprophyres and their relation to the North Atlantic alkaline province. Lithos **76**, 491–518.

Tappe, S., Foley, S.F., Jenner, G.A. & Kjarsgaard, B.A. 2005: Integrating ultramafic lamprophyres into the IUGS classification of igneous rocks: rational and implications. Journal of Petrology **46**, 1893–1900.

Authors' address

Geological Survey of Denmark and Greenland, Øster Voldgade 10, DK-1350 Copenhagen K, Denmark. E-mail: *tfn@geus.dk*

Using zircon geochronology to resolve the Archaean geology of southern West Greenland

Julie A. Hollis, Dirk Frei, Jeroen A.M. van Gool, Adam A. Garde and Mac Persson

Until recently, *in situ* U-Pb zircon geochronology could be carried out only using ion microprobes, requiring lengthy analysis times of *c.* 20 minutes. However, new developments in laser ablation inductively coupled plasma mass spectrometer technologies have resulted in zircon geochronology techniques that are much faster, simpler, cheaper, and more precise than before (e.g. Frei *et al.* 2006, this volume). Analyses approaching the precision obtained via ion microprobe can now be undertaken in 2–4 minutes using instruments such as the 213 nm laser ablation (LA) system coupled with Element2 sector-field inductively coupled plasma mass spectrometer (SF-ICP-MS) housed at the Geological Survey of Denmark and Greenland (GEUS). The up to tenfold decrease in analytical time means that zircon geochronology can now be used in a much wider range of studies.

The Godthåbsfjord region, southern West Greenland, contains some of the oldest rocks exposed on the Earth's surface reflecting a very complex Archaean geological evolution (Figs 1, 2). Over recent years GEUS has undertaken a range of mapping projects at various scales within the Godthåbsfjord region (see also below). These include the mapping of the 1:100 000 scale Kapisillit geological map sheet (Fig. 1), and regional and local investigations of the environments of formation and geological evolution of supracrustal belts, hosting potentially economic mineral occurrences.

Zircon geochronology is an important tool for investigating a range of geological problems in this region. By breaking down the complex geology into a series of simple problems that can be addressed using this tool, the geological evolution can be unlocked in a stepwise manner. Three examples are presented below: (1) the mapping of regional structures; (2) characterising and correlating supracrustal belts; and (3) dating metamorphism and mineralisation. Although focus is on the application of zircon geochronology to these problems, it is important to note that the resulting data must always be viewed within a wider context incorporating geological mapping and structural, geochemical and petrographic investigations.

Regional geology

The geology of the Godthåbsfjord region is dominated by orthogneiss formed during several distinct episodes of crustal growth during the Archaean (Fig. 2). These different-aged gneisses are thought to represent distinct small continental blocks that were amalgamated during the Neoarchaean (at

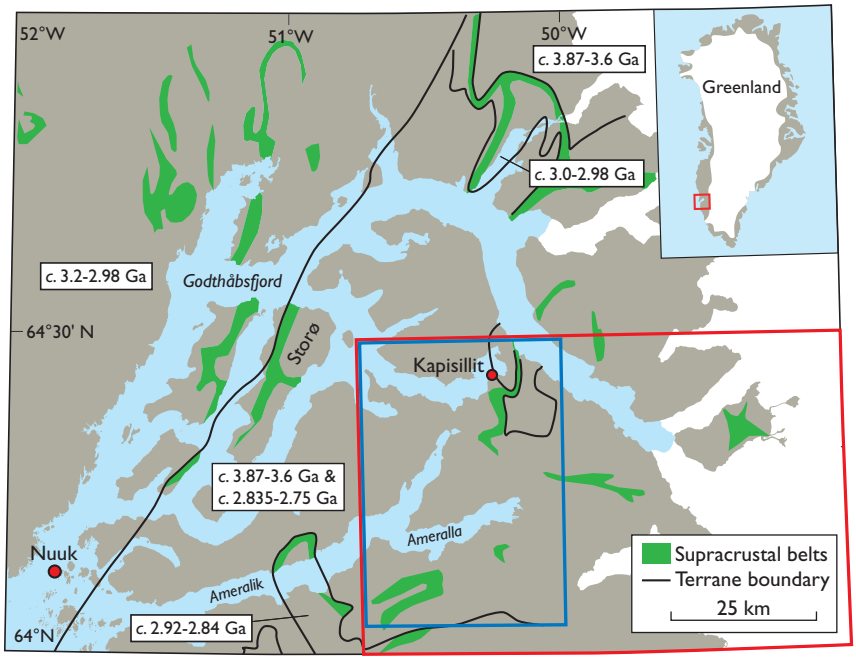

Fig. 1. Overview map of the Godthåbsfjord region. Inset shows the location of the main map in Greenland. Supracrustal belts are shown in **green**. The boundaries of the 1:100 000 scale Kapisillit geological map sheet area are in **red**. **Blue lines** outline the area shown in Fig. 3. **Bold black lines** are inferred terrane boundaries, with the major age components of the different terranes indicated (after Friend & Nutman 2005).

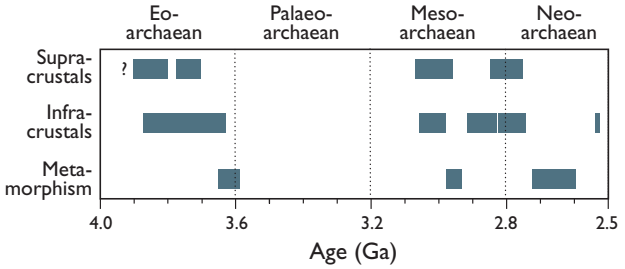

Fig. 2. Simplified summary of the major thermal events in the Godthåbsfjord region.

c. 2.7–2.6 Ga) during collisional tectonism (similar to that seen in modern mountain belts). Within, and often between, these different crustal blocks, or terranes, supracrustal belts made up of metasedimentary and metavolcanic rocks occur. Some of these are known to host potentially economic mineral occurrences, e.g. gold-mineralised supracrustal rocks on the island Storø (Fig. 1).

Several high-grade metamorphic events and associated deformation have affected different parts of the region from the Palaeoarchaean through to the Neoarchaean. These events resulted in partial melting, variable development of high-strain structural fabrics, and several generations of large-scale folds.

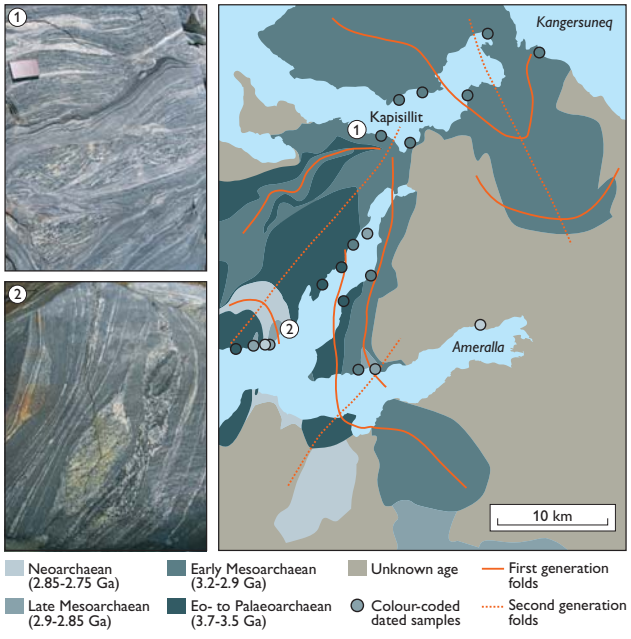

Fig. 3. Simplified version of map of major fold structures in the Kapisillit 1:100 000 scale geological map area. **Coloured circles** indicate the sites where zircons from rock samples have been dated. The **fill colours** indicate the obtained ages. These ages have been used to constrain the surface geometry of the folds. Photographs of outcrops of orthogneiss from two localities show that rocks of very similar appearance can be very different ages and therefore geochronology is useful in distinguishing them.

Mapping major regional structures

Although the orthogneisses that dominate the geology of the region were formed during several distinct events, different generations of orthogneisses are often very difficult to distinguish in the field owing to their similarity of composition (Fig. 3). The geometry of supracrustal belts is very useful in identifying the nature of regional structures, as these are lithologically very different from the orthogneisses and can be used as structural markers. However, where these are absent reconnaissance geochronology can be applied. Having identified several of the main crust-forming events in the region, it is possible to use the emplacement ages of orthogneisses as a guide to field mapping and the delineation of large-scale structures.

Selected samples collected during the 2004 field mapping were dated using LA-SF-ICP-MS U-Pb zircon geochronology (Fig. 2). Major fold structures inferred from field mapping data were dated using this method, in some cases resulting in significant advances in understanding. So far the results indicate that Mesoarchaean rocks were thrust northwards over Neo- and Eo- to Palaeoarchaean rocks and then deformed in kilometre-scale refolded folds (Fig. 3). The resulting map was used to identify problematic areas to investigate during the 2005 mapping.

Identifying and correlating supracrustal belts

Figure 1 shows the distribution of known supracrustal belts in the Godthåbsfjord region, typically comprising high-grade metamorphic volcanic, ultramafic, subordinate aluminous and siliceous sedimentary rocks. These were once thought to represent a single, dismembered suite of Mesoarchaean supracrustal rocks. It is now known that there are in fact several distinct belts deposited at *c.* 3.87 and 3.7 Ga (the Isua supracrustal belt), *c.* 3.0 Ga, and at *c.* 2.8 Ga (Fig. 2). These belts commonly occur along tectonised boundaries between chronologically distinct terranes.

Correlation between different supracrustal belts is important for understanding the regional structures and identifying areas of potentially economic mineral occurrences. Some belts show lithological and geochemical differences, and similarities that can be used to compare and contrast them. These indicate that there are at least three different environments that were important in forming the different belts: (1) basic volcanism in extensional oceanic environments; (2) gabbro-anorthosite magmatism at deeper levels within oceanic crust; and (3) andesitic volcanism and associated hydrothermal syngenetic alteration in island-arc environments (Garde 2005; Hollis 2005). However, the majority of

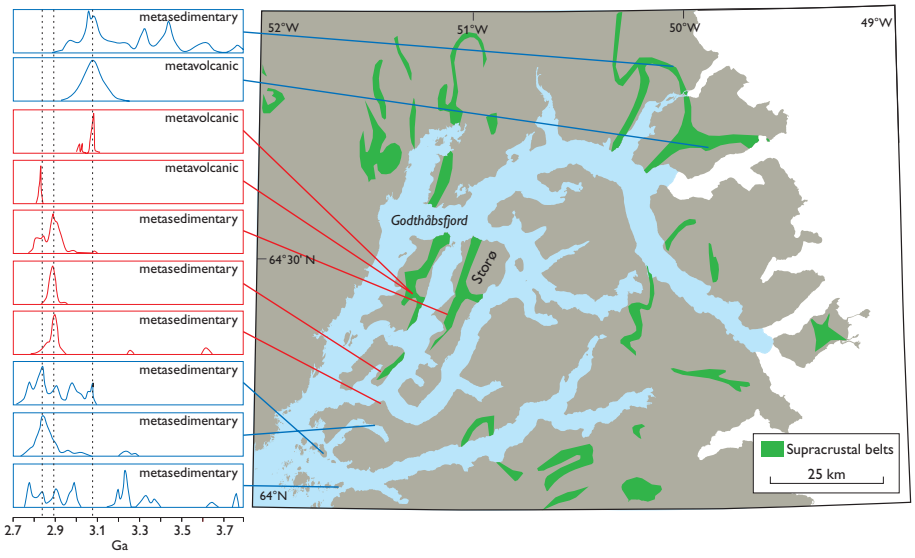

Fig. 4. Detrital zircon populations linked to the distribution of supracrustal belts. Inset shows the location of the main map in Greenland. **Red** zircon spectra were collected using the GEUS LA-SF-ICP-MS. **Blue** zircon spectra are taken from Nutman *et al.* (2004) and Schiøtte *et al.* (1988). **Dotted lines** show regionally significant age peaks at 3.07, 2.89 and 2.83 Ga.

the belts are strongly tectonised and extensive recrystallisation occurred during high-grade metamorphism. Locally hydrothermal alteration is very intense. Therefore, the protoliths are difficult to recognise and the different supracrustal belts are difficult to distinguish without detailed geochemical and geochronological information.

One of the most important tools for correlation is the study of detrital zircons. Siliceous and aluminous metasedimentary rocks carry detrital zircons derived from the erosion of the source regions for the sediments. Thus studies of their detrital zircons allow an assessment of both likely sources and their maximum age of deposition (given by the youngest detrital zircon). Furthermore, the detrital zircon age spectrum of a metasedimentary rock from a specific supracrustal belt is often characteristic, as the zircons are typically derived from the same source area. The detrital spectra can therefore be used to correlate between widely spaced supracrustal belts that would otherwise be difficult to compare from petrographic or geochemical data alone.

A compilation of existing and recently obtained detrital zircon data for metasedimentary rocks and primary zircons from metavolcanic or volcanoclastic rocks in the Godthåbsfjord region is shown in Fig. 4 (see also Hollis 2005). Distinct sources for supracrustal rocks of different ages are readily apparent. The volcanic rocks that form part of the Mesoarchaean supracrustal belts were deposited at *c.* 3.07 Ga, which is just slightly older than the dominant Mesoarchaean regional orthogneiss. Similarly, metasedimentary rocks within the Mesoarchaean supracrustal belts show dominant zircon age peaks at *c.* 3.07 Ga. However, significant proportions of older zircons show that there was also a contribution from Palaeo- and Eoarchaean sources. The Neoarchaean volcanic rocks were deposited at *c.* 2.83 Ga, which is also an age that is well represented in the detrital zircon population of most of the Neoarchaean metasedimentary rocks. A few metasedimentary samples show relatively minor contributions from older Meso- to Eoarchaean material. The synchronous sedimentation and generation of volcanic material at *c.* 3.07 Ga (Mesoarchaean) and at *c.* 2.83 Ga (Neoarchaean) suggests there may have been a common tectonic environment operating at both times.

When did metamorphism and mineralisation occur?

The Godthåbsfjord region records a complex history of high-grade metamorphism, which affected different parts of the Godthåbsfjord region at different times, from *c.* 3.8–2.5 Ga. The record of particular metamorphic events in different parts of the region has been used to establish the times when different terranes were amalgamated via collisional tectonism (e.g. Friend & Nutman 2005). The timing of metamorphism and contemporaneous deformation has also been used to constrain the timing of mineralisation events.

On Storø in central Godthåbsfjord (Fig. 1) detailed studies of the nature and timing of gold mineralisation have been carried out. Here gold-mineralised strataform horizons and cross-cutting quartz veins occur within a Neoarchaean supracrustal belt that was deposited at or after 2.8 Ga. The gold-bearing horizons are deformed by the kilometre-wide, high-grade Storø shear zone; thus the generation of the shear fabric post-dates the gold-mineralising event. To place absolute constraints on the timing of gold mineralisation the timing of emplacement of some of the abundant granitic pegmatites that either cross-cut or are deformed by the shear fabric has been investigated (Fig. 5). Four pegmatites contained

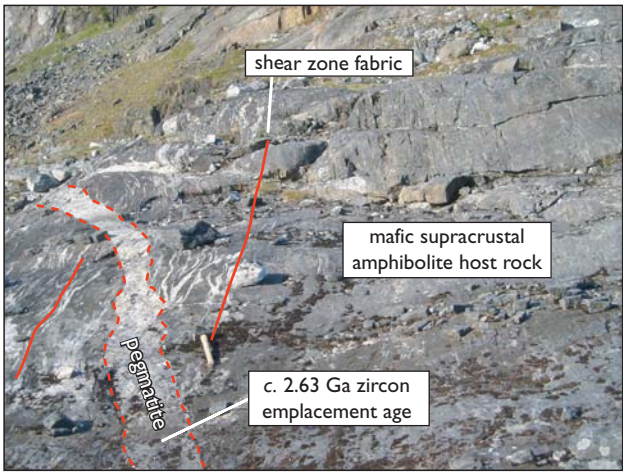

Fig. 5. Pegmatite on Storø cross-cutting and deformed by the Storø shear zone fabric, and Neoarchaean supracrustal amphibolite host rock. Zircons from the pegmatite indicate it was formed at *c.* 2.63 Ga, placing a minimum age constraint on gold mineralisation in the host rocks.

igneous zircon crystallised at *c.* 2.63–2.60 Ga. This is the same age as yielded by metamorphic zircons separated from a leucocratic amphibolite, and from metamorphic overgrowths on detrital zircons taken from a melt layer within a migmatised metasedimentary rock, both within the same supracrustal sequence on Storø. These results show that a gold-mineralising event occurred within the Neoarchaean supracrustal belt during or after sedimentation at *c.* 2.8 Ga and before the formation of the Storø shear zone during high-grade metamorphism and partial melting at *c.* 2.63 Ga. These results constrain the timing of mineralisation and may be extended to the investigation of rocks of similar age and setting elsewhere in the region.

Further work

This work forms part of ongoing studies of the supracrustal belts in the Godthåbsfjord region carried out with support from the Greenland Bureau of Minerals and Petroleum. In addition to the examples given here, the GEUS LA-SF-ICP-MS system can also be used to investigate the cooling history of rocks via U-Pb dating of zircon and other minerals, including titanite and monazite. Furthermore, by exploring other aspects of zircon geochemistry, such as Hf and O isotopes it may also be possible to delve deeper into issues of crustal evolution of the North Atlantic Craton through the Archaean.

References

Garde, A.A. 2005: A mid-Archaean island arc complex with gold mineralisation at Qussuk, Akia terrane, southern West Greenland. In: Hollis, J.A. (ed.): Greenstone belts in the central Godthåbsfjord region, southern West Greenland: Geochemistry, geochronology and petrography arising from 2004 field work, and digital map data. Danmarks og Grønlands Geologiske Undersøgelse Rapport **2005/42**, 215 pp., 1 DVD.

Hollis, J.A. (ed.) 2005: Greenstone belts in the central Godthåbsfjord region, southern West Greenland: Geochemistry, geochronology and petrography arising from 2004 field work, and digital map data. Danmarks og Grønlands Geologiske Undersøgelse Rapport **2005/42**, 215 pp., 1 DVD.

Frei, D., Hollis, J.A., Gerdes, A., Harlov, D., Karlsson, C., Vasquez, P., Franz, G. & Knudsen, C. 2006: Advanced *in situ* geochronological and trace element microanalysis by laser ablation techniques. Geological Survey of Denmark and Greenland Bulletin **10**, 25–28.

Friend, C.R.L. & Nutman, A.P. 2005: New pieces to the Archaean terrane jigsaw puzzle in the Nuuk region, southern West Greenland: Steps in transforming a simple insight into a complex regional tectonothermal model. Journal of the Geological Society (London) **162**, 147–162.

Nutman, A.P., Friend, C.R.L., Barker, S.L.L. & McGregor, V.R. 2004: Inventory and assessment of Palaeoarchaean gneiss terraines and detrital zircons in southern West Greenland. Precambrian Research **135**, 281–314.

Schiøtte, L., Compston, W. & Bridgwater, D. 1988: Late Archaean ages for the deposition of clastic sediments belonging to the Malene supracrustals, southern West Greenland: evidence from an ion probe U-Pb zircon study. Earth and Planetary Science Letters **87**, 45–58.

Authors' addresses

J.A.H., D.F., J.v.G., A.A.G., *Geological Survey of Denmark and Greenland, Øster Voldgade 10, DK-1350 Copenhagen K, Denmark.* E-mail: *jho@geus.dk*

M.P., *University of Copenhagen, Øster Voldgade 10, DK-1350 Copenhagen K.*

Five slices through the Nuussuaq Basin, West Greenland

Asger Ken Pedersen, Lotte Melchior Larsen, Gunver Krarup Pedersen and Keld S. Dueholm

In 2006 an important milestone will be reached in the study of the three-dimensional structure and architecture of the Nuussuaq Basin in West Greenland. The fifth and last of a series of detailed geological profiles through the sedimentary and volcanic rocks of the Nuussuaq Basin on Disko and Nuussuaq will be published (Fig. 1). At the same time, the last geological map at scale 1:100 000 of the basin area will be completed. These studies have been carried out over more than two decades by a group of scientists within Geocenter Copenhagen and the Technical University of Denmark.

The five geological profiles are at scale 1:20 000 and have been published as coloured plates in the same format as the geological maps (Pedersen *et al.* 1993, 2002a, 2003, 2005, 2006). In total, the profiles cover about 500 km of cross-sections through a classic sedimentary-volcanic basin and its crystalline basement. This is one of the best exposed basins of its kind on Earth, and it serves as a reference area for studies of similar basins on the continental shelves of Greenland, north-western Europe and elsewhere.

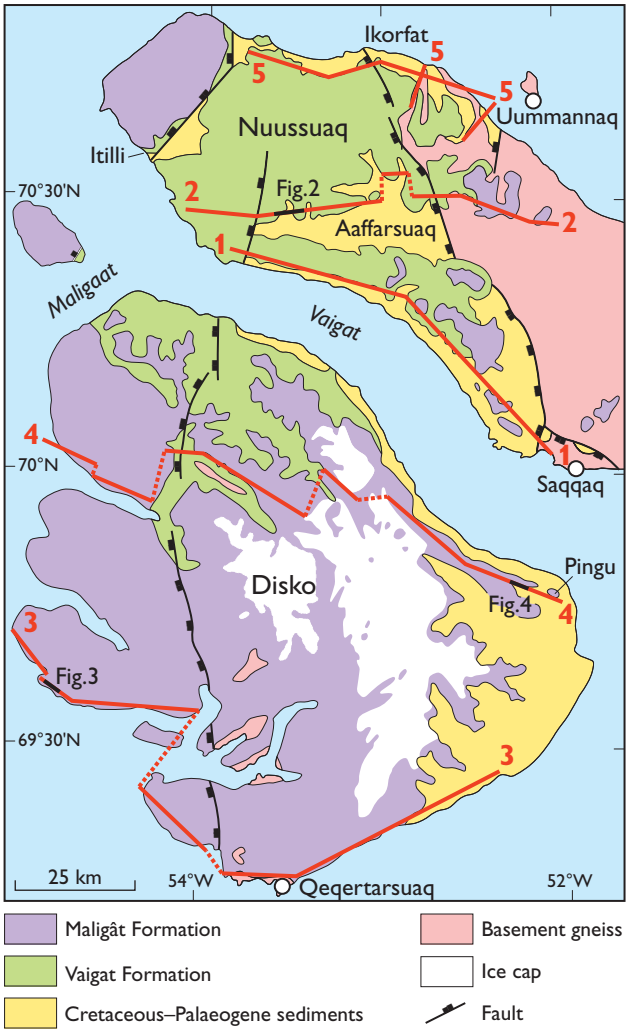

Fig. 1. Index map, with **red lines** showing the location of the five geological profiles through Disko and Nuussuaq. Profile **1**: Pedersen *et al.* (1993); profile **2**: Pedersen *et al.* (2002a); profile **3**: Pedersen *et al.* (2003); profile **4**: Pedersen *et al.* (2005); profile **5**: Pedersen *et al.* (2006).

The Nuussuaq Basin

During the late Mesozoic, a series of linked sedimentary basins were established along the West Greenland continental margin. The Nuussuaq Basin is the only one of these basins that extends into the onshore areas where Late Cretaceous to Paleocene sediments overlain by volcanic rocks can be studied in detail. From the Late Albian, sandstones and shales were deposited in a fluvial to deltaic environment in eastern Disko and central Nuussuaq. Towards west and north the delta fanned into deeper water. Several tectonic phases affected the basin and gave rise to an uplifted rift margin of Precambrian gneiss in eastern Nuussuaq and a gneiss ridge in central Disko (Chalmers *et al.* 1999). In the Paleocene around 62 Ma (Storey *et al.* 1998), volcanism started on the sea floor in the western part of the area. The volcanic pile rapidly became emergent and the lavas prograded eastwards into the marine embayment and gradually filled it with thick foreset-bedded hyaloclastites capped by subaerial lava flows. Thus, most of the early volcanic units exist in both subaerial and subaqueous facies. Eventually the marine basin, and also some slightly younger lake basins, was obliterated. The volcanic rocks interfingered with fluvial sandstones and lake sediments in southern Nuussuaq and eastern Disko, whereas in eastern Nuussuaq they lapped onto the Precambrian highlands.

The volcanic rocks form two formations: the older Vaigat Formation of thin pahoehoe flows of magnesia-rich picrites and their equivalent hyaloclastites, and the overlying Maligât Formation of thick, extensive lava flows of basalt and their

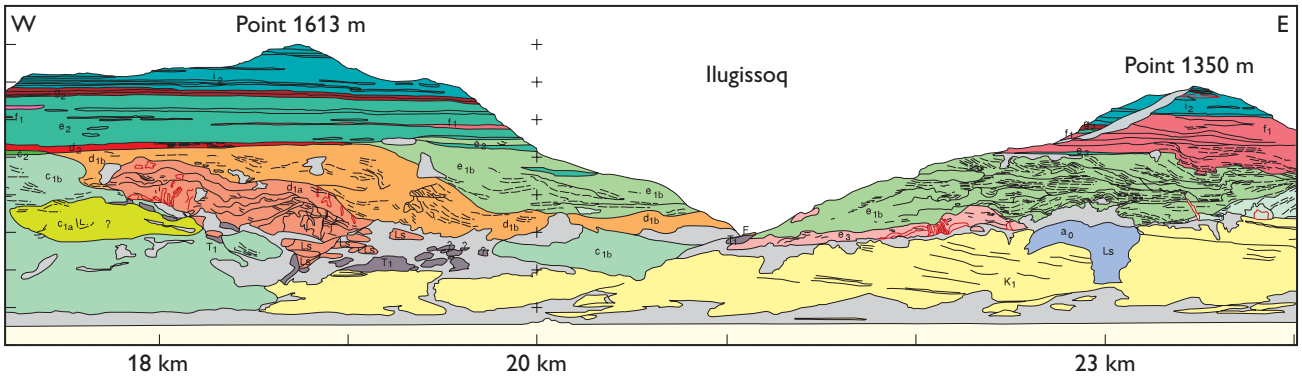

Fig. 2. Part of the geological section through the Aaffarsuaq valley (profile **2**), central Nuussuaq (Pedersen *et al.* 2002a) at 17-24 km on the section base line. No vertical exaggeration. Sediments of the Cretaceous Atane Formation (K_1) and the Paleocene Eqalulik Formation (T_1) are overlain by several volcanic units of the Vaigat Formation. The Atane Formation was faulted and tilted prior to the deposition of the volcanic rocks, and a large fault crosses the profile at 18.5 km west of which the Atane Formation is below exposure level. During the deposition of the volcanic rocks, subaqueous hyaloclastite breccias and subaerial lava flows prograded into the basin from the west to the east. Lava flows and hyaloclastite breccias from the same volcanic unit are shown with respectively darker and lighter colour shades; such subaerial–subaqueous pairs are c_2 and $c_{1(a+b)}$; d_2 and $d_{1(a+b)}$ (Nuuk Killeq Member), and e_2 and $e_{1(a+b)}$ (Naujánguit Member). The hyaloclastite breccias show east-dipping foreset bedding (d_{1b}) or irregular bedding structures (d_{1a}, e_{1b}) near eruption sites (feeder dykes lined with red). The red unit f_1, at around 23-24 km, comprises the pyroclastic rocks of the Ilugissoq volcano (Asuk Member) which erupted on the margin of the shallow marine shelf. The younger units are banked up against the volcanic edifice, and the lavas of the unit i_2 (Ordlingassoq Member) overran and covered it.

equivalent hyaloclastites. A detailed stratigraphy of the volcanic succession has been established based on lithology and geochemical analyses; several distinct units of crustally contaminated rocks form particularly good marker horizons because they are interbedded with the normal lithologies.

Oil seepages are found in the volcanic rocks in western Nuussuaq and northern Disko, and the Nuussuaq Basin is a key area in the exploration for oil both onshore and offshore West Greenland. Exploration for nickel and platinum has been focused on some of the contaminated volcanic units in which these elements are missing from the surface deposits and may have formed accumulations at depth in magma chambers.

Methods

Many mountain walls in the Nuussuaq Basin are excellently exposed but largely inaccessible. However, they can be photographed from boat or helicopter. The key data for the five geological profiles consists of long series of colour stereo photographs taken with ordinary, but calibrated, small-frame cameras. These photographs have been orientated and measured using multi-model photogrammetry as described by Dueholm (1992) and Pedersen & Dueholm (1992). In combination with field logging, sampling, geochemistry and petrography, this has enabled us to establish a detailed stratigraphical framework for the volcanic rocks and hence to trace the evolution and facies changes of the volcanic and sedimentary units with time.

The profiles

The individual profiles (Fig. 1), at scale 1:20 000, are between 80 km and 131 km long and show altitudes up to 2100 m with no vertical exaggeration. Three examples illustrating aspects of the contents and details of the profiles are shown in Figs 2-4.

Figure 2 shows progradation of hyaloclastite breccias and associated lava flows into a marine basin; this structure, with giant foresets in the hyaloclastite breccias, has been widely used as a model for the interpretation of seismic sections in offshore areas. An unusual feature of central Nuussuaq is the presence of submarine feeder systems and eruption sites for several of the volcanic units, which make the bedding structures in the hyaloclastites very irregular. The concentration of feeder sites in this small area is due to the presence of a deep fault zone, along which magma ascent from the mantle was focused.

Figure 3 illustrates late tectonic movements and subsequent dyke intrusion. Near the west coast of Disko the lava pile is faulted and tilted seawards at low angles that can be read very accurately on the profile. The reading of the dips requires that the strikes are perpendicular to the section which is mostly, but not always, the case; the index maps accompanying each profile sheet show strikes and dips of the lavas along the profiles.

Figure 4 illustrates sediments and lava flows and their interaction on the flood plain in the eastern part of the basin in north-east Disko. Fluvial sandstones are interbedded with

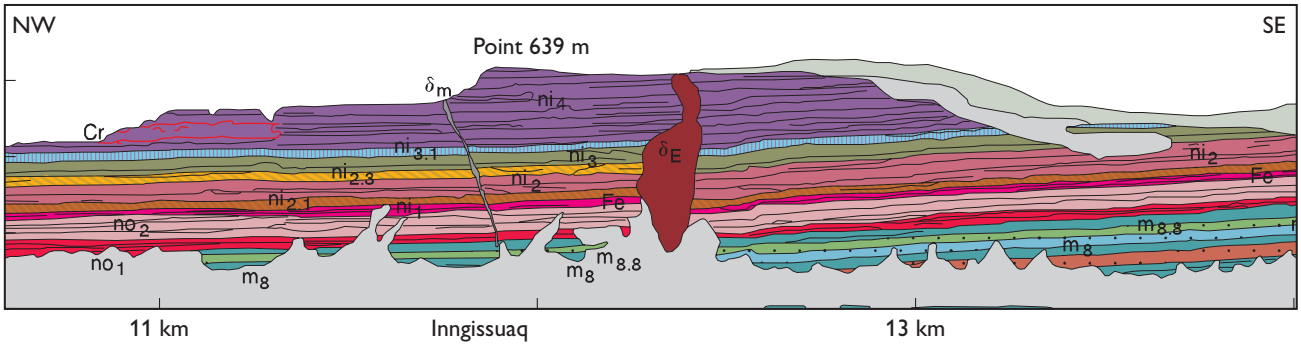

Fig. 3. Part of the geological section along the south-west coast of Disko (Pedersen *et al.* 2003) at 10.6-14 km on the section base line (profile **3**). No vertical exaggeration. The pile of formerly flat-lying subaerial lava flows is tilted and the lavas dip 2°-4° seawards (to the left), preserving some of the stratigraphically highest lava flows of the Maligât Formation on the mountain tops. The unit $m_{8.8}$ is the uppermost part of the Rinks Dal Member in which individual lava flows are indicated with separate colours and annotation (e.g. m_8); such individual flows extend typically over 5-15 km and then peter out. Units no_1 to no_2 are crustally contaminated lavas of the Nordfjord Member, and ni1 to ni_4 are crustally contaminated lavas of the Niaqussat Member, of which ni_1 carries native iron (Fe). A crater area (Cr) with thick, irregular, red-oxidised material is seen in the left part of ni_4. The lava pile is cut by younger dykes (δ_m and δ_E) of which the Eocene δE runs very obliquely to the section.

two units of Paleocene black shales, both of which were deposited in large and deep lakes. The Paleocene sediments are contemporaneous with volcanic rocks in the western part of the basin; the first volcanic unit to reach so far east was the middle part of the Rinks Dal Member of the Maligât Formation.

The boundaries between the major volcanic units form important near-isochronous surfaces that allow the tracing of regional syn- and post-volcanic tectonic movements in the Nuussuaq Basin. For example, the boundary between the upper Rinks Dal Member and the Nordfjord Member of the Maligât Formation is tilted below sea level in western Disko (Fig. 3) and rises eastwards towards the Disko Gneiss Ridge to more than 1600 m altitude in central Disko. East of the gneiss ridge the surface is gently tilted towards the south-east by slow syn- and post-volcanic regional movements, so that in eastern Disko (Fig. 4) it is situated at 940 m altitude. In eastern Nuussuaq the same surface is situated at up to 1800 m altitude (not shown here).

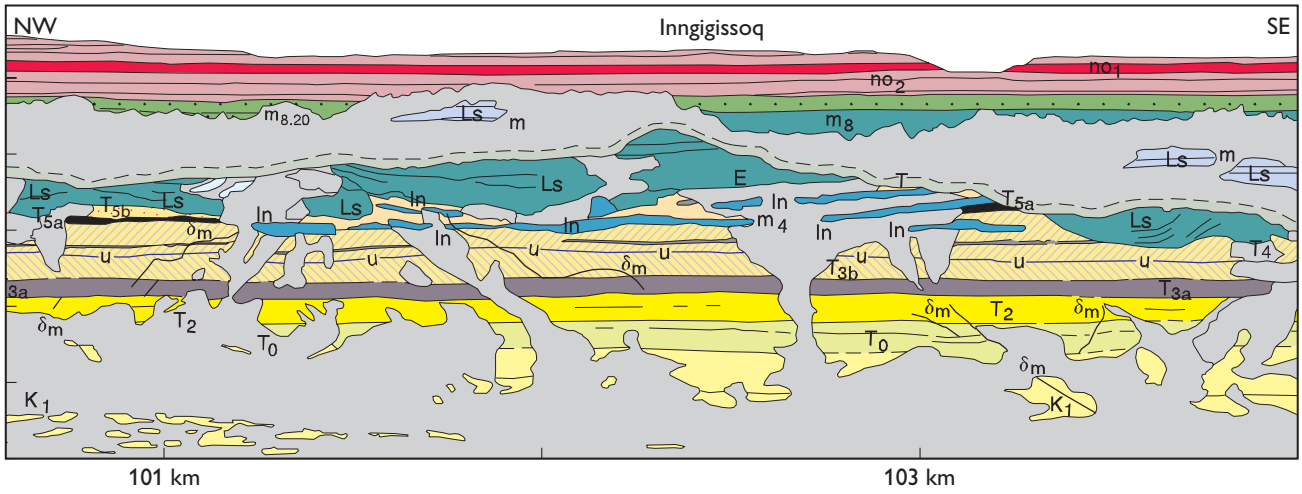

Fig. 4. Part of the geological section across Disko, near Pingu in eastern Disko (Pedersen *et al.* 2005) at 100.6-104 km on the section base line (profile 4). No vertical exaggeration. Sediments and lava flows are shown as viewed from the south, but are projected into the section both from the south (upper part) and from the north (lower part below the broken line: exposures along the Vaigat coast). Fluvial sandstones of Cretaceous (K_1) and Paleocene (T_2) age are separated by an interval of uncertain age (T_0). Two lake complexes each show filling with a coarsening-upwards succession of black mudstones and fluvial sandstones: the Pingu Member (T_{3a}-T_{3b}) and the Assoq Member (T_{5a}-T_{5b}). The level marked 'u' is an unconformity within the sandstones. Lava flows invaded the unconsolidated sediments to form three sill-like bodies (invasive lavas, In), and finally the sediments were over-run by entirely subaerial lava flows. The entablature zone (E) of the lowest flow indicates a moist environment. The lava flows are from the Maligât Formation, upper Rinks Dal Member (m_8) and Nordfjord Member (iron-bearing no_1, and no_2).

Perspectives

The completion of the five profiles, and the complementary geological maps at scale 1:100 000, has provided a significantly improved understanding of the overall three-dimensional structure and stratigraphy of the southern part of the Nuussuaq Basin, in particular of the well-exposed volcanic formations. In addition to the published profiles, an extensive web of colour stereo panels has been constructed wherever helicopter logistics allowed the photography, so that the total coverage now exceeds 1500 km of stereo panels. The existence of this web, assisted by complete on-line coverage of vertical aerial photograph models, has opened for a range of quantitative geological studies centred on volcanology, sedimentology, palaeomagnetics and tectonics. Using palaeomagnetic information, Pedersen *et al.* (2002b) calculated eruption rates and basin subsidence rates for an early part of the Vaigat Formation, and found eruption rates to be much in excess of those characterising modern Iceland. Measurements of lake depths and lateral correlation of subaqueous volcanic units over more than 20 km were instrumental for the understanding of the environment that gave rise to unique subaqueous rootless volcanic cones in the Assoq lake (Larsen *et al.* in press). The ability of the photogrammetrical method to identify volcanic eruption sites within the web of stereo panels has been demonstrated by the discovery of a large number of crater sites within the Vaigat Formation on Nuussuaq. Of particular significance is the observation that economically interesting crustally contaminated volcanic rocks tend to erupt along older fault zones within the basin. Such an example is provided by the Ilugissoq graphite andesite volcano (Pedersen & Larsen in press), which is the largest eruption site within the Vaigat Formation. It is believed that continued 3-D based work within the Nuussuaq Basin will be of considerable interest for a broad range of geoscientists from both universities and industry.

Acknowledgements

The work was partly supported by the Carlsberg Foundation, grant no. 0385/30.

References

Chalmers, J.A., Pulvertaft, T.C.R., Marcussen, C. & Pedersen, A.K. 1999: New insight into the structure of the Nuussuaq Basin, central West Greenland. Marine and Petroleum Geology **16**, 197–224.

Dueholm, K.S. 1992: Geological photogrammetry using standard small-frame cameras. In: Dueholm, K.S. & Pedersen, A.K. (eds): Geological analysis and mapping using multi-model photogrammetry. Rapport Grønlands Geologiske Undersøgelse **156**, 7–17.

Larsen, L.M., Pedersen, A.K. & Pedersen, G.K. 2006: A subaqueous rootless cone field at Niuluut, Disko, Paleocene of West Greenland. Lithos **92**, 20–32.

Pedersen, A.K. & Dueholm, K.S. 1992: New methods for the geological analysis of Tertiary volcanic formations on Nuussuaq and Disko, central West Greenland, using multi-model photogrammetry. In: Dueholm, K.S. & Pedersen, A.K. (eds): Geological analysis and mapping using multi-model photogrammetry. Rapport Grønlands geologiske Undersøgelse **156**, 19–34.

Pedersen, A.K. & Larsen, L.M. 2006: The Ilugissoq graphite andesite volcano, Nuussuaq, central West Greenland. Lithos **92**, 1–19.

Pedersen, A.K., Larsen, L.M. & Dueholm, K.S. 1993: Geological section along the south coast of Nuussuaq, central West Greenland. 1:20 000 coloured geological sheet. Copenhagen: Geological Survey of Greenland.

Pedersen, A.K., Larsen, L.M. & Dueholm, K.S. 2002a: Geological section along the north side of the Aaffarsuaq valley and central Nuussuaq, central West Greenland. 1:20 000 coloured geological sheet. Copenhagen: Geological Survey of Denmark and Greenland.

Pedersen, A.K., Larsen, L.M., Riisager, P. & Dueholm, K.S. 2002b: Rates of volcanic deposition, facies changes and movements in a dynamic basin: the Nuussuaq Basin, West Greenland, around the C27n–C26r transition. In: Jolley, D.W & Bell, B.R. (eds): The North Atlantic Igneous Province: Stratigraphy, tectonics, volcanic and magmatic processes. Geological Society (London) Special Publications **197**, 157–181.

Pedersen, A.K., Larsen, L.M., Pedersen, G.K., Heinesen, M.V. & Dueholm, K.S. 2003: Geological section along the south and south-west coast of Disko, central West Greenland. 1:20 000 coloured geological sheet. Copenhagen: Geological Survey of Denmark and Greenland.

Pedersen, A.K., Larsen, L.M., Pedersen, G.K. & Dueholm, K.S. 2005: Geological section across north central Disko from Nordfjord to Pingu, central West Greenland. 1:20 000 coloured geological sheet. Copenhagen: Geological Survey of Denmark and Greenland.

Pedersen, A.K., Larsen, L.M., Pedersen, G.K., Sønderholm, M., Midtgaard, H.H., Pulvertaft, T.C.R. & Dueholm, K.S. 2006: Geological section ≠along the north coast of the Nuussuaq peninsula, central West Greenland. 1:20 000 coloured geological sheet. Copenhagen: Geological Survey of Denmark and Greenland.

Storey, M., Duncan, R.A., Pedersen, A.K., Larsen, L.M. & Larsen, H.C. 1998: $^{40}Ar/^{39}Ar$ geochronology of the West Greenland Tertiary volcanic province. Earth and Planetary Science Letters **160**, 568–586.

Authors' addresses

A.K.P., *Geological Museum, University of Copenhagen, Øster Voldgade 5–7, DK-1350 Copenhagen K, Denmark.* E-mail: *akp@snm.ku.dk*

L.M.L., *Geological Survey of Denmark and Greenland, Øster Voldgade 10, DK-1350 Copenhagen K, Denmark.*

G.K.P., *Geological Institute, University of Copenhagen, Øster Voldgade 10, DK-1350 Copenhagen K, Denmark.*

K.S.D., *Information and Mathematical Modelling, Richard Petersens Plads, DTU-Bygning 321, DK-2800 Lyngby, Denmark.*

Earthquake seismology in Greenland – improved data with multiple applications

Tine B. Larsen, Trine Dahl-Jensen, Peter Voss, Thomas Møller Jørgensen, Søren Gregersen and Hans Peter Rasmussen

Earthquake seismology is a rapidly evolving field that has provided a wealth of new information about deep geological structures on a regional scale over the last decade as well as information about dynamic processes in the Earth. A major leap forward was the development of portable digital broad band (BB) seismographs around 1990. Without any changes in configuration, these are able to record the signals from large distant earthquakes, as well as the signals from weak local events. BB seismographs typically cover a frequency range from 0.0083 Hz to 50 Hz, making them useful for studies ranging from the high frequency signals from explosions to the very low frequency oscillations following major earthquakes. The first seismological observatory in Greenland was established in 1907 in Qeqertarsuaq (GDH) and was in service for about five years (Hjelme 1996). Later, seismographs were established in Ivittut (1927) and Illoqqortoormiut (1928; SCO), and the network has been regularly upgraded and expanded ever since (Fig. 1). Prior to the development of BB seismographs, each station was equipped with a set of seismographs with different frequency sensitivities in an attempt to cover both distant and local earthquakes. Now just one small instrument is needed at each location.

The Geological Survey of Denmark and Greenland (GEUS) operates four permanent BB seismographs in Greenland (Fig. 1), two of them in collaboration with foreign institutions. In addition to the permanent network, there are currently 13 temporary BB seismographs active in Greenland, of which eight are operated by GEUS. Three of the temporary seismograph stations were established as part of the Danish Continental Shelf Project (Marcussen *et al.* 2004), and the remainder in connection with research projects. Three temporary seismographs were deployed during 2005 as part of a research project aiming to resolve very deep regional structures in North Greenland: the Citronen Fjord station (CFJ, Continental Shelf Project), and the stations in Kullorsuaq (KUL) and Daneborg (DBG).

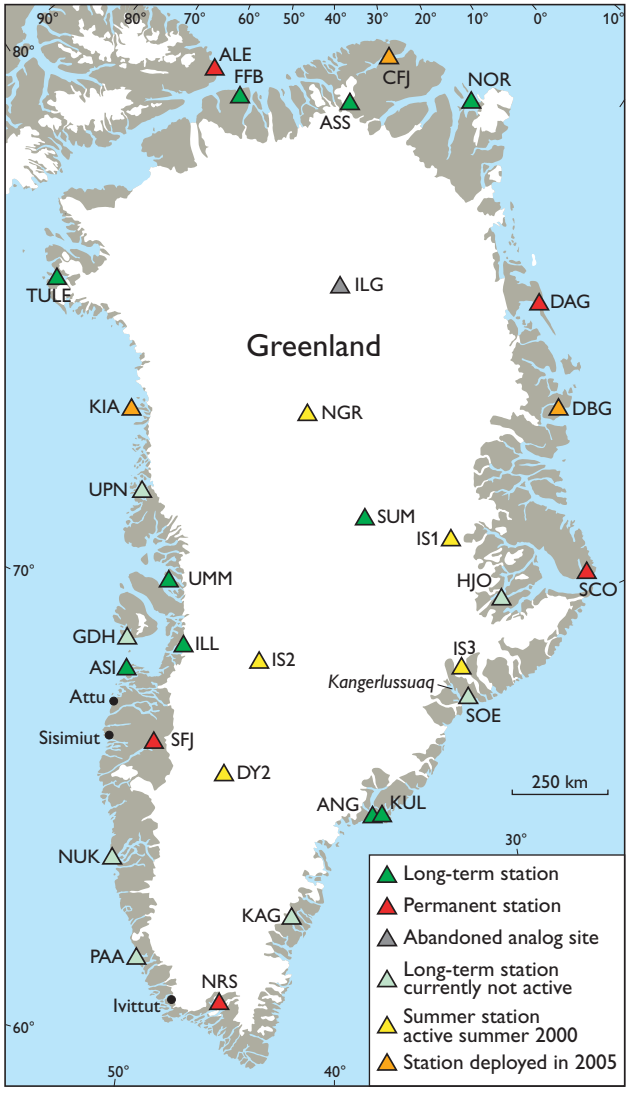

Fig. 1. Seismograph stations in Greenland.

The seismological service in Greenland

The study of earthquakes is international by nature. Large earthquakes can be recorded world wide, and a good coverage of high quality data is crucial for an accurate determination of an epicentre. Epicentral determination for large earthquakes is carried out at international data centres through collaboration of seismic services in almost all countries of the world. The primary task for the seismology group at GEUS is to maintain the seismological service for Denmark and Greenland (see Gregersen *et al.* 2004). The seismological service runs the permanent network of seismographs, that collects high quality continuous data, analyses the data, and reports registered earthquake signals (phases) for local earthquakes as well as for regional and teleseismic events. The

continuous digital waveform data are freely available directly from a GEUS server, as well as through international data centres. Due to Greenland's size and geographical location, data from Greenland are particularly important to the international seismological community. Currently, the Kangerlussuaq (SFJ) seismograph and the seismograph at the Summit ice camp (SUM) are the only two in Greenland with real-time data transmission. Data from other stations are available with varying time delay. The phase readings are reported to international data centres such as the United States Geological Survey (USGS) and the International Seismological Centre (ISC) through the weekly bulletin and the revised monthly bulletin. In 2005, GEUS reported a total of 3999 earthquake signals from the permanent seismograph network in Greenland, including many of the aftershocks that continued for several months after the Sumatra earthquake on 26 December, 2004, as well as the devastating 7.6 Richter Scale Kashmir earthquake on 8 October, 2005 (Fig. 2).

The seismograph in Kangerlussuaq was moved 300 m in February 2005 to a vault protected from local radar antenna disturbances. This was carried out in order to serve better the needs of the Comprehensive Test Ban Treaty Organisation (CTBTO). CTBTO financed the move, and provides in addition the real-time satellite transmission of the continuous data. The instrumentation was supplemented in 2005 with an extra BB seismograph. The CTBTO is an organisation under the United Nations, and its goal is to detect nuclear explosions of more than 5 kg fissionable material anywhere on Earth. An important tool for the organisation is seismological surveillance carried out by a primary and a secondary global network of designated secure seismograph stations. The Kangerlussuaq seismograph is part of the secondary network, and was officially certified by CTBTO on 24 November 2005. GEUS is Denmark's National Authority for the CTBTO.

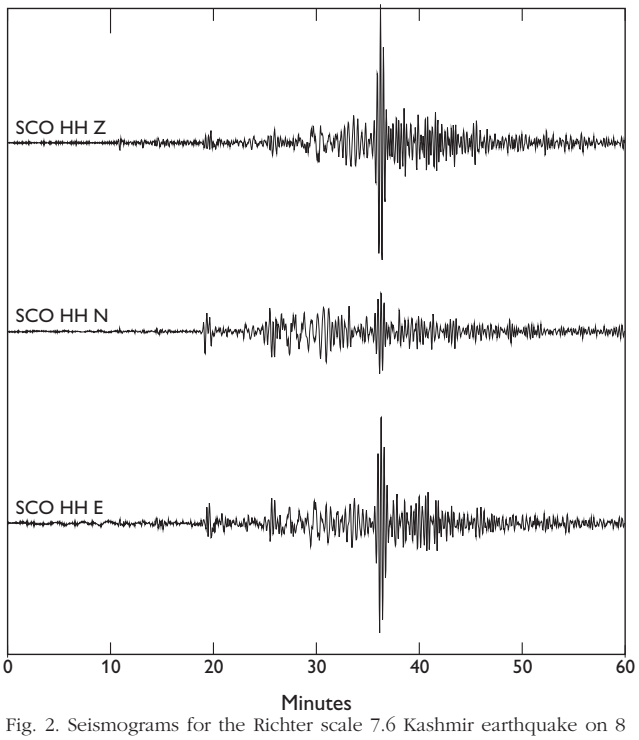

Fig. 2. Seismograms for the Richter scale 7.6 Kashmir earthquake on 8 October, 2005 recorded at Illoqqortoormiut. The **top** seismogram shows the vertical motion, the **middle** seismogram motion in the north–south direction, and the **bottom** seismogram motion in the east–west direction.

Several minor earthquakes occurred in Greenland in 2005. GEUS received reports that earthquakes were felt in Qeqertarsuaq (GDH) on 30 March, in Sisimiut on 23 July, at Station Nord (NOR) on 30 August, and in Attu on 23 October. Tasiilaq (ANG) is normally the place in Greenland where most earthquakes are felt; however, no earthquakes were reported in 2005. Including the reports of felt earthquakes noted above, GEUS has so far registered 20 earthquakes in Greenland in 2005 (Fig. 3). This number may increase when the preliminary earthquake catalogue is quality controlled and revised, and data from the temporary seismographs are recovered and included.

Studies on deep crustal and mantle structures

Denmark ratified the United Nations Convention on the Law of the Sea (UNCLOS) in November 2004. After ratification of UNCLOS, a country has ten years to collect the appropriate information and submit a claim for an extended continental shelf beyond 200 nautical miles. One of the potential claim areas is the continental shelf north of Greenland (Marcussen *et al*. 2004). Three BB seismographs have been placed along the North Greenland coast (Fig. 1) with the aim of learning more about the thickness and structure of the crust of North Greenland through receiver function analysis. This method has previously been used at many sites in Greenland during the GLATIS (*Greenland Lithosphere Analysed Teleseismically on the Ice Sheet*) project, but all BB seismographs used in previous studies were located further south (Dahl-Jensen *et al*. 2003). The stations at Frankfield Bugt (FFB) and Aftenstjernesø (ASS) have been in operation since 2004, whereas the Citronen Fjord station (CFJ) started recording data in 2005. These stations record signals from distant (teleseismic) earthquakes that can be processed to obtain information about crustal structure, e.g. depth to Moho and even deeper structures. The data retrieved so far are of excellent quality. Normally it is necessary to record data for more than a year in order to obtain a reliable estimate for the depth to Moho, but for the Aftenstjernesø station a depth to Moho of 41 km and a Vp/Vs of 1.71 was determined using just a few months of data. The relatively

large depth to Moho at Aftenstjernesø indicates that the station is on the rim of the Precambrian shield area (Fig. 3), and data from other locations are therefore necessary to resolve the question of crustal thickness in the Franklinian Basin that extends along the North Greenland coastal region.

Surface waves from teleseismic earthquakes can provide information on deep geological structures between two seismographs recording the same earthquake. Provided that two seismographs are located on the same great circle as the epicentre, differences in the signal recorded on the two instruments will reflect the geology affecting the wave propagating between the two stations. A dense web of epicentres and station pairs will make it possible to construct a seismic velocity model from depths of about 60 km to about 300 km. This kind of analysis was successfully carried out during the GLATIS project (Darbyshire *et al.* 2004). Similar studies were made previously by Gregersen (1970, 1982) for the crust, using various kinds of seismic waves. In addition to the studies of velocity structure in the mantle, measurements of amplitude attenuation have been carried out (Jørgensen 2005), resulting in preliminary maps of differences in the wave absorption properties of the deep structures.

In order to take full advantage of the seismographs along the north coast of Greenland and improve coverage inland north of 72°N, it was necessary to deploy two extra seismographs, one in the settlement of Kullorsuaq (KUL), and another at Daneborg (DBG) that was previously used by the GLATIS project (Fig. 1). Both seismographs were installed in 2005 and will remain in operation until 2007. It is expected that a first-order model of the very deep velocity structures inland in North Greenland can be constructed within the framework of the project. In 2006 another deep-structure seismological project will deploy a short profile of five BB seismographs across the Safartoq kimberlite region south-east of Sisimiut. The aim of this project is to reveal the crustal thickness in the area. The Safartoq project will be initiated as a pilot study of the area in order to facilitate a proposal for a large-scale deep structure study with international partners. A larger array of instruments is necessary for studies of the deep lithospheric structures.

Glacial earthquakes

Glacial earthquakes are a peculiar type of seismological event primarily located in Greenland. They were first described by Ekström *et al.* (2003). The signals are dispersive, lack the characteristic P- and S- waves known from ordinary earthquakes and all signals appear to have their source beneath large glaciers. The focal mechanisms that can be calculated for the earthquakes are consistent with a large mass of ice moving abruptly downhill over an elastic medium (landslide model).

In 2005 Geocenter Copenhagen funded a joint research project on glacial earthquakes involving GEUS and the Institute of Geography, University of Copenhagen. Through the GLATIS project GEUS possesses a unique seismological data set for Greenland, previously used only for structural studies. When the majority of BB seismographs in Greenland were installed, the existence of glacial earthquakes had not been recognised. However, after the start of the glacial earthquake project in 2005, it has become clear that the BB seismological data from Greenland are a unique data set for the study of glacial earthquakes.

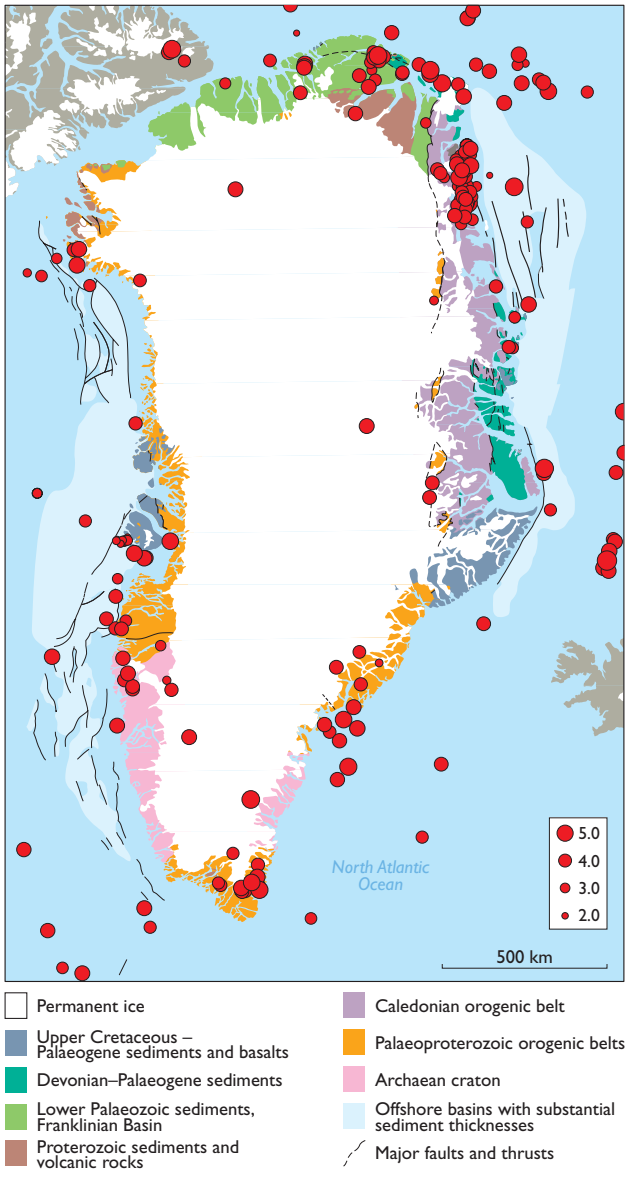

Fig. 3. Map of earthquake locations in and around Greenland for 1970-2005. Only earthquakes with a magnitude of 2.0 or more on the Richter Scale are shown. The map is compiled from the GEUS earthquake database, supplemented with epicentre locations from the Geological Survey of Canada, the United States Geological Survey and NORSAR in Norway.

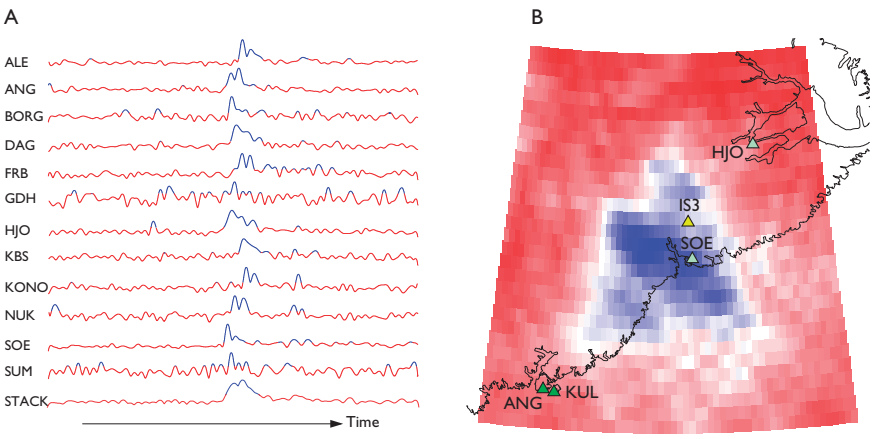

Fig. 4. **A**: Seismogram envelopes for a glacial earthquake, that occurred on 20 October, 2000. Signal from the earthquake is shown in blue. The bottom seismogram is a stack of the twelve seismograms, relative to a chosen test epicentre. When the test epicentre is close to the true epicentre, stacking will produce a strong signal. For location of Greenland stations see Fig. 1. ALE: Alert, Arctic Canada. BORG: Borganes, Iceland. FRB: Frobisher Bay, Arctic Canada. KBS: Kingsbay, Svalbard; KONO: Kongsberg, Norway. **B**: Correlation for the signal in the stack, with the best correlation in blue. Many test epicentres are modelled before the true epicentre can be determined, in this case centred in Kangerlussuaq in East Greenland (see Fig. 1).

Glacial earthquakes have not previously been studied extensively using a local data set (Fig. 4). One purpose of the project is to significantly improve the location accuracy for the earthquakes, and to improve the detection threshold by an order of magnitude from 4.7 on the Richter Scale to 3.7. Detecting smaller earthquakes opens the possibility of revealing unknown ice streams within the Greenland ice sheet.

The occurrence of glacial earthquakes shows strong seasonal variation, with most earthquakes occurring during summer. This implies that the glacial earthquakes could contribute information as to how variations in climate parameters affect ice sheet dynamics. GPS fieldwork is planned for summer 2006, when glacial earthquakes will be recorded simultaneously on both seismographs and differential GPS. The objective of the project is to shed light on the mechanisms controlling the glacial earthquakes, with the possibility that glacial earthquakes can be used as a surveillance tool to study Greenland ice sheet dynamics.

Acknowledgements

GeoForschungsZentrum-Potsdam (GFZ), Germany provides instrumentation and technical support to the seismograph in Danmarkshavn, and together with the Incorporated Research Institutions for Seismology (IRIS), USA to the seismograph in Kangerlussuaq. The Bureau of Minerals and Petroleum, Government of Greenland, provided financial support to several of the projects described in this paper. Geocenter Copenhagen provides financial support for the project on glacial earthquakes.

References

Dahl-Jensen, T., Larsen, T.B., Woelbern, I., Bach, T., Hanka, W., Kind, R., Gregersen, S., Mosegaard, K., Voss, P. & Gudmundsson, O. 2003: Depth to Moho in Greenland: Receiver-function analysis suggests two Proterozoic blocks in Greenland. Earth and Planetary Science Letters **205**, 379–393.

Darbyshire, F.A., Larsen, T.B., Mosegaard, K., Dahl-Jensen, T., Gudmundsson, O., Bach, T., Gregersen, S., Pedersen, H.A. & Hanka, W. 2004: A first detailed look at the Greenland lithosphere and upper mantle, using Rayleigh wave tomography. Geophysical Journal International **158**, 267–287.

Ekström, G., Nettles, M. & Abers, G.A. 2003: Glacial earthquakes, Science **302**, 622–624.

Gregersen, S. 1970: Surface wave dispersion and crust structure in Greenland. Geophysical Journal of the Royal Astronomical Society **22**, 22–39.

Gregersen, S. 1982: Seismicity and observations of Lg wave attenuation in Greenland. Tectonophysics **89**, 77–93.

Gregersen, S., Glendrup, M., Larsen, T.B., Voss, P. & Rasmussen, H.P. 2004: Seismology: neotectonics and structure of the Baltic Shield. Bulletin of the Geological Survey of Denmark and Greenland **7**, 25–28.

Hjelme, J. 1996: History of seismological stations in Denmark and Greenland. In: Wahlström, R. (ed.) Seismograph recording in Sweden, Norway – with arctic regions, Denmark – with Greenland, and Finland. Proceedings from the Uppsala Wiechert Jubilee Seminar, 49–57. Uppsala: Seismological Department, Uppsala University, Sweden.

Jørgensen, T.M., 2005: Attenuation of Rayleigh waves in Greenland, 78 pp. Unpublished M.Sc. thesis, University of Copenhagen, Denmark.

Marcussen, C., Christensen, F.G., Dahl-Jensen, T., Heinesen, M., Lomholt, S., Møller, J.J. & Sørensen, K 2004: Exploring for extended continental shelf claims off Greenland and the Faroe Islands. Bulletin of the Geological Survey of Denmark and Greenland **4**, 61–64.

Authors' address

Geological Survey of Denmark and Greenland (GEUS), Øster Voldgade 10, DK-1350 Copenhagen K, Denmark. E-mail: *tbl@geus.dk*

Radical past climatic changes in the Arctic Ocean and a geophysical signature of the Lomonosov Ridge north of Greenland

Naja Mikkelsen, Niels Nørgaard-Pedersen, Yngve Kristoffersen, Susanne Juul Lassen and Emma Sheldon

The Arctic Ocean is a landlocked basin, at present covered by perennial sea ice. During the past few decades a significant thinning and shrinking of the sea ice has been observed, and modelling studies indicate that the Arctic Ocean ice cover could, by the end of this century, almost disappear from most parts of the Arctic Ocean during peak summer seasons. It remains uncertain, however, whether the environmental changes are an enhanced greenhouse-warming signal or a result of natural (long-term) variability, but palaeoceanographic studies can contribute to our understanding of the natural variability of environmental parameters, e.g. sea-ice cover and oceanographic changes on time-scales of centuries to millennia.

As part of the multidisciplinary EU project *Greenland Arctic Shelf Ice and Climate Experiment* (GreenICE), sediment coring and seismic reflection measurements have been undertaken in a hitherto unexplored part of the Arctic Ocean, the margin of the Lomonosov Ridge in the Lincoln Sea (Fig. 1). The aim of the project was to study the structure and dynamics of the sea-ice cover and attempt to relate these to longer-term records of climate variability retrieved from sediment cores. The main field work was carried out in May 2004 from an ice camp established by a Twin Otter aircraft on drifting sea ice at 85°N, 65°W, *c.* 170 km north of Alert, Arctic Canada. The camp was deployed over the shallowest part of the Lomonosov Ridge off the northern Greenland/Canada continental margin (Fig. 1). The sea-ice drift would normally be between east and south, but persistent easterly winds resulted in a fast drift trajectory towards the WSW, such that the camp drifted a distance of approximately 62 km during the two weeks camp period.

At present the study area is heavily ice covered, and forecast models of future shrinking Arctic sea-ice cover suggest that this area is one of the least sensitive to warming in the Arctic. The results obtained from the GreenICE project challenge this view.

An unexplored area

The reduction and thinning of Arctic sea ice in recent decades (e.g. Rothrock *et al.* 1999; ACIA 2004) has drawn attention to whether these environmental changes are an early reaction to global warming, or whether they are part of a long-term variation of the Arctic environment. Modelling studies of global warming effects indicate that the Arctic is

Fig. 1. **Upper**: The GreenICE field camp area (marked by a red square) was deployed north of Arctic Canada and North Greenland at the shallowest part of the submarine Lomonosov Ridge, in a region where no geologic record has hitherto been retrieved. **Lower**: Drift path of the field camp is shown by arrow and **red line** and coring stations by yellow and **red dots**.

likely to show a significant temperature increase, and that sea-ice cover could, by the end of this century, almost disappear during peak summer seasons (Johannessen *et al.* 2004). Such a scenario would not only have a dramatic impact on Arctic ecosystems, navigation and indigenous people, but could also influence the thermohaline circulation and regional climate in the sub-Arctic and North Atlantic region. In a discussion of these scenarios, there is an urgent need for high-latitude Arctic records of variations in climate, oceanography and sea-ice cover representing long time periods and, in particular, records of natural environmental change during earlier warm periods, which can be used to evaluate present-day changes. In spite of its importance, the recent geological record of many parts of the Arctic Ocean, including the Lincoln Sea, are still poorly known and hampered by difficult access.

Reduced ice cover during interglacial periods

Seismic data and sediment cores were collected from the drifting GreenICE station in this normally inaccessible area of the Lincoln Sea. During the camp period, 15 gravity core stations were established (Figs 1, 2), and the retrieved cores were subsequently subjected to a wide array of investigations including AMS-^{14}C dating, faunal analysis of nannofossils and benthic and planktonic foraminifers, and stable isotope and geochemical analysis. The two longest cores, GreenICE Core 10 (176 cm) and GreenICE Core 11 (64 cm), show several characteristic colour cycles previously recorded in other parts of the Arctic Ocean (Fig. 3; Phillips & Grantz 1997; Nørgaard-Pedersen *et al.* 1998; Jakobsson *et al.* 2000; Polyak *et al.* 2004; Spielhagen *et al.* 2004). The stratigraphy of Core 11 is based on nannoplankton, benthic foraminiferal assemblages and AMS-^{14}C dates and provides a record of the last *c.* 130 000 years, including the last interglacial period (Eemian). Preliminary investigations indicate that the longer Core 10 contains a record of the last *c.* 200 000 years.

Planktonic foraminiferal assemblages are used as a key palaeoceanographic proxy, and a surprisingly large variability of these foraminifers was observed for an interior Arctic Ocean site. The discovery of abundant numbers of the small subpolar foraminifers *Turborotalita quinqueloba* in two core sections, corresponding to the last interglacial and a younger warm interstadial (Fig. 3), is an enigma, as this species indicates fairly strong subsurface Atlantic water advection and possibly a much reduced summer sea-ice cover in the area compared to present-day conditions. The youngest part of the retrieved sediment record is condensed, but samples taken from close to the surface, representing Holocene and Recent conditions, lack the subpolar foraminifer species and thus indicate a consistent thick perennial sea-ice cover in accordance with present-day conditions (Nørgaard-Pedersen *et al.* in press)

The results support the concept that interglacial conditions in the interior Arctic Ocean can vary considerably. At present, however, it is not known whether the influx of subpolar foraminifers was related to an ice-margin or polynya-type setting, or whether it reflects a generally reduced sea-ice cover of the interior Arctic Ocean. Ongoing work aims to explore whether the observed trends can be traced to other key sites in the Arctic Ocean.

Seismic investigations and active faulting

A 62 km long seismic reflection profile was collected during the drift of the GreenICE field camp (Figs 1, 4). Seismic reflection data were obtained from the shallowest part of the

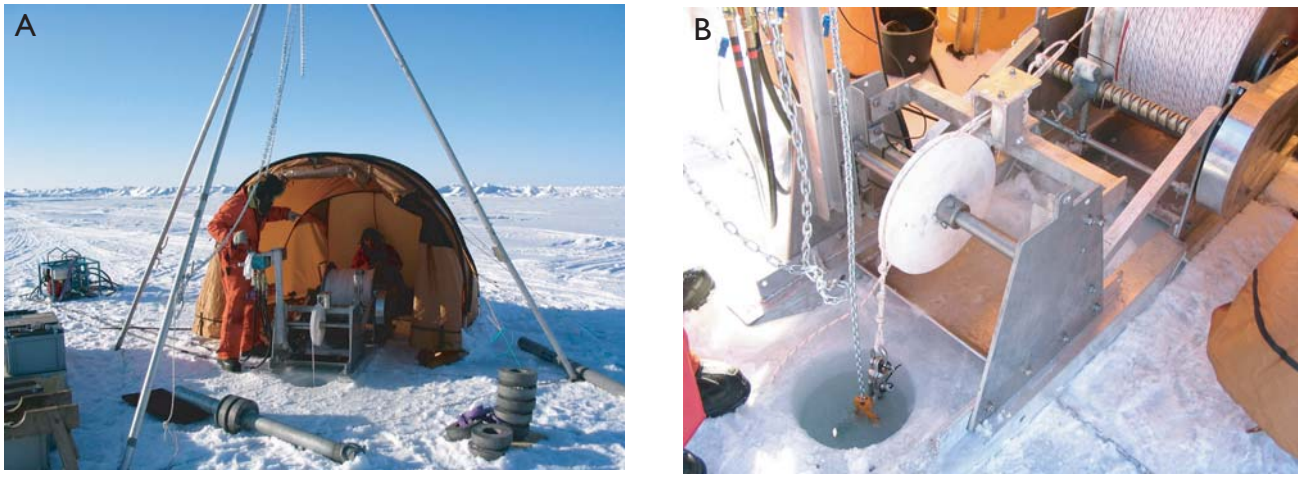

Fig. 2. **A**: Lightweight gravity coring equipment (constructed by J. Boserup, GEUS) used during the drift of the GreenICE camp. **B**: Sediment cores were retrieved through a hole drilled in the ice.

Fig. 4. Seismic line retrieved during the ice drift over the Lomonosow Ridge north of Canada and Greenland (adapted from Kristoffersen & Mikkelsen 2006).

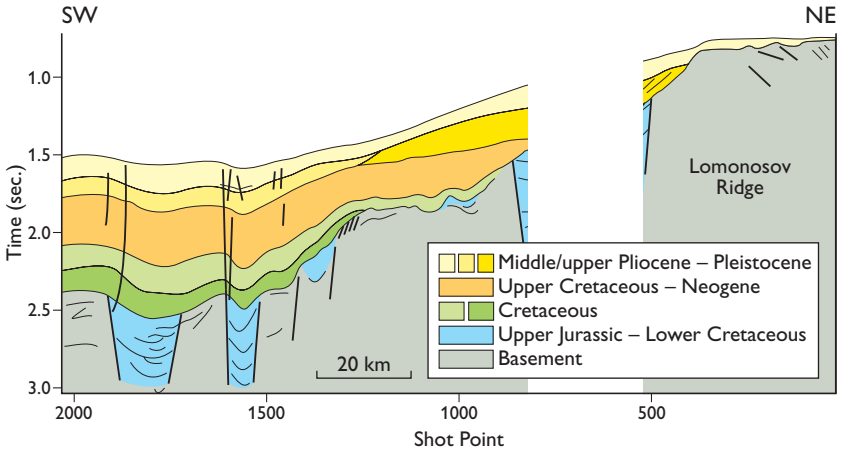

submarine Lomonosov Ridge facing the Canadian/Greenlandic continental margin, and comprise two parallel single channel lines (Kristoffersen & Mikkelsen 2006). The data reveal that the top of Lomonosov Ridge is bevelled at a water depth of 550 m and that only a thin sediment cover (less that 50 m) overlies the acoustic basement. Pre-Pleistocene sediments were probably eroded by a grounded marine ice sheet extending north from Ellesmere Island, and/or by deep draft icebergs. In the deep passage between the Lomonosov Ridge and the Lincoln Sea continental margin, more than 1 km of sediment is present. The uppermost 300 m of this succession reflects a significant sediment drift possibly related to

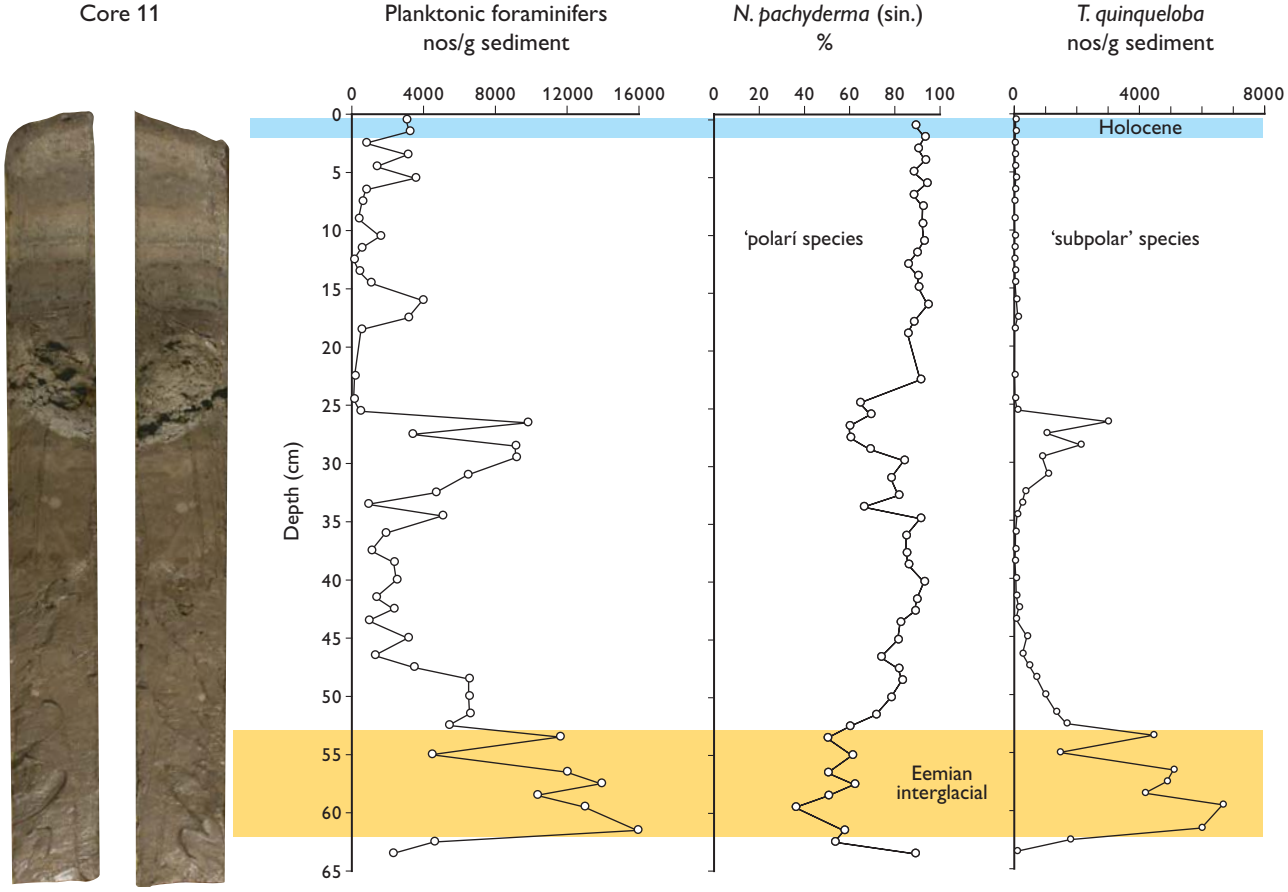

Fig. 3. The GreenICE sediment cores show marked colour cycles. GreenICE Core 11 covers a time span of *c.* 130 000 years and includes the Eemian interglacial marine isotope stage 5e. Abundant subpolar foraminifers (*Turborotalita quinqueloba*) in Eemian deposits indicate open water conditions not far from the GreenICE site. This is in contrast to Holocene sediments that show a total dominance of polar species (*Neogloboquadrina pachydermal*).

increased Plio-Pleistocene sediment input, and the underlying 700 m of sediment onlap a subsiding ridge slope. Blocks of older margin sediments may represent the acoustic basement in the area. A basal unconformity, which may correspond to the Hauterivian break-up unconformity of Embry & Dixon (1994), caps a series of NW–SE-trending grabens, and several of the main graben faults extend to the sea bed and appear to have been active until recent times.

Acknowledgements

The Greenland Arctic Shelf Ice and Climate Experiment (GreenICE) was supported by EU-grant EVK2-2001-00280.

References

ACIA, 2004: Impacts of a warming Arctic – arctic climate impact assessment, 144 pp. Cambridge: Cambridge University Press.

Embry, A.F. & Dixon, J. 1994: The age of the Amerasian Basin. In: Thurston, D.K. & Fujita, K. (eds): 1992 Proceedings, International Conference on Arctic Margins, 289–294. Anchorage, Alaska, USA: U. S. Department of the Interior, Minerals Management Service.

Jakobsson, M., Løvlie, R., Al-Hanbali, H., Arnold, E., Backman, J.& Mörth, M. 2000: Manganese and color cycles in Arctic Ocean sediments constrain Pleistocene chronology. Geology **28**, 23–26.

Johannessen, O.M. *et al.* 2004: Arctic climate change: observed and modelled temperature and sea-ice variability. Tellus A **56**, 559–560.

Kristoffersen, Y. & Mikkelsen, N. 2006: On sediment deposition and nature of the plate boundary at the junction between the submarine Lomonosov Ridge, Arctic Ocean and the continental margin of Arctic Canada /North Greenland. Marine Geology **225**, 265–278.

Nørgaard-Pedersen, N., Spielhagen, R.F., Thiede, J. & Kassens, H. 1998: Central Arctic surface ocean environment during the past 80,000 years. Paleoceanography **13**, 193–204.

Nørgaard-Pedersen. N., Mikkelsen, N., Lassen, S.J., Kristoffersen, Y. & Sheldon, E. in press: Arctic Ocean sediment cores off northern Greenland reveal reduced sea-ice concentrations during the last interglacial period. Paleoceanography.

Phillips, R.L. & Grantz, A. 1997: Quaternary history of sea ice and paleoclimate in the Amerasia basin, Arctic Ocean, as recorded in the cyclical strata of Northwind Ridge. Geological Society of America Bulletin **109**, 1101–1115.

Polyak, L., Curry, W.B., Darby, D.A., Bischof, J. & Cronin, T.M. 2004: Contrasting glacial/interglacial regimes in the western Arctic Ocean as exemplified by a sedimentary record from the Mendeleev Ridge. Palaeogeography, Palaeoclimatology, Palaeoecology **20**, 73–93.

Rothrock, D.A., Yu, Y. & Maykut, G.A. 1999: Thinning of the Arctic sea-ice cover. Geophysical Research Letters **26**, 3469–3472.

Spielhagen, R.F., Baumann, K.-H., Erlenkeuser, H., Nowaczyk, N.R., Nørgaard-Pedersen, N., Vogt, C. & Weiel, D. 2004: Arctic Ocean deep-sea record of northern Eurasian ice sheet history. Quaternary Science Reviews **23**, 1455–1483.

Authors' addresses

N.M., N.N.-P., S.J.L. & E.S., *Geological Survey of Denmark and Greenland (GEUS), Øster Voldgade 10, DK-1350 Copenhagen K, Denmark;* E-mail: *nm@geus.dk*

Y.K., *Department of Earth Science, University of Bergen, Allegaten 41, N-5007 Bergen, Norway.*

KenSea – development of an environmental sensitivity atlas for coastal areas of Kenya

John Tychsen, Ole Geertz-Hansen and Jesper Kofoed

The Kenya coastline extends 600 km from the border of Tanzania in the south to the border of Somalia in the north (Fig. 1). The Kenyan coast features a diverse marine environment, including estuaries, mangroves, sea grass beds and intertidal reef platforms and coral reefs, which are vital for the reproduction of marine organisms. These coastal ecosystems are regarded as some of the most valuable in Kenya but face serious threats from the ever increasing human pressure of tourism, industrial pollution, destructive fishing, mangrove logging and other unsustainable uses of marine resources.

Another serious threat is the maritime transportation activities along the coast and at the ports. It is estimated that at any given time more than 50 ships operate in the major shipping lanes off the Kenyan coast, of which about nine are oil tankers with capacities ranging from 50 000 to 250 000 tonnes. Furthermore, the harbour of Mombasa serves as the major port for countries in East Africa.

In recognition of the risks posed by oil pollution the government of Kenya and the commercial petroleum industry agreed to develop a National Oil Spill Response Contingency Plan (NOSRCP) with the purpose of enabling a speedy and effective response to any oil spill within the territorial waters of Kenya. An important element of this plan was the mapping of the coastal resources and the development of an environmental sensitivity atlas showing the vulnerability of the coast to marine oil spills.

In 2004, the Government of Kenya approached the United Nations Development Program (UNDP) in Kenya for financial support to develop an environmental sensitivity atlas. The project was approved and forwarded for funding by the Danish Consultancy Trust Fund administrated by United Nations Operational Program (UNOPS) in Copenhagen. The project was announced in Denmark, and the KenSea group headed by the Geological Survey of Denmark and Greenland (GEUS) was awarded the contract.

The project comprises four phases: (1) data compilation and development of the KenSea database, (2) development of a coastal classification for Kenya, (3) development of the sensitivity index jointly with a group of stakeholders, and (4) compilation of the KenSea environmental sensitivity atlas (Tychsen 2006).

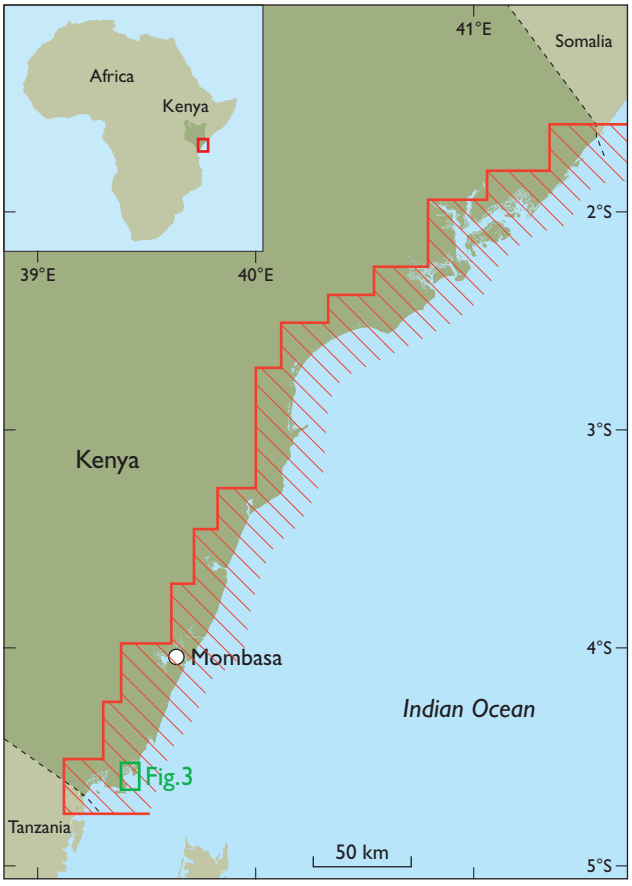

Fig. 1. The coastal area of Kenya (**red frame** on index map) showing coverage of the KenSea coastal sensitivity map (**ruled area**). **Green frame**, location of maps shown in Fig. 3.

Development of the KenSea database

In the 1990s the Eastern Africa Coastal and Marine Resources Database and Atlas (UNEP 1998) was developed by the United Nations Environmental Programme. This database contains a variety of datasets covering bioscience, geoscience and human use, which have been incorporated either directly or as guidelines for further investigations in the KenSea database (KenSeaBase). However, the UNEP atlas has been produced at the scale of 1:250 000, implying a lower degree of spatial resolution than the scale of 1:50 000 requested for the KenSea project.

Fig. 2. Pleistocene coral limestone cliffs typical of the Kenyan coast.

Following a kick-off seminar with all stakeholders, the team from the KenSea group visited a large number of government agencies, ministries, private companies and national as well as international non-governmental organisations to collect additional and updated data. All collected data were digitised and included in the KenSeaBase, and preliminary maps were printed. Based on these preliminary maps, a field programme for data verification and additional data collection was developed and carried out. The results were integrated into the KenSeaBase and logistic and topographic maps and coastal resource maps were produced.

Development of a coastal classification for Kenya

Many attempts have been made worldwide to classify coastlines with respect to their vulnerability to oil pollution. These classifications are usually based on the geomorphology, the degree of exposure to wind and waves, and other relevant conditions. Most of these classifications were inspired by Gundlach & Hayes (1978) and Baker *et al.* (1994).

The classification adopted for the KenSea project is a further development of these classifications to meet the conditions in Kenya. In addition to coastal geomorphology and degree of exposure, the ecological value and biodiversity of this particular stretch of coastline is taken into account, as well as the ability of the particular coastal types to facilitate self-cleaning and the conditions for removing a potential oil spill. The resulting classification comprises seven categories, each of which can be described in terms of its geomorphology, ecological value and vulnerability to an oil spill (Tychsen 2006).

Rocky coast

Much of the Kenyan coast is formed by 4–6 m high Pleistocene coral limestone cliffs (Fig. 2). At present-day sea level they are exposed to wave erosion, resulting in an irregular and rugged appearance. In the upper part of the intertidal zone biological activity is sparse. Subtidal rocks and man-made hard-surface structures such as piers and wharfs may develop a richer flora and fauna, resembling the conditions found on reefs. The exposed cliffs are regarded as less sensitive to oil pollution than most other habitats because of the sparse biological activity, and because the exposure to waves makes the surface to some extent self-cleaning.

Sandy beaches and dunes

Two types of sandy shores are present along the Kenyan coast: (1) gentle to steep sandy beaches without protection from a reef. The beach is often backed by one or a series of wind-blown sand dunes. The sand may be of terrestrial origin and supplied by the larger rivers. (2) Gently sloping beaches sheltered behind a reef are common along the coast and the sand is often white calcareous sand of marine origin (coral sand).

Species diversity on sandy beaches is usually low. Above the high-water line, only a few burrowing crabs and amphipods are usually found. The density and diversity of crabs, bivalves, polychaetes and other marine invertebrates increases in the intertidal zone, but remains low compared to most other habitats. Fine-grained sandy beaches are less sensitive to oil pollution due to their relatively sparse biological activity. Furthermore, they are relatively easy to clean since oil does not penetrate deep and can be removed either manually or by use of machinery. On the other hand, coarse sand or gravel is more sensitive as the oil can sink deep into it, and the oil may therefore be impossible to remove.

Coral reefs and reef flats

Most of the Kenya coastline is fringed by a major barrier reef complex that includes the most diverse ecosystems in the marine environment. The up to 2 km wide shallow-water reef flats between the coastal cliffs and the reef crest comprise fossil reefs currently eroded by wave action. Active reef growth occurs at the reef crest and on the slope facing the ocean where coral reef growth occurs to depths between 20 and 25 m. The main part of the reefs are subtidal, and are therefore sheltered from direct contact with a possible oil slick. However, reef crests are usually exposed at low tide and the intertidal corals will be killed immediately by contact with oil. The deeper parts of the reef may also be endangered as waves break on the crest and fine oil droplets become dispersed in the water column. Recovery of damaged coral reefs may take several decades, and restoration techniques are usually not very successful.

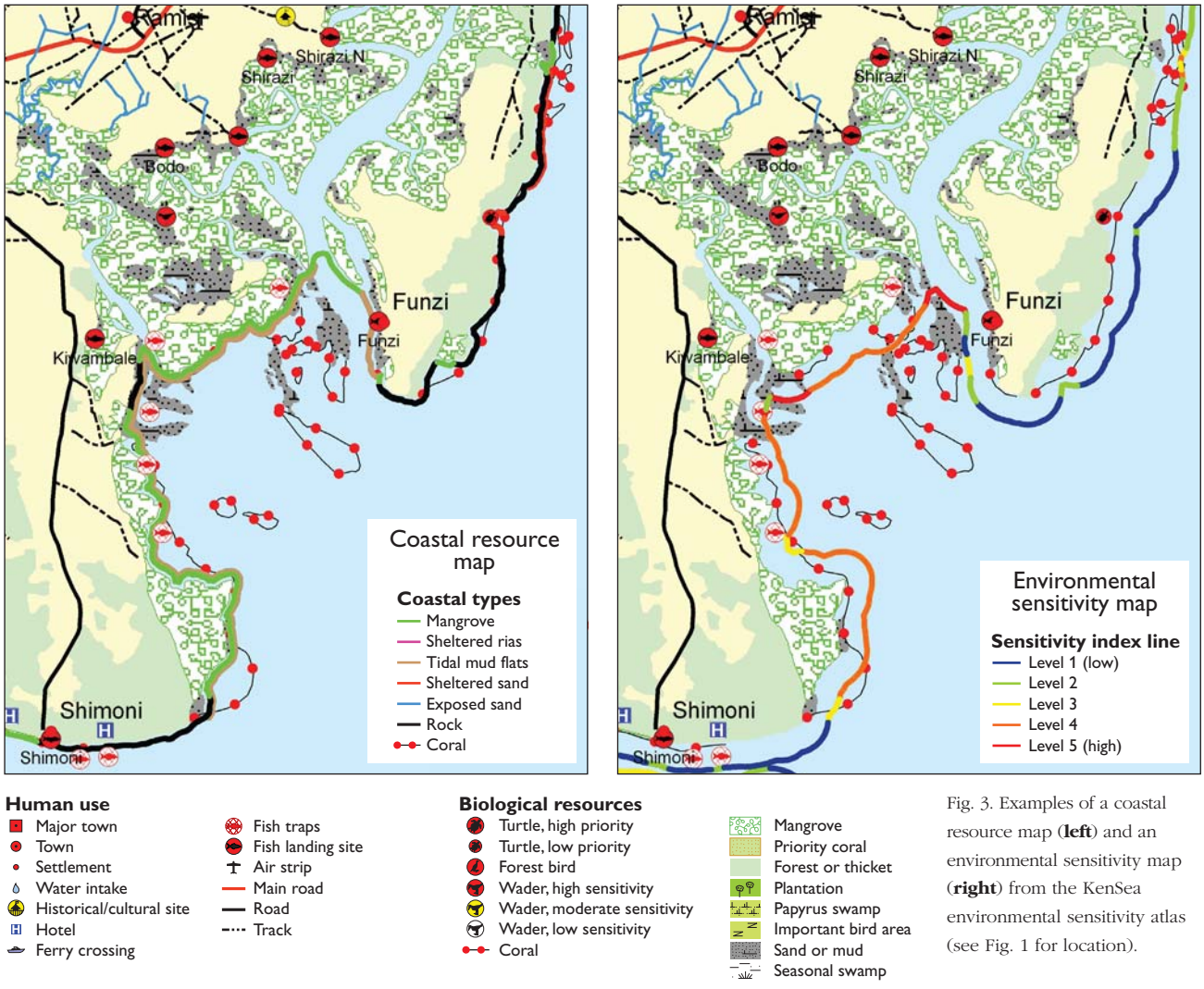

Fig. 3. Examples of a coastal resource map (**left**) and an environmental sensitivity map (**right**) from the KenSea environmental sensitivity atlas (see Fig. 1 for location).

Rias

Rias are drowned river valleys or estuaries. The typical ria has a steep slope or a sheltered cliff, often with a narrow subtidal muddy beach with a few mangrove trees. The sheltered environment of the ria has only little self-cleaning capacity, although it is often possible to clean from the seaward side because of its narrow extent.

River mouths and estuaries

The rivers in the area form large, gently sloping floodplains with extensive estuarine zones characterised by fluctuating salinity. The mouths of smaller rivers are often hidden behind mangrove creeks.

Few plant species apart from mangroves are adapted to low or fluctuating salinities. The biodiversity is therefore low within the estuaries, although the density is usually very high due to the continuous supply of food and nutrient from the river. The high density of bivalves, snails and other benthic invertebrates usually attracts many birds. Tidal currents can carry any oil pollution far into the estuary and thus into contact with a high density of food items. Therefore the sensitivity is very high. Flushing and self-cleaning is limited to the seasonal high flow situations.

Mangroves

Mangroves have a high productivity as they profit from nutrients from both land and sea, and mangrove detritus is often the main source of energy fuelling the estuarine food webs. Mangroves are favoured by fine-grained nutrient-rich sediment, and are therefore often associated with estuaries and other freshwater outlets.

While the diversity of mangrove tree species is limited, they create a multitude of niches suitable for a vast diversity of other organisms. Oil can be acutely toxic to the mangrove as clogging of the aerial roots by oil may hinder proper ventilation

of subsurface parts and lead to suffocation and stress, and eventually death. Clean-up operations may prove extremely difficult due to the low energy environment of mangrove forests.

Intertidal mud flats

Sheltered mangroves in creeks or bays are often fringed by a broad intertidal mudflat. These are characterised by a high density of marine invertebrates such as mussels, snails and crustaceans. Although diversity is usually low they are important feeding grounds for aquatic birds. The mudflats are sensitive to oil spills since they are difficult to clean mechanically without mixing the oil into the sediment. Where mangrove forests are associated with mudflats the clean-up is even more difficult for both habitats.

Development of a sensitivity index

The oil spill sensitivity ranking is designed to help decision-makers to prioritise the available resources and to focus the emergency response on the most vulnerable areas, both (1) during the pre-spill planning, in order to prepare appropriate response strategies and (2) during an oil spill combat in order to plan and continuously optimise the response strategy under the given conditions and limitations (oil type, weather, equipment, crew, etc.).

Planning the clean-up operation and avoiding post-spill damage

The goal of oil spill response is to minimise the overall impacts on natural and economic resources as well as cultural assets, but some aspects will be of greater concern than others. The sensitivity ranking for a given stretch of coastline therefore includes the actual sensitivity of the present resources or assets, and a more subtle evaluation of importance or value.

The ranking should integrate a multitude of data such as geomorphological and geological properties, wave exposure, biological diversity and productivity, oil behaviour, ease of clean-up, human use and cultural assets. Although these properties are not directly comparable or quantifiable the outcome should ideally be a simple statement, a numerical index value, or a colour code. The comparison and evaluation of incomparable properties is a matter of balancing often conflicting interests, and no perfect system can be devised. A complicated system is not necessarily better or more accurate than a simple system or qualified judgments. Therefore, it is essential that the amount of detail matches the purpose, and leaves the decision-makers with some alternatives.

The total sensitivity index developed for the KenSea atlas embraces three main themes: (1) coastal type, (2) biological resource, and (3) human use. For each theme an index value that incorporates the index values for the various attributes encompassed by the particular theme has been allocated for a particular stretch of coastline.

The index value for the individual attributes used in each of the themes and the formula for calculating the total index were developed during a seminar with participants from government agencies, ministries, private sector as well as national and international NGOs. This joint development of the formula is crucial for the future use of the sensitivity index. The sensitivity index line has been reproduced on the environmental sensitivity maps (Fig. 3).

Environmental sensitivity atlas

The atlas covers the entire coastline and comprises three types of maps, each of which have been produced in 16 map sheets at scale 1:50 000 (Fig 1; Tychsen 2006).

References

Baker, J.M., Spalding, M.D., Moore, J. & Tortell, P. 1994:. Sensitivity mapping for oil spill response. IMO/IPIECA Report Series **1**, 24 pp.

Gundlach, E.R. & Hayes, M.O. 1978: Vulnerability of coastal environments to oil spill impacts. Marine Technology Society Journal **12**, 18–27.

Tychsen, J. 2006 (ed.): KenSea – environmental sensitivity atlas for coastal area of Kenya, 76 pp. Copenhagen: Geological Survey of Denmark and Greenland.

UNEP 1998. Eastern Africa atlas of coastal resources, Kenya, 119 pp. Nairobi: UNEP.

Authors' address

J.T., *Geological Survey of Denmark and Greenland, Øster Voldgade 10, DK-1350 Copenhagen K, Denmark.* E-mail: *jt@geus.dk*

O.G.-H., *AquaSim, Slagslunde Bygade 37, DK-3660 Stenløse, Denmark.*

J.K., *GeoQuest, Gyldenløvesgade 16, DK-1369 Copenhagen K, Denmark.*

Danmarks og Grønlands Geologiske Undersøgelse (GEUS)

Geological Survey of Denmark and Greenland
Øster Voldgade 10, DK-1350 Copenhagen K
Denmark

Geological Survey of Denmark and Greenland Bulletin is a new series started in 2003 to replace the two former bulletin series of the Survey, viz. *Geology of Greenland Survey Bulletin* and *Geology of Denmark Survey Bulletin*. The twenty-one volumes published since 1997 in those two series are listed below after the new bulletin series. The new series, together with *Geological Survey of Denmark and Greenland Map Series*, now form the peer-review scientific series of the Survey.

Geological Survey of Denmark and Greenland Bulletin (new series)

1 The Jurassic of Denmark and Greenland, 948 pp. (28 articles), 2003.
Edited by J.R. Ineson & F. Surlyk. 500.00

2 Fish otoliths from the Paleocene of Denmark, 94 pp., 2003.
By W. Schwarzhans. 100.00

3 Late Quaternary environmental changes recorded in the Danish marine molluscan faunas, 268 pp., 2004.
By K.S. Pedersen. 200.00

4 Review of Survey activities 2003, 100 pp. (24 articles), 2004.
Edited by M. Sønderholm & A.K. Higgins. 180.00

5 The Jurassic of North-East Greenland, 112 pp. (7 articles), 2004.
Edited by L. Stemmerik & S. Stouge. 160.00

6 East Greenland Caledonides: stratigraphy, structure and geochronology, 93 pp. (6 articles), 2004.
Edited by A.K. Higgins and F. Kalsbeek. 160.00

7 Review of Survey activities 2004, 80 pp. (19 articles), 2005.
Edited by M. Sønderholm & A.K. Higgins. 180.00

8 Structural analysis of the Rubjerg Knude Glaciotectonic Complex, Vendsyssel, northern Denmark, 2005.
By S.A.S. Pedersen. 300.00

9 Scientific results from the deepened Lopra-1 borehole, Faroe Islands, 156 pp. (11 articles), 2006.
Edited by J.A. Chalmers and R. Waagstein. 240.00

10 Review of Survey activities 2005, 68 pp. (15 articles), 2006.
Edited by M. Sønderholm & A.K. Higgins.

11 Precambrian crustal evolution and Cretaceous–Palaeogene faulting in West Greenland, 204 pp. (12 articles), 2006.
Edited by A.A. Garde & F. Kalsbeek.

Geological Survey of Denmark and Greenland Map Series (new series)

1 Explanatory notes to the Geological map of Greenland, 1:500 000, Humboldt Gletscher, Sheet 6, 48 pp., 2004.
By P.R. Dawes 280.00

2 Explanatory notes to the Geological map of Greenland, 1:500 000, Thule, Sheet 5 (1991), 97 pp. + map, 2006.
By P.R. Dawes. 300.00

Geology of Greenland Survey Bulletin (discontinued)

176 Review of Greenland activities 1996, 112 pp. (18 articles), 1997.
Edited by A.K. Higgins & J.R. Ineson. 200.00

177 Accretion and evolution of an Archaean high-grade grey gneiss – amphibolite complex: the Fiskefjord area, southern West Greenland, 115 pp., 1997.
By A.A. Garde. 200.00

178 Lithostratigraphy, sedimentary evolution and sequence stratigraphy of the Upper Proterozoic Lyell Land Group (Eleonore Bay Supergroup) of East and North-East Greenland, 60 pp., 1997.
By H. Tirsgaard & M. Sønderholm. 200.00

179 The Citronen Fjord massive sulphide deposit, Peary Land, North Greenland: discovery, stratigraphy, mineralization and structural setting, 40 pp., 1998.
By F.W. van der Stijl & G.Z. Mosher. 200.00

180 Review of Greenland activities 1997, 176 pp. (26 articles), 1998.
Edited by A.K. Higgins & W.S. Watt. 200.00

181 Precambrian geology of the Disko Bugt region, West Greenland, 179 pp. (15 articles), 1999.
Edited by F. Kalsbeek. 240.00

182 Vertebrate remains from Upper Silurian – Lower Devonian beds of Hall Land, North Greenland, 80 pp., 1999.
By H. Blom. 120.00

183 Review of Greenland activities 1998, 81 pp. (10 articles), 1999.
Edited by A.K. Higgins & W.S. Watt. 200.00

184 Collected research papers: palaeontology, geochronology, geochemistry, 62 pp. (6 articles), 1999. 150.00

185 Greenland from Archaean to Quaternary. Descriptive text to the Geological map of Greenland, 1:2 500 000, 93 pp., 2000.
By N. Henriksen, A.K. Higgins, F. Kalsbeek & T.C.R. Pulvertaft. 225.00

186 Review of Greenland activities 1999, 105 pp. (13 articles), 2000.
Edited by P.R. Dawes & A.K. Higgins. 225.00

187 Palynology and deposition in the Wandel Sea Basin, eastern North Greenland, 101 pp. (6 articles), 2000.
Edited by L. Stemmerik. 160.00

188 The structure of the Cretaceous–Palaeogene sedimentary-volcanic area of Svartenhuk Halvø, central West Greenland, 40 pp., 2000.
By J. Gutzon Larsen & T.C.R. Pulvertaft. 130.00

189 Review of Greenland activities 2000, 131 pp. (17 articles), 2001.
Edited by A.K. Higgins & K. Secher. 160.00

190 The Ilímaussaq alkaline complex, South Greenland: status of mineralogical research with new results, 167 pp. (19 articles), 2001.
Edited by H. Sørensen. 160.00

191 Review of Greenland activities 2001, 161 pp. (20 articles), 2002.
Edited by A.K. Higgins, K. Secher & M. Sønderholm. 200.00

Geology of Denmark Survey Bulletin (discontinued)

36 Petroleum potential and depositional environments of Middle Jurassic coals and non-marine deposits, Danish Central Graben, with special reference to the Søgne Basin, 78 pp., 1998.
By H.I. Petersen, J. Andsbjerg, J.A. Bojesen-Koefoed, H.P. Nytoft & P. Rosenberg. 250.00

37 The Selandian (Paleocene) mollusc fauna from Copenhagen, Denmark: the Poul Harder 1920 collection, 85 pp., 2001.
By K.I. Schnetler. 150.00

Prices are in Danish kroner exclusive of local taxes, postage and handling

Note that information on the publications of the former Geological Survey of Denmark and the former Geological Survey of Greenland (amalgamated in 1995 to form the present Geological Survey of Denmark and Greenland) can be found on the Survey's website: *www.geus.dk*